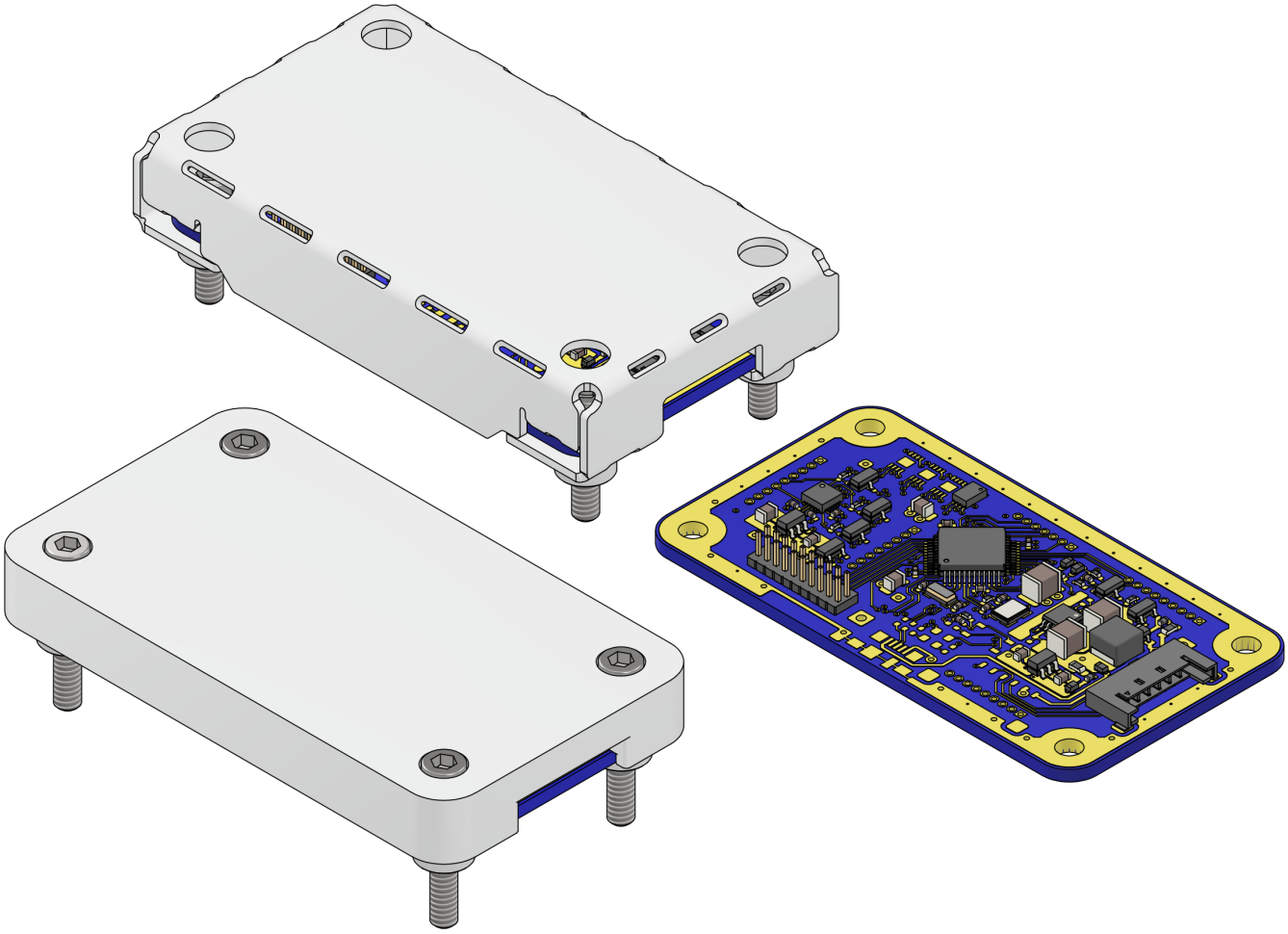
Wave-field Inertial Measurement System (WIMS)
User Manual

Hardware v5.02

Firmware v2.01.00617b



doc. rev. 3.22 (2026-11-03) DRAFT

Disclaimers

---

1. STORM AND OTHER WEATHER CONDITIONS. WIMS data, and any information, products, or analyses derived from them, including those presented in this manual (collectively, "WIMS Data"), are not intended or warranted for use, and shall not be used, as the basis of any decision concerning actions taken or not taken in response to storm or other weather conditions where such decision or action could result in death, personal injury, damage to or loss of property, or other harm. WIMS Data are not an official forecast, warning, watch, or advisory, and are not a substitute for one.

2. NO WARRANTY. WIMS DATA ARE PROVIDED "AS IS", WITHOUT WARRANTY OF ANY KIND, EXPRESS OR IMPLIED, INCLUDING ANY WARRANTY OF ACCURACY, COMPLETENESS, TIMELINESS, OR FITNESS FOR A PARTICULAR PURPOSE. ANY PERSON WHO USES WIMS DATA DOES SO AT THEIR OWN RISK.

3. AUTHORITATIVE GUIDANCE. For guidance on storm and other weather conditions, and on the actions to take in response to them, users should seek and follow the advice of the appropriate local, state, and federal authorities, including the National Oceanic and Atmospheric Administration (NOAA), the National Weather Service (NWS), the National Hurricane Center (NHC), the Federal Emergency Management Agency (FEMA), and local emergency management agencies.

4. USE OF ARTIFICIAL INTELLIGENCE. The analysis presented in Sections 7.8 to 7.10 of this manual, including its data processing, analysis software, figures, and text, was produced with the assistance of Claude Code (Anthropic), an artificial intelligence coding assistant. All such material has been reviewed by the author. The author accepts full responsibility and accountability for the content and validity of the analysis, and any errors or omissions in it are the responsibility of the author.



Contents

1 Absolute Maximum Ratings 13

2 Recommended Operating Conditions 14

3 Electrical Characteristics 15
- 3.1 D.C. Electrical Characteristics . . . 15
- 3.2 A.C. Electrical Characteristics . . . 17
- 3.3 Recommendations for Electrical Integration . . . 18

4 Mechanical Properties 19
- 4.1 Dimensions . . . 20
- 4.2 Assembly Drawings . . . 21
- 4.3 Renders . . . 22
- 4.4 Recommendations for Mechanical Integration . . . 23

5 Connectors 24
- 5.1 Connector Pinouts . . . 25
- 5.2 Recommendations for Primary Cable Assembly . . . 29

6 Operation 30
- 6.1 Calibration . . . 32
  - 6.1.1 Accelerometer Calibration . . . 32
  - 6.1.2 Gyroscope Calibration . . . 34
  - 6.1.3 Magnetometer Calibration . . . 36
- 6.2 Orientation Filter . . . 38
  - 6.2.1 Formulation . . . 38
- 6.3 Reset Behavior . . . 41
- 6.4 Run Behavior . . . 42
  - 6.4.1 Run Duration . . . 42
- 6.5 Low-power Shutdown . . . 44

7 Spectral Data Processing 45
- 7.1 Naming Conventions . . . 45
- 7.2 Spectra Frequencies . . . 46
- 7.3 Scale Sensitivity . . . 47
- 7.4 Converting from Acceleration to Displacement Spectra . . . 49
- 7.5 Directional Spectra . . . 50

7.6 Derived Wave Parameters . . . 52
7.7 Shore-Side Data Validation and Post-Processing . . . 53
7.7.1 Decoding . . . 53
7.7.2 Post-Processing Steps . . . 53
7.8 Low-Frequency Response Correction . . . 56
7.8.1 Data . . . 56
7.8.2 Method . . . 56
7.8.3 Results . . . 60
7.8.4 Storm-Relative Position . . . 64
7.8.5 Rejection Criteria Evaluation . . . 67
7.8.6 Limitations . . . 68
7.9 Wave Direction Validation . . . 70
7.9.1 Directional Fourier Coefficients and Spreading Parameters . . . 71
7.10 NDBC Buoy Intercomparison . . . 78
7.10.1 Method . . . 78
7.10.2 Results . . . 81
7.10.3 Tropical Cyclones . . . 85
7.10.4 Limitations . . . 86

8 Serial Interface 88
8.1 Special Characters and Strings . . . 88
8.2 Serial Interface Commands . . . 89
8.2.1 baud . . . 90
8.2.2 get . . . 90
8.2.3 help . . . 91
8.2.4 load . . . 91
8.2.5 mcal . . . 92
8.2.6 mst . . . 93
8.2.7 read . . . 93
8.2.8 reset . . . 94
8.2.9 run . . . 95
8.2.10 runinfo . . . 95
8.2.11 save . . . 97
8.2.12 set . . . 97
8.2.13 shutdown . . . 98
8.2.14 sleep . . . 98
8.2.15 vers . . . 98
8.3 Output Message Formats . . . 99



8.3.1 Comment Lines . . . 99
8.3.2 Run Output Records . . . 99
8.3.3 Error Messages and Status Codes . . . 100

9 Configuration Parameters 105
9.1 brd.leds . . . 108
9.2 cal.acof[A] and cal.acsc[A] . . . 108
9.3 cal.gcof[A] and cal.gcsc[A] . . . 109
9.4 cal.mcof[A] and cal.mcsc[A] . . . 110
9.5 imu.dlpf . . . 110
9.6 imu.fsra . . . 111
9.7 imu.fsrg . . . 111
9.8 imu.srate . . . 111
9.9 log.level . . . 112
9.10 run.rmode . . . 112
9.11 run.smode . . . 113
9.12 serialnum . . . 113
9.13 wav.afilt . . . 114
9.14 wav.fbmax . . . 115
9.15 wav.fbmin . . . 115
9.16 wav.gaina . . . 115
9.17 wav.mxsam . . . 116
9.18 wav.mxseg . . . 116
9.19 wav.nfwax . . . 116
9.20 wav.nupax . . . 116
9.21 wav.obeta . . . 117
9.22 wav.omode . . . 117
9.23 wav.ostsc . . . 119
9.24 wav.ozeta . . . 120
9.25 wav.slen . . . 120
9.26 wav.smode . . . 120
9.27 wav.srdiv . . . 120
9.28 wav.twalp . . . 121

10 Schematic 123

11 Mechanical Drawings 128

12 Firmware Change Log **135**
v2.01.00617b (2026-10-27) . . . 135
v2.01.00616b (2026-10-26) . . . 135
v2.01.00615b (2026-10-26) . . . 135
v2.01.00614b (2026-10-26) . . . 136
v2.01.00613b (2025-05-14) . . . 136
v2.01.00612b (2025-05-06) . . . 136
v2.01.00611a (2025-03-25) . . . 136
v2.01.00604a (2025-03-21) . . . 136
v2.01.00596a (2025-03-18) . . . 136
v2.01.00591a (2025-03-18) . . . 136
v2.00.00487a (2024-12-27) . . . 137
v2.00.00426a (2024-12-03) . . . 137
v2.00.00416a (2024-11-22) . . . 137
v2.00.00394a (2024-11-18) . . . 138
v2.00.00365a (2024-11-12) . . . 138
v2.00.00336a (2024-11-06) . . . 138
v2.00.00324a (2024-11-05) . . . 138
v2.00.00323a (2024-11-04) . . . 138
v2.00.00322a (2024-11-04) . . . 138
v2.00.00317a (2024-09-17) . . . 139
v1.09 . . . 139
v1.08 . . . 139
v1.07 . . . 140
v1.06 . . . 140
v1.05 . . . 140
v1.04 . . . 140
v1.03 . . . 141
v1.02 . . . 141
v1.01 . . . 141

13 Document Revision Change Log **142**
v3.22 (2026-11-03) . . . 142
v3.21 (2026-10-31) . . . 142
v3.20 (2026-10-29) . . . 143
v3.19 (2026-10-29) . . . 144
v3.18 (2026-10-29) . . . 144
v3.17 (2026-10-29) . . . 144

v3.16 (2026-10-29) . . . 144
v3.15 (2026-10-28) . . . 145
v3.14 (2026-10-27) . . . 146
v3.13 (2026-10-26) . . . 146
v3.12 (2026-10-26) . . . 146
v3.11 (2026-10-26) . . . 146
v3.10 (2025-10-16) . . . 147
v3.09 (2025-09-02) . . . 147
v3.08 (2025-08-27) . . . 147
v3.07 (2025-05-28) . . . 147
v3.06 (2025-05-15) . . . 147
v3.05 (2025-05-14) . . . 147
v3.04 (2025-05-12) . . . 147
v3.03 (2025-05-08) . . . 148
v3.02 (2025-05-07) . . . 148
v3.01 (2025-05-06) . . . 148
v3.00 (2025-05-02) . . . 148

14 References **149**

List of Tables

1 Absolute maximum ratings. . . . 13
2 Recommended operating conditions. . . . 14
3 D.C. Electrical characteristics - power supply. . . . 15
4 D.C. Electrical characteristics - digital I/O. . . . 16
5 A.C. Electrical characteristics. . . . 17
6 Mechanical properties. . . . 19
7 WIMS connector descriptions. . . . 24
8 Primary connector J1 pinout. . . . 25
9 Primary (alternate) connector J2 pinout. . . . 25
10 USB connector J3 pinout. . . . 26
11 JTAG/SWD connector J4 pinout. . . . 27
12 Auxiliary connector J10 pinout. . . . 28
13 Low-frequency response correction coefficients. . . . 54
14 Spectra rejection criteria. . . . 55
15 Intercomparison data sets. The WIMS segment length was 256, except for floats 9287 and 9291 (512). . . . 59
16 Colocation criteria and colocated pairs in the same storm quadrant or both more than 600 km from the center of the storm, after rejection of WIMS spectra and of the A-DWSD outliers. . . . 60
17 Significant wave height of colocated WIMS and reference spectra, from 0.04 Hz to 0.48 Hz. Bias and RMS are of the WIMS minus the reference value. The ratio is that of the mean values; the median ratio is $\exp(\mathrm{median}(\ln(H_{m0,\mathrm{WIMS}}/H_{m0,\mathrm{ref}})))$. . . . 63
18 Median ratio of WIMS to reference significant wave height, with the adopted correction, by the storm quadrant of the WIMS and reference positions, with the number of pairs. Quadrants are within 600 km of the center of the storm. The 33 NDBC 41047 pairs in the same quadrant of Hurricane Imelda or Melissa, not shown, have a median ratio of 0.90. 64
19 Evaluation of rejection criteria, for the 2977 WIMS spectra of both storms and their 11699 colocated pairs with all three data sets, in the same storm quadrant or both outside the storm, without the A-DWSD outliers. Low-frequency criteria are the maximum acceleration spectral density at or below 0.05 Hz, for the axes given. . . . 67
20 WIMS bulk mean wave direction, 0.06 Hz to 0.25 Hz, compared with the reference directions, for the pairs in the same storm quadrant or both outside the storm. . . . 70
21 WIMS bulk mean wave direction, 0.06 Hz to 0.25 Hz, compared with the reference directions, by the storm quadrant of both positions, and for the pairs with both positions outside the storm (more than 600 km from the center). . . . 71



22 WIMS bulk directional coefficients and parameters, 0.0625 Hz to 0.3 Hz, compared with the reference instruments: bias (WIMS minus reference) / RMS difference / correlation coefficient for the coefficients, and bias / RMS difference / median absolute difference for the directions. Directions are from which the waves come; principal direction differences are modulo $180°$. The spread is the bulk circular spread, $\sqrt{2(1-r_1)}$. 73
23 Median ratio of WIMS to reference r_1 / r_2, at each frequency bin, by frequency band. . 73
24 NDBC buoys: location, deployments in effect during the colocated pairs, from the NDBC station metadata, with the position of each deployment, the water depth at that position from the ETOPO 2022 bathymetry [14], and the period and number of the colocated pairs. Deployments at the same position are combined. 80
25 WIMS compared with NDBC buoys, by ALAMO float and NDBC buoy, in order of the first colocated pair, with the period of the colocated pairs. 81
26 WIMS compared with NDBC buoys, by NDBC significant wave height. 83
27 Colocated WIMS and NDBC pairs during tropical cyclones, with both instruments within 600 km of the center of the storm: Saffir-Simpson peak of the storm, floats and buoys, number of pairs (in the same storm quadrant), closest approach of the float and of the buoy to the center, largest WIMS and NDBC significant wave height, median ratio of WIMS to NDBC significant wave height (same quadrant), and median absolute difference of the bulk mean wave direction (same quadrant). 86
28 Serial interface special characters and strings. 88
29 Serial interface commands. 89
30 Status codes. 100
31 Command interface error messages. 101
32 Configuration memory error messages. 102
33 Run error messages. 103
34 IMU error messages. 104
35 Configuration parameters. 105
36 Serial interface log levels. 112
37 Run mode (`run.rmode`) bitmask. 113
38 Start mode (`run.smode`) bitmask. 113
39 Acceleration finite-impulse response (FIR) low-pass filter (LPF) characteristics. 114
40 Axis enumeration for `wav.nfwax` and `wav.nupax`. 117
41 Equivalent orientation representation for combinations for `wav.nfwax` and `wav.nupax`. . 118
42 Output modes. 119
43 Sample modes. 121

List of Figures

1 WIMS PCB dimensions. 20
2 PCB assembly drawing - front. 21
3 PCB assembly drawing - back. 21
4 PCB assembly render - front. 22
5 PCB assembly render - back. 22
6 Primary cable assembly. 29
7 Digital signal processing overview in full-spectra output mode. 30
8 Calibration fixture. 33
9 Example magnetometer calibration - transient response. 37
10 Example magnetometer calibration - ellipsoid fitting. 37
11 Hurricane Erin and the intercomparison data sets: (a) best track of Hurricane Erin [11], with the position every 6 hours colored by Saffir-Simpson category, the area shown in (b) (rectangle), and NDBC buoy 41047 (star); (b) positions of the WIMS spectra, the A-DWSD drifter spectra, and NDBC buoy 41047, with the 220 km colocation radius around the buoy, the track of Hurricane Erin, and the extent of the 34, 50, and 64 kt winds (outlines) at the closest approach of the storm to the floats, over the GOES-19 band 13 infrared image of that hour (brightness temperature from 190 K, white, to 305 K, black) [12]; (c) distance of the ALAMO floats, of NDBC buoy 41047, and of the A-DWSD drifters (grey dots) from the center of the storm, with the mean radii of the 34, 50, and 64 kt winds, and the maximum sustained wind of the storm. Float 9302, which had no GPS fixes during the passage of the storm, is not shown in (c). 57
12 Hurricane Lowell and the intercomparison data sets: (a) best track of Hurricane Lowell [10], with the position every 6 hours colored by Saffir-Simpson category, and the area shown in (b) (rectangle); (b) positions of the WIMS spectra and the A-DWSD drifter spectra, with the track of Hurricane Lowell, labelled every 12 hours, and the extent of the 34, 50, and 64 kt winds (outlines) at the closest approach of the storm to the floats, over the GOES-18 band 13 infrared image of that hour (brightness temperature from 190 K, white, to 305 K, black) [12]; (c) distance of the ALAMO floats and of the A-DWSD drifters (grey dots) from the center of the storm, with the mean radii of the 34, 50, and 64 kt winds, and the maximum sustained wind of the storm. 58
13 Per-bin scale factors, reference / WIMS, of the three data sets, as (a) the ratio of the means, with that of all data sets combined, and (b) the median ratio, and the adopted correction factor, $T(f)$. 61
14 Colocated NDBC 41047 during Hurricane Erin: difference of each pair of vertical acceleration spectra, WIMS minus NDBC, without and with the correction, as the median and interquartile range, and the mean. 61

15 Colocated A-DWSD drifters during Hurricane Erin: difference of each pair of vertical acceleration spectra, WIMS minus A-DWSD, without and with the correction, as the median and interquartile range, and the mean. 62
16 Colocated A-DWSD drifters during Hurricane Lowell: difference of each pair of vertical acceleration spectra, WIMS minus A-DWSD, without and with the correction, as the median and interquartile range, and the mean. 62
17 Significant wave height of colocated WIMS and reference spectra, with the adopted correction. The horizontal rows of points are WIMS spectra colocated with several drifters. 63
18 Storm-relative positions of the references within 400 km of the center of the storm, along and across its track (cubic spline through the best track positions), colored by the logarithm of the ratio of WIMS to reference significant wave height, with the adopted correction, with the number of pairs. The arrow is the direction of motion of the storm. 64
19 Storm-relative positions of the WIMS spectra within 400 km of the center of the storm, along and across its track, colored by the WIMS significant wave height, with the adopted correction. The arrow is the direction of motion of the storm. 65
20 Storm-relative positions of the WIMS spectra within 400 km of the center of the storm, along and across its track, colored by the WIMS mean swell direction, 0.06 Hz to 0.10 Hz, toward which the waves propagate, relative to the direction of motion of the storm (up). 66
21 Storm-relative positions of the WIMS spectra within 400 km of the center of the storm, along and across its track, colored by the WIMS mean wind-wave direction, 0.10 Hz to 0.25 Hz, toward which the waves propagate, relative to the direction of motion of the storm (up). 66
22 WIMS and reference bulk mean wave directions, 0.06 Hz to 0.25 Hz, toward which the waves propagate, referenced to true north, for the pairs in the same storm quadrant or both outside the storm (top), and the difference of the mean wave directions, θ_1, at each frequency, with the median and interquartile range (bottom). 72
23 Differences of the directional Fourier coefficients, WIMS minus reference, in the NDBC convention, against frequency: median (line) and interquartile range (shading), for each reference data set. 74
24 Differences of the spreading parameters, r_1 and r_2, WIMS minus reference, against frequency: median (line) and interquartile range (shading), for each reference data set. . . 75
25 Bulk r_1 (a) and r_2 (b), 0.0625 Hz to 0.3 Hz, WIMS against the reference instruments, with the number of pairs and the median ratio of each data set. Horizontal rows of points are WIMS spectra colocated with several references. 75
26 Differences of the mean direction, α_1, and of the principal direction, α_2 (modulo $180°$), WIMS minus reference, against frequency: median (line) and interquartile range (shading), for each reference data set. 76

27 The NDBC buoys at their deployment positions during the colocated pairs, with their number of colocated pairs, the ALAMO float positions of the colocated WIMS spectra, in the color of their buoy, and the excluded buoys in water shallower than 50 m. 79
28 WIMS compared with NDBC buoys: significant wave heights, by buoy, with the number of pairs (a); ratio of significant wave heights against the NDBC significant wave height, with the median and interquartile range in 0–1, 1–2, 2–3, 3–5, and above 5 m bins (b); bulk mean wave directions, 0.06 Hz to 0.25 Hz, toward which the waves propagate, referenced to true north (c); and difference of the bulk mean wave directions, with ± the median absolute difference in the same bins (d). 84
29 Effect of Tukey window alpha parameter. 122
30 WIMS 5.02 schematic (1/4) - root. 124
31 WIMS 5.02 schematic (2/4) - power management. 125
32 WIMS 5.02 schematic (3/4) - microcontroller unit (MCU). 126
33 WIMS 5.02 schematic (4/4) - inertial measurement unit (IMU). 127
34 WIMS 5.02 mechanical drawing (1/6) - overview. 129
35 WIMS 5.02 mechanical drawing (2/6) - PCB assembly. 130
36 WIMS 5.02 mechanical drawing (3/6) - billet aluminum shield. 131
37 WIMS 5.02 mechanical drawing (4/6) - laser-cut, folded aluminum shield. 132
38 WIMS 5.02 mechanical drawing (5/6) - primary cable assembly. 133
39 WIMS 5.02 mechanical drawing (6/6) - calibration fixture. 134

1 Absolute Maximum Ratings

Table 1: Absolute maximum ratings[1].

Supply					
Symbol	Parameter	Conditions	Min.	Max.	Units
V_{IN}[2]	Supply input voltage	Continuous	-0.3	19.4	V
V_{IN}[2]	Supply input voltage	Momentary	-0.3	31.9	V
I_{IN}[3]	Supply input current			80	mA
Digital I/O					
Symbol	Parameter	Conditions	Min.	Max.	Units
V_{DI}[2]	Digital input voltage		-0.3	4.0	V
$V_{DI,SHDN}$[2]	Shutdown digital input voltage	All I/O pins except ENABLE state = shutdown	-0.3	0.6	V
I_{DO}[2]	Digital output current source			20	mA
I_{DO}[2]	Digital output current sink			20	mA
Temperature					
Symbol	Parameter	Conditions	Min.	Max.	Units
T_A[2]	Operating temperature		-40	85	$°C$
T_{STG}[2]	Storage temperature		-40	85	$°C$
Acceleration					
Symbol	Parameter	Conditions	Min.	Max.	Units
a[2]	Acceleration	Any axis, unpowered, for 2 ms		20,000	g

[1] These are stress ratings only, which do not imply functional operation of the device at these or any other conditions beyond those indicated under Table 2: Recommended operating conditions.. Exposure to absolute-maximum-rated conditions for extended periods may permanently affect device performance and/or reliability.

[2] Guaranteed by design.

[3] Supply input currents beyond those indicated under Table 3: D.C. Electrical characteristics - power supply. imply a fault condition.

2 Recommended Operating Conditions

Table 2: Recommended operating conditions.

Supply						
Symbol	Parameter	Conditions	Min.	Typ.	Max.	Units
V_{IN}	Supply input voltage		6.0		16.5	V
Digital I/O						
Symbol	Parameter		Min.	Typ.	Max.	Units
V_{DIH}	Digital input high voltage		2.9		3.3	V
V_{DIL}	Digital input low voltage		0.0		0.4	V
$V_{DI,SHDN}$	Shutdown digital input voltage	All I/O pins except ENABLE state = shutdown		0.0	0.3	V
I_{DO}	Digital output current source				4	mA
I_{DO}	Digital output current sink				4	mA
f_{SER}	Serial port speed			115200		$baud$
Temperature						
Symbol	Parameter		Min.	Typ.	Max.	Units
T_A	Operating temperature		-5		50	$°C$
T_{STG}	Storage temperature		-20		65	$°C$

3 Electrical Characteristics

3.1 D.C. Electrical Characteristics

Table 3: D.C. Electrical characteristics - power supply.

Supply						
Symbol	Parameter	Conditions	Min.	Typ.	Max.	Units
V_{IN}[1]	Supply input voltage		5.3		16.8	V
I_{IN}[2]	Supply input current	$V_{IN} = 15.0V$ state = running		3.04	3.10	mA
I_{IN}[2]	Supply input current	$V_{IN} = 15.0V$ state = idle		1.06	1.09	mA
I_{IN}[2]	Supply input current	$V_{IN} = 15.0V$ state = sleep		672	681	μA
I_{IN}[2]	Supply input current	$V_{IN} = 15.0V$ $V_{EN} \leq 0.6V$ state = shutdown			0.1	μA
P_{IN}[2]	Supply input power	$V_{IN} = 15.0V$ state = running		45.6	46.5	mW
P_{IN}[2]	Supply input power	$V_{IN} = 15.0V$ state = idle		15.9	16.3	mW
$I_{IN,PH}$[1]	Input PTC fuse hold current	$0°C \leq T_A \leq 50°C$	64	80	98	mA
$I_{IN,PT}$[1]	Input PTC fuse trip current	$0°C \leq T_A \leq 50°C$	160	200	246	mA

[1] Guaranteed by design.
[2] Derived from characterization or validation of components.

Table 4: D.C. Electrical characteristics - digital I/O.

Digital I/O						
Symbol	Parameter	Conditions	Min.	Typ.	Max.	Units
V_{DIH}[1]	Digital input high voltage	All I/O pins except ENABLE	2.3			V
V_{DIL}[1]	Digital input low voltage	All I/O pins except ENABLE			0.9	V
I_{DI}[1]	Digital input current	All I/O pins except ENABLE $0.0V \leq V_{DI} \leq 3.3V$	-1		1	μA
V_{ENH}[1]	ENABLE pin input high voltage		2.3			V
V_{ENL}[1]	ENABLE pin input low voltage				0.6	V
I_{EN}[1]	ENABLE pin input current	$V_{EN} = 3.3V$			33	μA
V_{DOH}[1]	Digital output high voltage	All I/O pins except TX $\lvert I_{DO} \rvert = 4mA$	2.8			V
V_{DOL}[1]	Digital output low voltage	All I/O pins except TX $\lvert I_{DO} \rvert = 4mA$			0.4	V
V_{TXH}[1]	TX pin output high voltage	$\lvert I_{DO} \rvert = 4mA$	2.4			V
V_{TXL}[1]	TX pin output low voltage	$\lvert I_{DO} \rvert = 4mA$			0.8	V
I_{DO}[1]	Digital output current source				20	mA
I_{DO}[1]	Digital output current sink				20	mA

[1] Guaranteed by design.

3.2 A.C. Electrical Characteristics

Table 5: A.C. Electrical characteristics.

Clock						
Symbol	Parameter	Conditions	Min.	Typ.	Max.	Units
f_{SYS}[1]	System clock			8		MHz
Δf_{SYS}[1]	System clock tolerance	$-40°C \leq T_A \leq 85°C$	-20		20	ppm
f_{RTC}[1]	RTC clock			32.768		kHz
Δf_{RTC}[1]	RTC clock tolerance	$-40°C \leq T_A \leq 85°C$	-20		20	ppm
Δf_{IMU}[2]	IMU clock tolerance	$-40°C \leq T_A \leq 85°C$	-2		2	%
Digital I/O						
Symbol	Parameter	Conditions	Min.	Typ.	Max.	Units
f_{SER}[1,3]	USART serial data rate		9600	115200	460800	baud

[1] Guaranteed by design.
[2] Derived from characterization or validation of components.
[3] Minimum viable USART serial data rate dependent on output mode.

3.3 Recommendations for Electrical Integration

- **Power supply.** Supply V_{IN} within the range of Table 2, 6.0 V to 16.5 V, at the WIMS connector, allowing for the voltage drop of the cable. The supply must provide the running current of Table 3 with margin. The input is protected by a resettable PTC fuse; a sustained fault current above the hold current trips it, and it resets when the fault is removed and the power is cycled.

- **Grounds.** Return the supply current through the GND pin and reference the serial and ENABLE signals to the $DGND$ pin, using separate wires in the cable. Join the host's supply and signal grounds at one point (see Section 5.2: Recommendations for Primary Cable Assembly).

- **Logic levels.** The serial (TX, RX) and ENABLE signals are 3.3 V logic. Do not drive any I/O pin above 3.3 V. Use a level translator to connect a host with 5 V logic or an RS-232 interface. Limit the current drawn from TX to 4 mA.

- **Serial receive line.** The WIMS RX input has no internal pull-up resistor. Keep it driven high (idle) by the host, or pulled up to 3.3 V, whenever WIMS is powered and ENABLE is asserted. A floating input can pick up noise that is received as framing or noise errors, which can leave the serial interface unresponsive until WIMS is reset (see Section 8.3.3: Error Messages and Status Codes).

- **Shutdown.** Use the ENABLE pin to shut WIMS down between measurements (see Section 6.5: Low-power Shutdown). Drive ENABLE high (≥ 2.9 V) while WIMS is in use; de-asserting it for more than 100 ms shuts WIMS down. During shutdown, hold all other I/O pins at or below 0.3 V: a host that keeps its serial output high powers WIMS through the I/O pins and increases the shutdown current.

- **Magnetic interference.** The orientation filter uses the magnetometer, so magnetic fields from nearby currents corrupt the orientation estimate and the earth-frame acceleration. Route supply and other current-carrying wires away from the IMU, twist each supply pair so that its fields cancel, and avoid ferrous fasteners and components near the IMU. Do not switch large loads, such as pumps, motors, or radio transmitters, during a run.

- **Electrical noise.** Avoid running the WIMS cable alongside switching power supplies, motor drives, or antenna feeds. If the WIMS supply is shared with such loads, filter it at the WIMS end of the cable.

- **Calibration in the final assembly.** Perform the magnetometer calibration (Section 6.1.3: Magnetometer Calibration) with WIMS installed and wired as it will be deployed, since batteries, wiring, and the host electronics change the magnetic field at the IMU.

4 Mechanical Properties

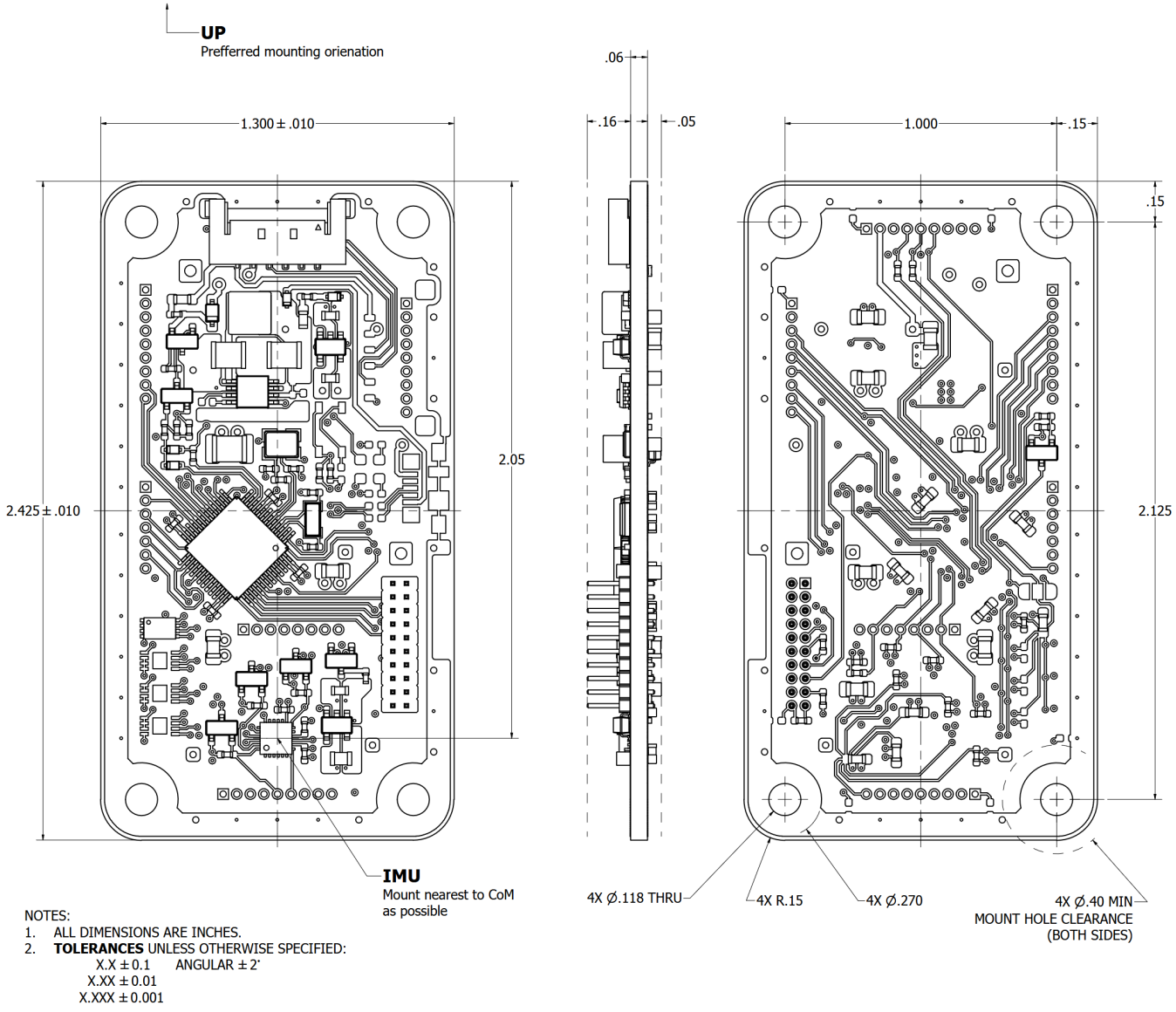
The mechanical properties of the WIMS 5.02 PCB assembly are given in Table 6, from the dimensions of Figure 1 and the mechanical drawing on page 130.

Table 6: Mechanical properties.

Parameter	Conditions	Inches	mm
PCB assembly			
Length		2.425	61.6
Width		1.300	33.0
PCB thickness		0.06	1.5
Component height	Connector (J1) side, above PCB	0.16	4.1
Component height	Opposite side, below PCB	0.05	1.3
Corner radius		0.15	3.8
Mounting holes	4, through	Ø0.118	Ø3.0
Mounting hole spacing	Center to center	1.000 × 2.125	25.4 × 54.0
Mounting hole position	Hole center from each adjacent edge	0.15	3.8
Mounting pad	Around each mounting hole	Ø0.270	Ø6.9
Mounting hole clearance	Keep-out around each hole, both sides, min.	Ø0.40	Ø10.2
IMU location	On the long centerline, from the J1 edge	2.05	52.1
Mounting hardware			
Screws	4, No. 4-40 socket cap screw		
Spacers	4, No. 4 unthreaded, Ø0.25 × 0.05 min.		

4.1 Dimensions

Figure 1: WIMS PCB dimensions.



4.2 Assembly Drawings

Figure 2: PCB assembly drawing - front.

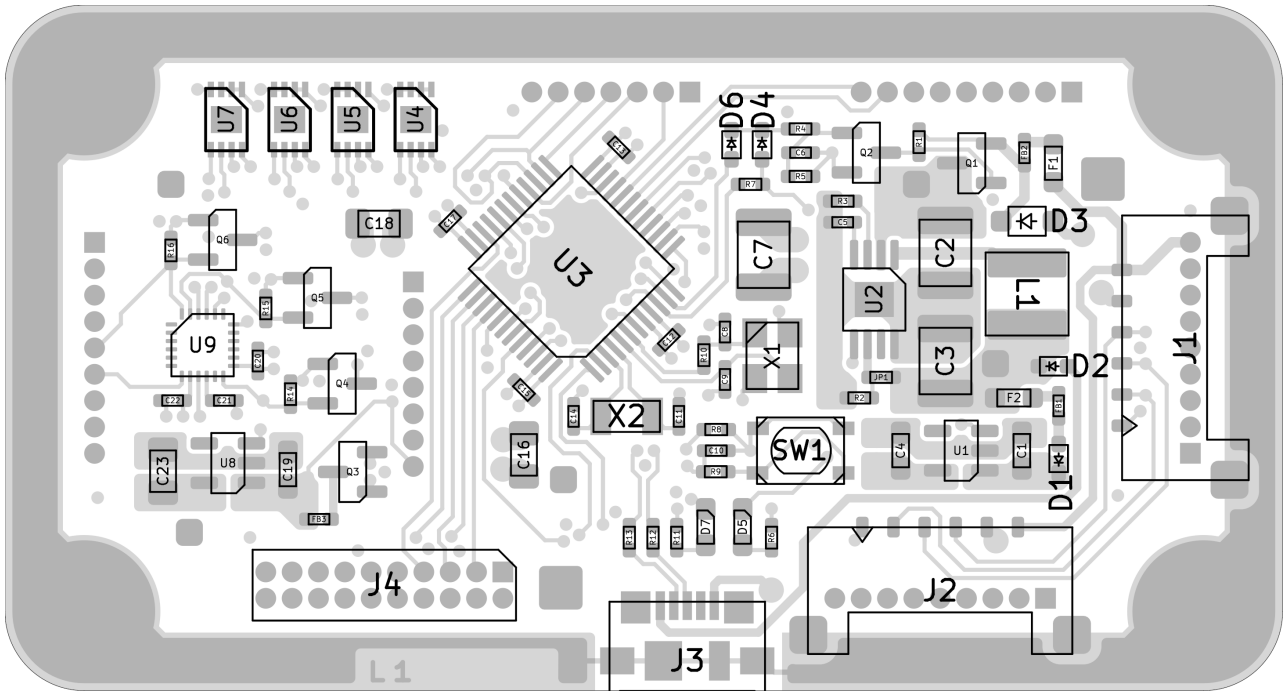
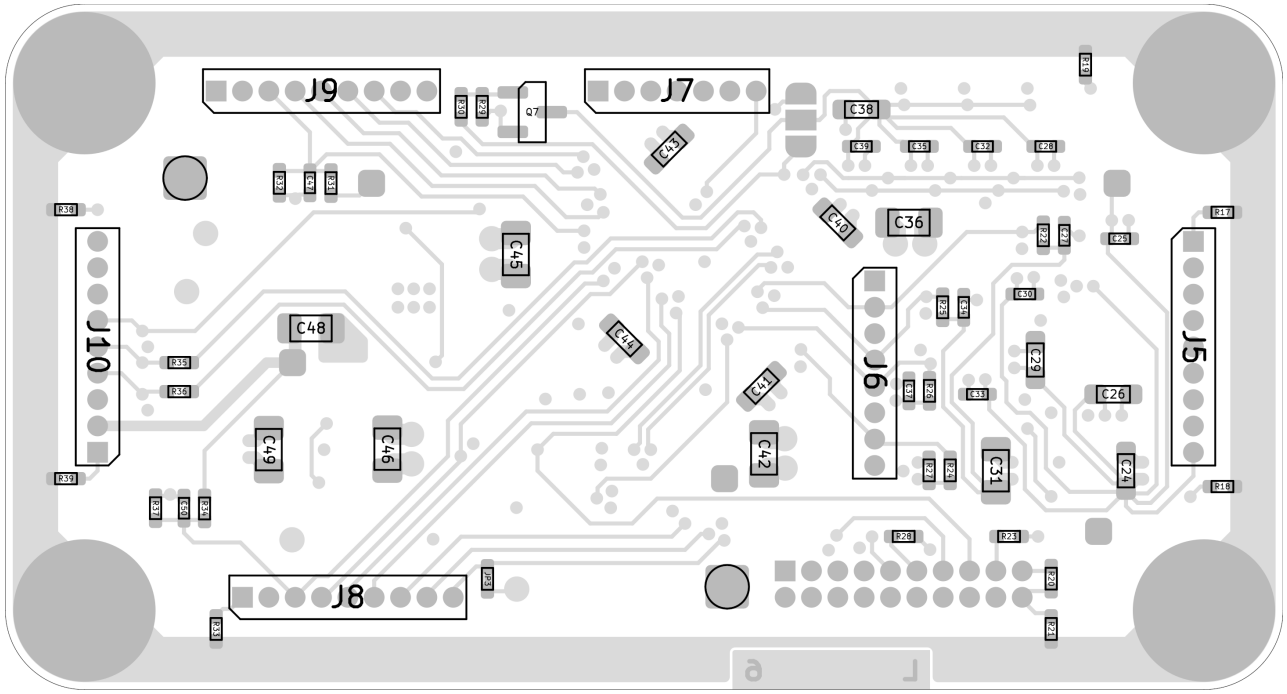


Figure 3: PCB assembly drawing - back.



4.3 Renders

Figure 4: PCB assembly render - front.

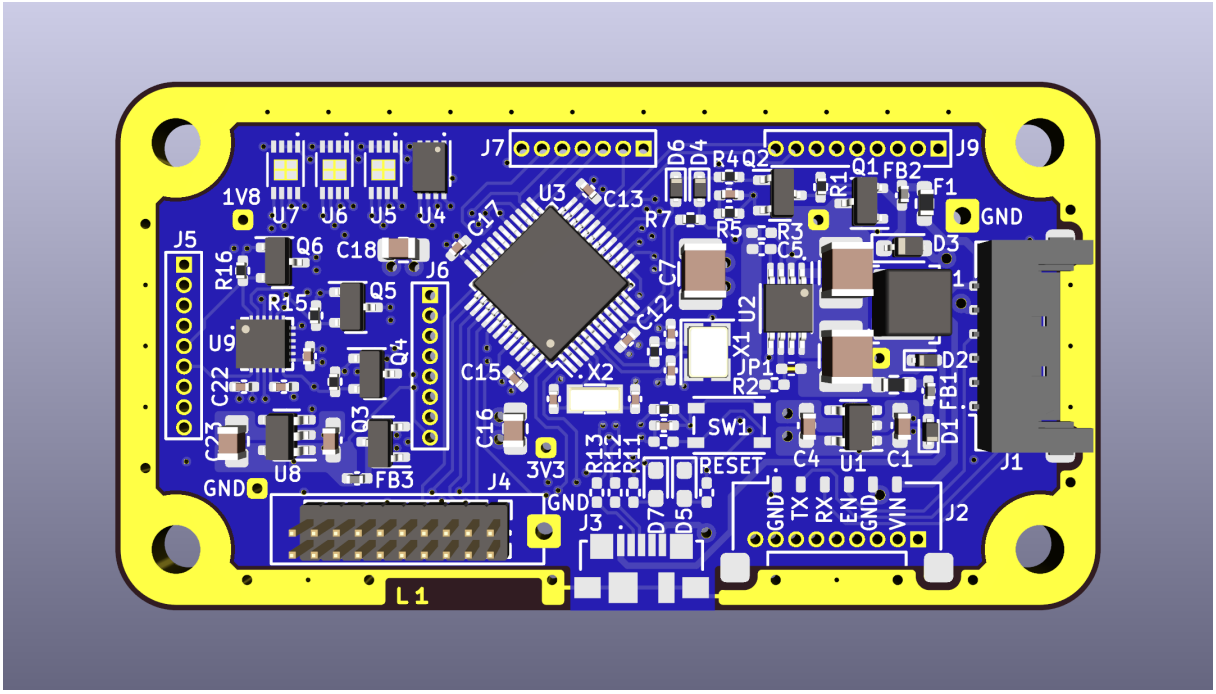
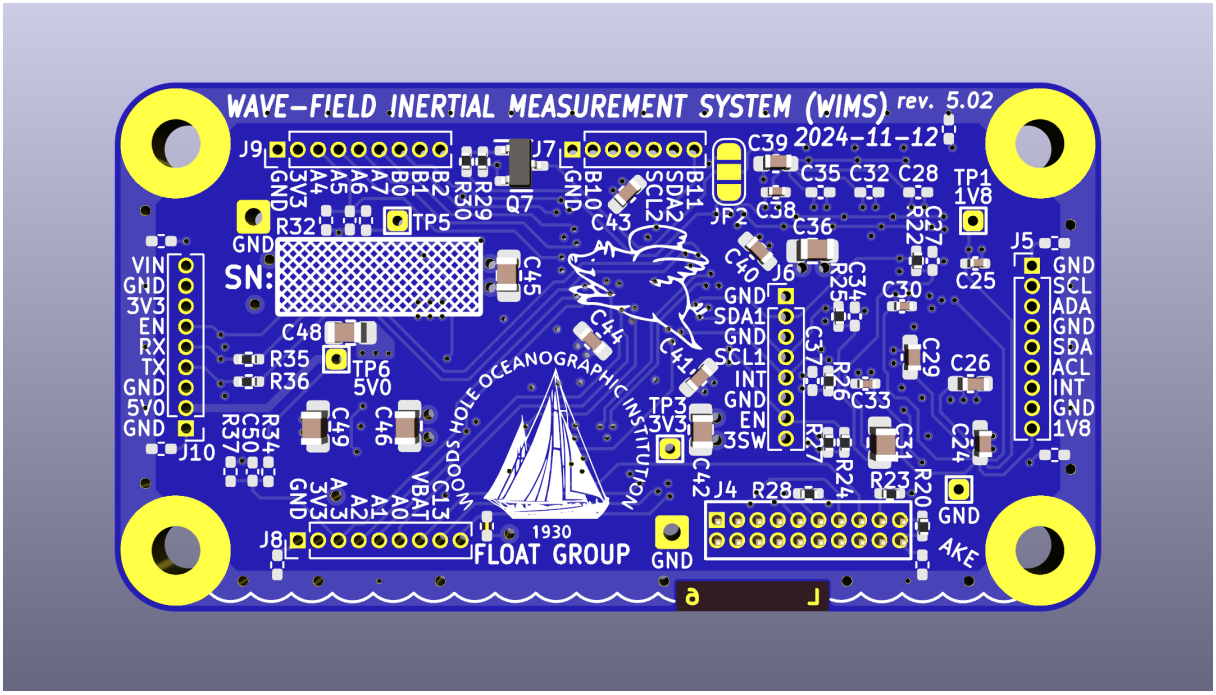


Figure 5: PCB assembly render - back.



4.4 Recommendations for Mechanical Integration

- **Vertical axis.** Mount WIMS so that the vertical axis is normally aligned with the IMU X- or Y-axis, not the Z-axis. Because of the planar structure of the silicon die, the IMU Z-axis is the least accurate of the three, while the vertical acceleration is the most important measurement of the wave field.
- **Location.** Mount the IMU as near to the center of mass of the platform as possible. Far from the center of mass, rotations of the platform add centripetal accelerations to the measured acceleration.
- **Mounting.** Fix WIMS rigidly to the platform, and isolate it from severe vibration and mechanical shock.
- **Magnetic interference.** Avoid ferromagnetic hardware near WIMS, which interferes with the magnetometer, and mount WIMS as far from sources of magnetic interference as possible (see Section 3.3: Recommendations for Electrical Integration).

5 Connectors

Table 7: WIMS connector descriptions.

Ref.	Type	Connector	Mating connector	Description	Table (Page)
J1	Primary	Molex 5040500691 Pico-Lock Header SMD R/A 6POS	Molex 5040510601 Pico-Lock RCPT HSG 6POS	Power, data	8 (25)
J2	Primary (alternate)	Molex 5040500691 Pico-Lock Header SMD R/A 6POS (unpopulated)	Molex 5040510601 Pico-Lock RCPT HSG 6POS	Power, data	9 (25)
J3	USB	Molex 0473460001 (unpopulated)	USB Micro-B	Power, programming	10 (26)
J4	JTAG/SWD Pin header	10x2 0.050" (1.27mm) pin header Sullins GRPB102VWVN-RC	e.g. CNC Tech 3230-20-0101-00	Programming, debug	11 (27)
J5	Auxiliary	9x1 0.050" (1.27mm) pin header (unpopulated)	-	Power, I^2C	-
J6	Auxiliary	8x1 0.050" (1.27mm) pin header (unpopulated)	-	Power, I^2C	-
J7	Auxiliary	7x1 0.050" (1.27mm) pin header (unpopulated)	-	Auxiliary GPIO, I^2C	-
J8	Auxiliary	9x1 0.050" (1.27mm) pin header (unpopulated)	-	Auxiliary GPIO, V_{BAT}	-
J9	Auxiliary	9x1 0.050" (1.27mm) pin header (unpopulated)	-	Auxiliary GPIO	-
J10	Auxiliary	9x1 0.050" (1.27mm) pin header (unpopulated)	-	Auxiliary power, data	12 (28)

5.1 Connector Pinouts

Table 8: Primary connector J1 pinout.

Pin	Symbol	Name	Type	Description
1	$DGND$	Digital ground	Supply	Ground return path for digital I/O.
2	TX	Serial out	Digital out	USART transmit pin. 3.3V TTL logic.
3	RX	Serial in	Digital in	USART receive pin. 3.3V TTL logic.
4	EN	Enable	Digital in	Wake/enable device. 3.3V TTL logic.
5	GND	Power supply ground	Supply	Ground return path for power supply V_{IN}.
6	V_{IN}	Power supply in	Supply	Circuit power supply. See Table 2: Recommended operating conditions..

Table 9: Primary (alternate) connector J2 pinout.

Pin	Symbol	Name	Type	Description
1	$DGND$	Digital ground	Supply	Ground return path for digital I/O.
2	TX	Serial out	Digital out	USART transmit pin. 3.3V TTL logic.
3	RX	Serial in	Digital in	USART receive pin. 3.3V TTL logic.
4	EN	Enable	Digital in	Wake/enable device. 3.3V TTL logic.
5	GND	Power supply ground	Supply	Ground return path for power supply V_{IN}.
6	V_{IN}	Power supply in	Supply	Circuit power supply. See Table 2: Recommended operating conditions..

Table 10: USB connector J3 pinout.

Pin	Symbol	Name	Description
1	V_{BUS}	+5V	USB power bus.
2	$D-$	Data minus	USB negative differential data signal.
3	$D+$	Data plus	USB positive differential data signal.
4	ID	Device identifier	Not internally connected.
5	GND	Ground	USB signal and power ground.
6	$SHLD$	Shield	USB shield. Connected to WIMS chassis ground.

Table 11: JTAG/SWD connector J4 pinout.

Pin	Symbol	Name	Type	Description
1	$VTREF$	Voltage reference	Supply	3.3V supply output.
2	$VSUPPLY$	Voltage Supply	Supply	3.3V supply output.
3	$JNRST$	Test reset	Digital in	JTAG asynchronous reset (active low) of the JTAG Test Access Port (TAP).
4	GND	Ground	Supply	Ground return path for supply and digital I/O.
5	$JTDI$	Test data in	Digital in	JTAG data signal from debugger to processor.
6	GND	Ground	Supply	Ground return path for digital I/O.
7	$JTMS$	Test mode select	Digital in	JTAG control signal for the TAP controller.
	$SWDIO$	Data I/O	Digital I/O	SWD data I/O.
8	GND	Ground	Supply	Ground return path for digital I/O.
9	$JTCK$	Test clock	Digital in	JTAG clock signal from debugger to processor.
	$SWCLK$	Clock	Digital in	SWD clock signal from debugger to processor.
10	GND	Ground	Supply	Ground return path for digital I/O.
11	NC	Not connected	Not connected	$10k\Omega$ resistor to GND.
12	GND	Ground	Supply	Ground return path for digital I/O.
13	$JTDO$	Test data out	Digital out	JTAG data signal from processor to debugger.
	SWO	Trace output	Digital out	SWD output for low-bandwidth trace.
14	GND	Ground	Supply	Ground return path for digital I/O.
15	$NRST$	System reset	Digital in	System reset (active low).
16	GND	Ground	Supply	Ground return path for digital I/O.
17	NC	Not connected	Not connected	$10k\Omega$ resistor to GND.
18	GND	Ground	Supply	Ground return path for digital I/O.
19	NC	Not connected	Not connected	$10k\Omega$ resistor to GND.
20	GND	Ground	Supply	Ground return path for digital I/O.

Table 12: Auxiliary connector J10 pinout.

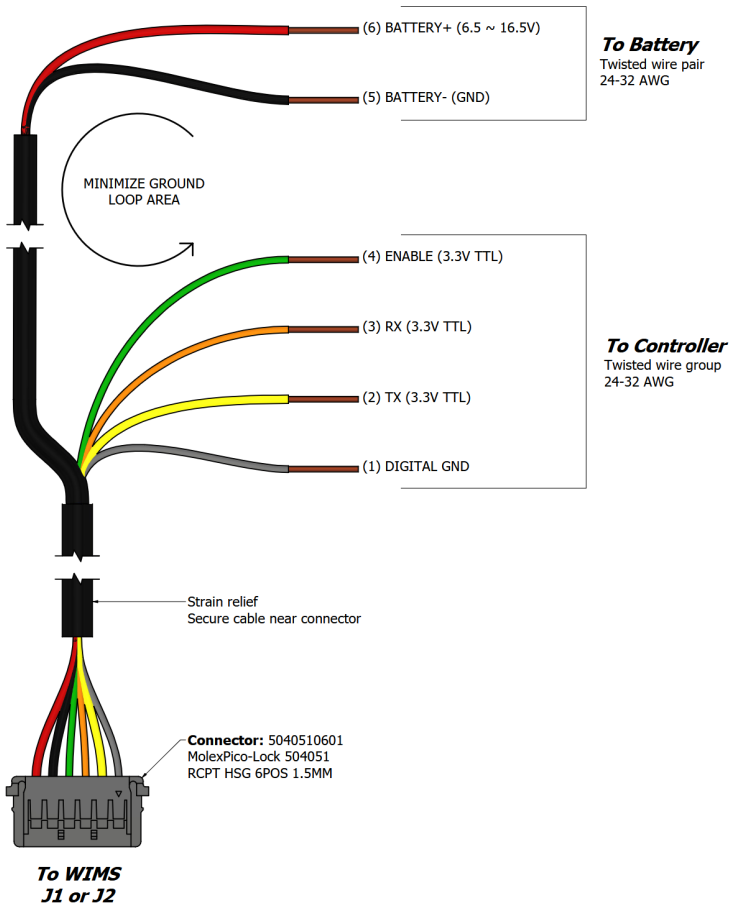
Pin	Symbol	Name	Type	Description
1	GND	Power supply ground	Supply	Ground return path for power supply $5V0$.
2	$5V0$	5.0V supply	Supply	5.0V supply output.
3	$DGND$	Digital ground	Supply	Ground return path for digital I/O.
4	TX	Serial out	Digital out	USART transmit pin. 3.3V TTL logic.
5	RX	Serial in	Digital in	USART receive pin. 3.3V TTL logic.
6	EN	Enable	Digital in	Wake/enable device. 3.3V TTL logic.
7	$3V3$	3.3V supply	Supply	3.3V supply output.
8	GND	Power supply ground	Supply	Ground return path for power supply V_{IN} and $3V3$.
9	V_{IN}	Power supply in	Supply	Circuit power supply. See Table 2: Recommended operating conditions..

5.2 Recommendations for Primary Cable Assembly

The primary cable assembly is shown in Figure 6.

- **Length.** Keep the cable and its leads as short as possible.
- **Twisted groups.** Organize the wires into two twisted groups, one for power and one for digital I/O.
- **Strain relief.** Secure the cable as near as possible to the primary connector to reduce mechanical stress. On final assembly, secure the primary WIMS connector with RTV.
- **Shared supply.** Where the power source, such as a battery, is shared with the host or controller, minimize the ground loop area to reduce radiated interference, and use a star ground where possible.
- **Routing.** Route the cable as far as possible from sources of electromagnetic interference, and route all cables away from the IMU to minimize magnetic interference.

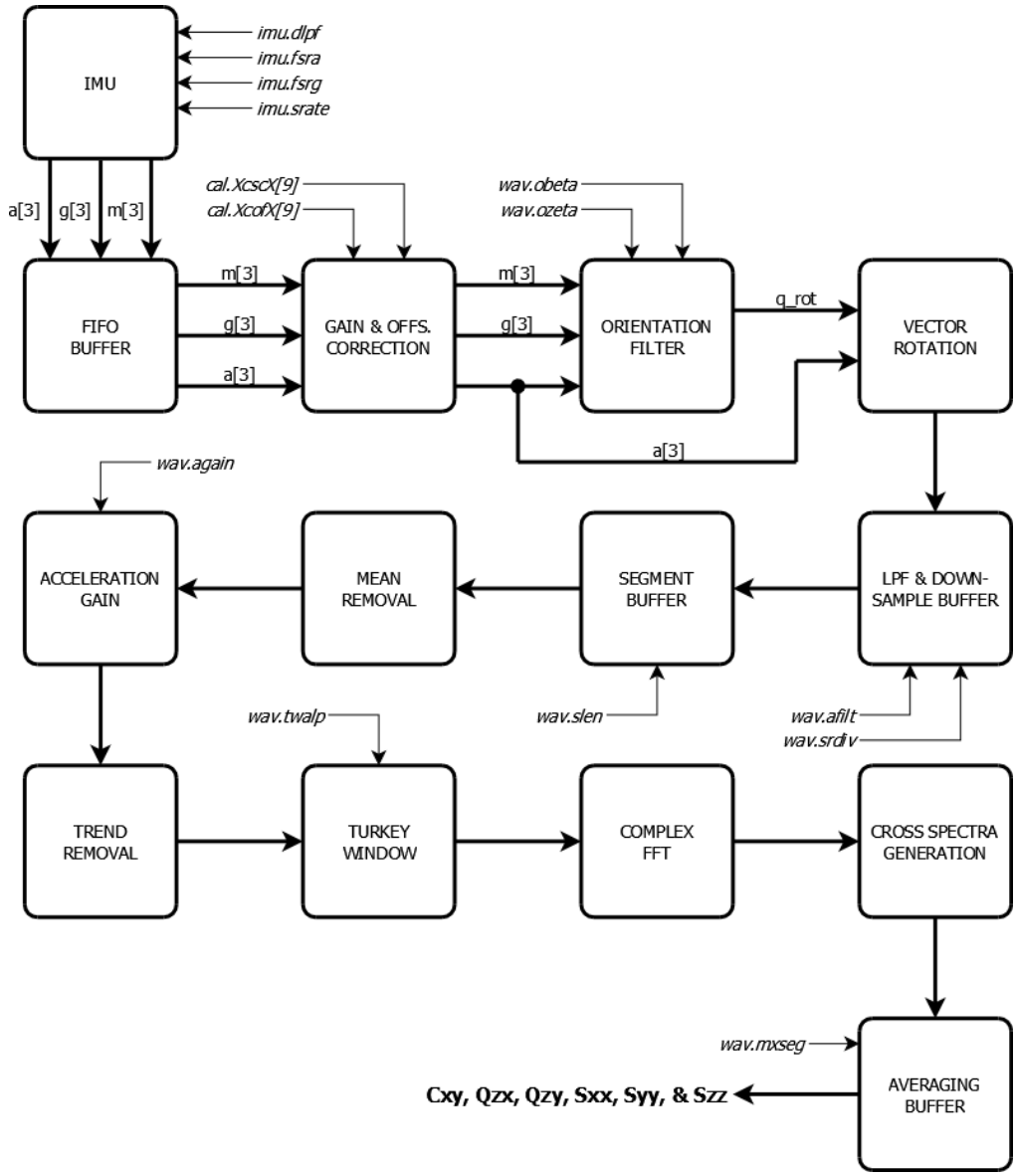
Figure 6: Primary cable assembly.



6 Operation

WIMS and its signal processing are described in U.S. Patent 12,650,303 [1]. It was developed for the Air-Launched Autonomous Micro Observer (ALAMO) profiling float [2]. A brief overview of signal processing in spectral output mode is shown in Figure 7. Samples from the IMU's accelerometer, gyroscope, and magnetometer are buffered before gain and offset corrections are applied. A gradient-descent sensor fusion algorithm is used by the orientation filter to estimate the device's orientation. That orientation estimate is used to rotate the acceleration vector from the sensor- to earth-frame.

Figure 7: Digital signal processing overview in full-spectra output mode.



After the acceleration vectors are rotated into the earth-frame, they are low-pass filtered and down-

sampled. The acceleration time-series are then divided into 50% overlapping segments. The mean is removed from each segment, a programmable gain is applied, and a linear regression is used to remove any trend. A cosine-taper Tukey window is then applied to reduce spectral leakage before a complex Fast Fourier Transform is performed. The complex amplitude spectra are then used to generate select Power- and Cross-Spectra, which are then averaged across each segment to produce the final result. In vertical spectral output mode, `wav.omode` = 4, the same processing is applied to the earth-frame vertical acceleration only, and only its power spectral density is reported.

6.1 Calibration

The calibration procedure for WIMS consists of two stages. First, a static calibration generates gain and offset corrections for the accelerometer and offset corrections for the gyroscope. The static calibration may be performed any time after assembly, before the WIMS module is installed in an instrument. The second stage of the calibration is a dynamic calibration to generate the gain and offset corrections for the magnetometer which is critical for proper operation. The magnetometer calibration must be performed after final assembly as it corrects for any residual magnetism in nearby batteries, electronics, or structures. Prior degaussing of nearby ferrous materials is not necessary, but may improve the performance of the WIMS module.

6.1.1 Accelerometer Calibration

The static calibration generates gain and offset corrections for the accelerometer. The procedure for performing the static calibration requires that the module is held in a fixed position in six different orthogonal orientations such that each of the acceleration axes are aligned vertically upward and downward, and that the average acceleration is recorded, producing a minimum and maximum acceleration for each of the three axes.

For each of the three axes, the acceleration offset coefficient value is computed from

$$a_o = 2^{(13-r_a)} \left(a_{max} + a_{min}\right), \tag{1}$$

where the acceleration radix[1], r_a, is given as a function of the configured accelerometer full-scale range, `imu.fsra`:

$$r_a = 15 - log2(\texttt{imu.fsra}) \in \{14, 13, 12, 11\}. \tag{2}$$

The acceleration gain correction coefficient is computed from

$$a_g = 2^{14} \left(1 - \frac{a_{max} - a_{min}}{2^{r_a+1}}\right). \tag{3}$$

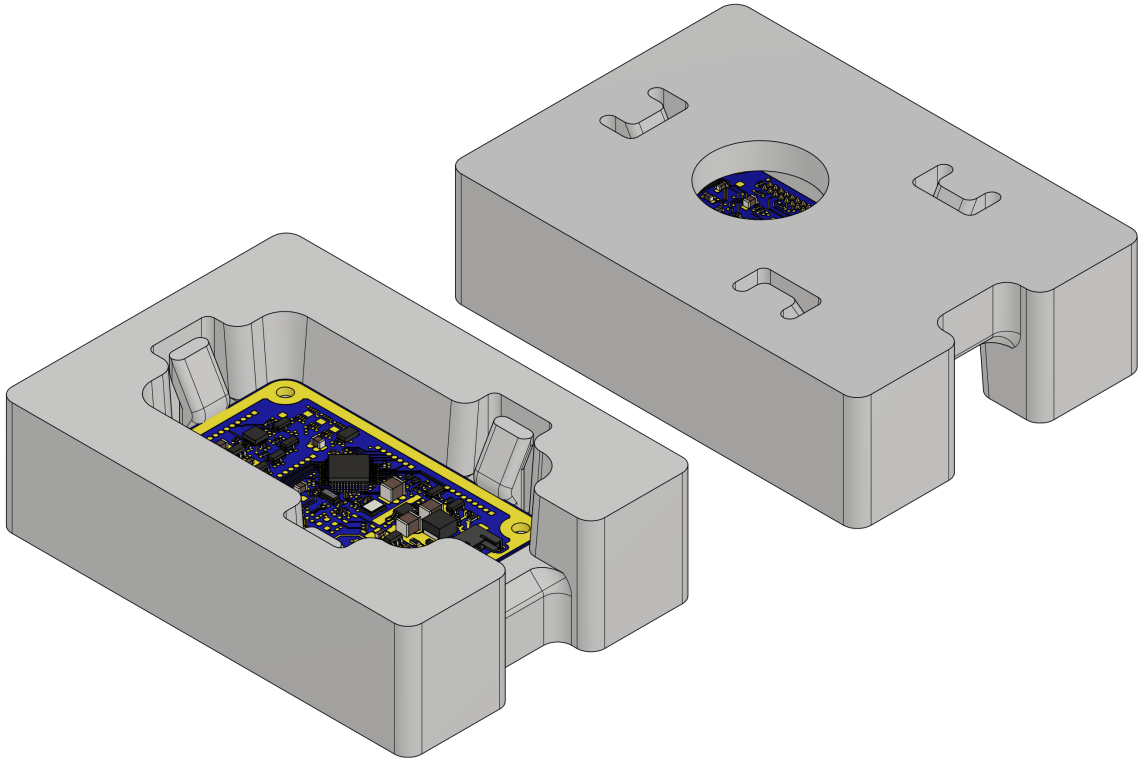
The accelerometer calibration procedure is as follows:

1. Load the saved configuration and ensure the accelerometer calibration coefficients are set to zero by issuing the following:

```
load
set cal.acofx 0
set cal.acofy 0
```

[1]The acceleration radix is the number of bits used to represent the fractional part of the fixed-point acceleration value.

Figure 8: Calibration fixture.



```
set cal.acofz 0
set cal.acscx 0
set cal.acscy 0
set cal.acscz 0
```

2. Set the full-scale range of the accelerometer to $\pm 2g$:

```
set imu.fsra 2
```

3. Disable remapping of the normally-forward and normally-upward axes (0 = none), so that the sensor axes are used directly:

```
set wav.nupax 0
set wav.nfwax 0
```

4. Set the output mode to raw counts, and set the base sample rate and divider to output 5 second time-averaged samples, then start a run:

```
set imu.srate 45
```

```
set wav.srdiv 224
set wav.omode 0
run
```

5. Using the calibration fixture shown in Figure 8, place the WIMS module on a flat, level surface with the z-axis aligned with the upward direction. Wait for the WIMS output to settle and record maximum value acceleration of the z-axis.

6. Flip the calibration fixture over so that the z-axis is aligned with the downward direction. Wait for the WIMS output to settle and record minimum value acceleration of the z-axis.

7. Repeat Items 5 and 6 for the x- and y-axes.

8. Revert changes to configuration parameters by using the `load` command or resetting or power cycling the device:

```
load
```

9. Calculate the accelerometer gain and offset coefficients using Equations (1) and (3), with the acceleration radix $r_a = 14$.

10. Set the accelerometer calibration coefficients and save the configuration parameters to EEPROM:

```
set cal.acofx XXX
set cal.acofy XXX
set cal.acofz XXX
set cal.acscx XXX
set cal.acscy XXX
set cal.acscz XXX
save
```

where the `XXX`s are replaced with the calculated scale and offset coefficients.

6.1.2 Gyroscope Calibration

The static calibration procedure for the gyroscope generates the offset calibration coefficients. The gyroscope offset calibration is critical for proper operation of the WIMS orientation filter, which is used in the calculation of acceleration spectra. While the WIMS orientation filter performs a dynamic gyroscope bias correction, the offset values are necessary to ensure that the bias estimate converges. Without them the orientation estimate may "spin", resulting in nonsensical and unrecoverable spectral data.

Gyroscope gain corrections are not typically calculated during calibration, as their measurement would require additional undeveloped procedures and fixturing for a dynamic gyroscope calibration. These calibration coefficients should be set to zero. In theory gyroscope gain corrections would improve WIMS performance. However, adequate performance can be achieved without these corrections.

The procedure for the static gyroscope calibration is as follows:

1. Load the saved configuration and ensure the gyroscope calibration coefficients are set to zero by issuing the following:

```
load
set cal.gcofx 0
set cal.gcofy 0
set cal.gcofz 0
set cal.gcscx 0
set cal.gcscy 0
set cal.gcscz 0
```

2. Ensure the gyroscope full-scale range is set to $\pm 500^{\circ}/s$:

```
set imu.fsrg 500
```

3. Disable remapping of the normally-forward and normally-upward axes (0 = none), so that the sensor axes are used directly:

```
set wav.nupax 0
set wav.nfwax 0
```

4. Set the output mode to raw counts, and set the base sample rate and divider to output 5 second time-averaged samples, then start a run:

```
set imu.srate 45
set wav.srdiv 224
set wav.omode 0
run
```

5. Using the calibration fixture shown in Figure 8, place the WIMS module on a flat, level surface such that the normally-upward facing axis is aligned with the upward direction. Wait for the WIMS output to settle and record the average values for the x-, y-, and z-axes. These values will be used as the gyroscope offset calibration coefficients.

6. Revert changes to configuration parameters by using the `load` command or resetting or power cycling the device:

```
load
```

7. Set the gyroscope offset calibration coefficients and save the configuration parameters to EEPROM.

```
set cal.gcofx XXX
set cal.gcofy XXX
set cal.gcofz XXX
save
```

6.1.3 Magnetometer Calibration

The dynamic calibration procedure generates the gain and offset corrections for the magnetometer, which are critical for proper operation. The magnetometer calibration must be performed after final assembly as it corrects for any residual magnetism in nearby batteries, electronics, or structures. Prior degaussing of nearby ferrous materials is not necessary, but may improve the performance of the WIMS module. The results of an example magnetometer calibration are shown in Figures 9 and 10.

The magnetometer calibration is performed with the mcal command:

1. Install WIMS in its final assembly, away from other magnetic disturbances.
2. Issue the mcal command.
3. Wait for the orientation filter settle time, `wav.ostsc`; samples received during this time are not used. Then slowly rotate the assembly through as many orientations as possible, so that each magnetometer axis points both toward and away from the magnetic field.
4. Send any character to end the calibration. The computed offset and scale coefficients are printed and applied to the `cal.mcof*` and `cal.mcsc*` parameters in RAM.
5. Check the coefficients with the get command, then save them with the save command. Unsaved coefficients are lost at the next reset.

Figure 9: Example magnetometer calibration - transient response.

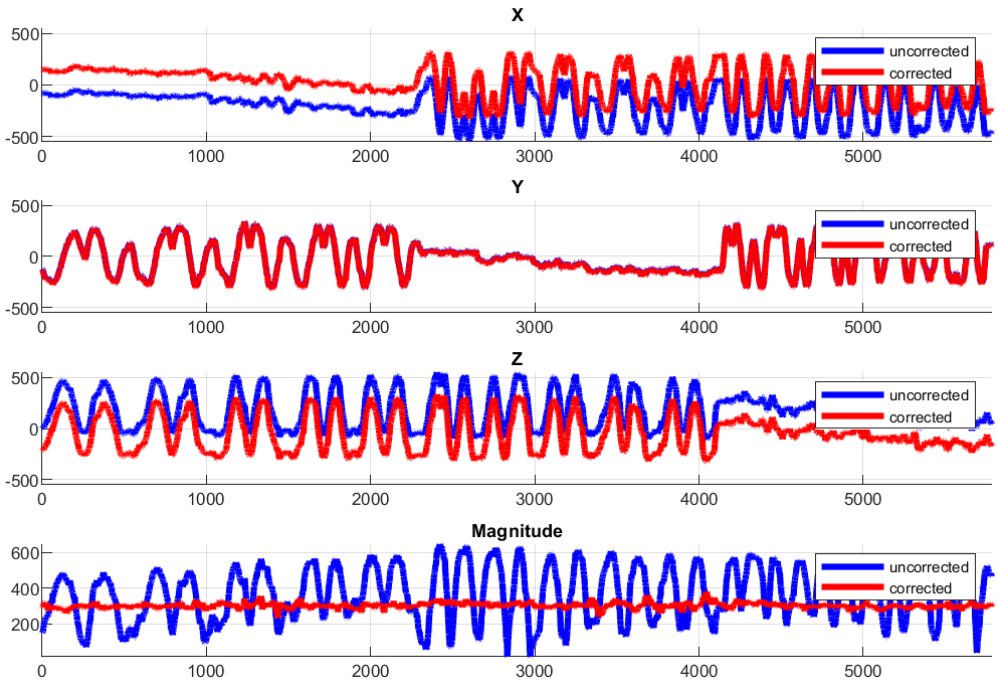
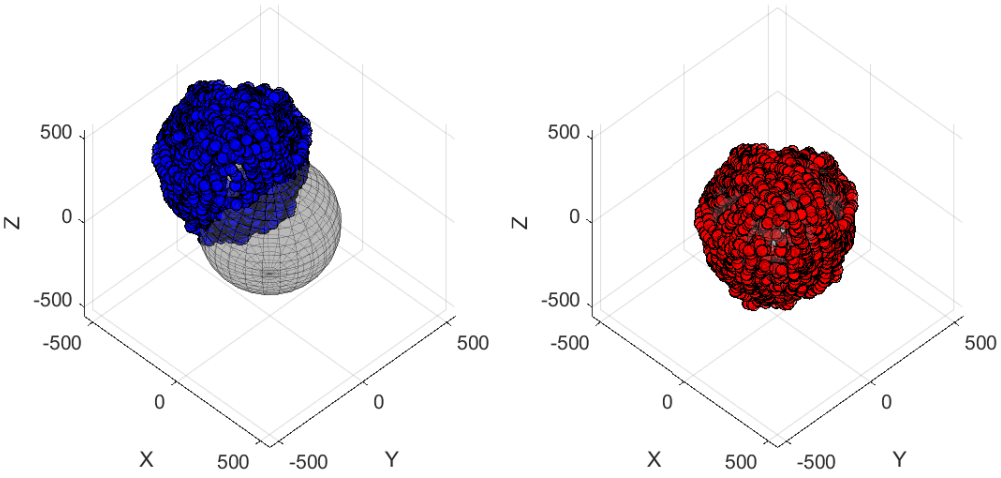


Figure 10: Example magnetometer calibration - ellipsoid fitting.



6.2 Orientation Filter

The orientation filter is used to rotate hull-fixed acceleration measurements into the Earth reference frame. The filter is based on a computationally efficient, quaternion-based gradient descent algorithm developed by Madgwick et al [3] and later improved by Wilson et al [4]. In the WIMS firmware, the filter has been uniquely implemented using only fixed-point integer arithmetic to further reduce computational complexity.

The low frequency component of measured acceleration and magnetism are combined with the high frequency component of angular rate from the gyroscope to produce a running estimate of the instruments' orientation, using a single tunable parameter, `wav.obeta`, to adjust the relative contributions of each. Additionally, the filter integrates the difference between the two components to automatically compute a gyroscope offset correction. The rate of convergence of the gyroscope offset correction is determined by the parameter `wav.ozeta`.

6.2.1 Formulation

The orientation is estimated as a unit quaternion, $\mathbf{q} = [q_0\ q_1\ q_2\ q_3]^T$, which rotates vectors from the sensor frame to the earth frame, with the x-axis pointing east, the y-axis north, and the z-axis up, referenced to magnetic north. The earth-frame acceleration is

$$[0\ \ \mathbf{a}^E] = \mathbf{q} \otimes [0\ \ \mathbf{a}^S] \otimes \mathbf{q}^*, \tag{4}$$

where $\otimes$ is the quaternion product, $\mathbf{q}^*$ is the conjugate of $\mathbf{q}$, and $\mathbf{a}^S$ is the calibrated sensor-frame acceleration, with its axes assigned by `wav.nfwax` and `wav.nupax`. The earth-frame acceleration includes gravity, $+1$ g in its vertical component. The filter is updated at every IMU sample, at the base sample rate `imu.srate`, before low-pass filtering and downsampling. At the start of each run, $\mathbf{q} = [1\ 0\ 0\ 0]^T$ and the gyroscope bias estimate is zero.

Reference vectors. At each sample k, the measured acceleration, $\mathbf{a}$, and magnetic field, $\mathbf{m}$, are normalized, and the magnetic reference vector is formed from their cross product, following Wilson et al [4]:

$$\hat{\mathbf{a}} = \frac{\mathbf{a}}{\|\mathbf{a}\|}, \qquad \hat{\mathbf{m}} = \frac{\mathbf{m}}{\|\mathbf{m}\|}, \qquad \hat{\mathbf{m}}' = \frac{\hat{\mathbf{a}} \times \hat{\mathbf{m}}}{\|\hat{\mathbf{a}} \times \hat{\mathbf{m}}\|}. \tag{5}$$

At rest, $\hat{\mathbf{a}}$ points up and $\hat{\mathbf{m}}'$ points horizontally toward magnetic west, $[-1\ 0\ 0]^T$ in the earth frame. $\hat{\mathbf{m}}'$ is orthogonal to $\hat{\mathbf{a}}$ and independent of the magnetic inclination, so magnetic disturbances affect only the heading.

Objective function. The objective function is the difference between the earth-frame up and west vectors, rotated into the sensor frame by $\mathbf{q}^* \otimes [0 \;\; \mathbf{v}] \otimes \mathbf{q}$, and the measured reference vectors:

$$\mathbf{f}(\mathbf{q}) = \begin{bmatrix} 2(q_1 q_3 - q_0 q_2) - \hat{a}_x \\ 2(q_0 q_1 + q_2 q_3) - \hat{a}_y \\ q_0^2 - q_1^2 - q_2^2 + q_3^2 - \hat{a}_z \\ -(q_0^2 + q_1^2 - q_2^2 - q_3^2) - \hat{m}'_x \\ 2(q_0 q_3 - q_1 q_2) - \hat{m}'_y \\ -2(q_0 q_2 + q_1 q_3) - \hat{m}'_z \end{bmatrix}, \tag{6}$$

with Jacobian

$$\mathbf{J}(\mathbf{q}) = 2 \begin{bmatrix} -q_2 & q_3 & -q_0 & q_1 \\ q_1 & q_0 & q_3 & q_2 \\ q_0 & -q_1 & -q_2 & q_3 \\ -q_0 & -q_1 & q_2 & q_3 \\ q_3 & -q_2 & -q_1 & q_0 \\ -q_2 & -q_3 & -q_0 & -q_1 \end{bmatrix}. \tag{7}$$

The normalized gradient of the objective function, which is the direction of the orientation error, is

$$\nabla \mathbf{f} = \mathbf{J}^T(\mathbf{q}_{k-1})\, \mathbf{f}(\mathbf{q}_{k-1}), \qquad \hat{\nabla} \mathbf{f} = \frac{\nabla \mathbf{f}}{\|\nabla \mathbf{f}\|}. \tag{8}$$

Gyroscope bias. The gyroscope bias is estimated, as in Madgwick et al [3], by integrating the angular rate error implied by the orientation error:

$$[0 \;\; \boldsymbol{\omega}_{\epsilon,k}] = 2\, \mathbf{q}^*_{k-1} \otimes \hat{\nabla} \mathbf{f}, \qquad \boldsymbol{\omega}_{b,k} = \zeta\, \Delta t \sum_{j \le k} \boldsymbol{\omega}_{\epsilon,j}, \tag{9}$$

where ζ is `wav.ozeta`, and each component of the sum is limited to $\pm 2^{14}$ rad/s. If $\zeta = 0$, the bias is not estimated. The estimate of the previous sample is subtracted from the measured angular rate, $\boldsymbol{\omega}$, in rad/s:

$$\dot{\mathbf{q}}_\omega = \frac{1}{2}\, \mathbf{q}_{k-1} \otimes [0 \;\; \boldsymbol{\omega}_k - \boldsymbol{\omega}_{b,k-1}]. \tag{10}$$

Fusion and update. The rate of change of the orientation combines the angular rate with a step of size β, `wav.obeta`, against the gradient, and is integrated over the sample period:

$$\dot{\mathbf{q}} = \dot{\mathbf{q}}_\omega - \beta\,\hat{\nabla}\mathbf{f}, \qquad \mathbf{q}_k = \frac{\mathbf{q}_{k-1} + \dot{\mathbf{q}}\,\Delta t}{\|\mathbf{q}_{k-1} + \dot{\mathbf{q}}\,\Delta t\|}. \tag{11}$$

The sample period, Δt, is initially $1/$`imu.srate`, and is measured from the IMU sample timestamps every 1024 samples, as the elapsed time of the last 1024 samples divided by 1024.

Settling. For the first 30 seconds of each run, the angular rate is ignored, $\dot{\mathbf{q}}_\omega = 0$, the step size is $\beta = 0.41$ instead of `wav.obeta`, and the gyroscope bias is not updated, so that the orientation converges quickly from the acceleration and magnetic field alone. Spectral processing begins only after the settle time `wav.ostsc`.

Fixed-point implementation. All quantities are fixed-point integers: the quaternion with radix 14, its rate of change with radix 12, the angular rate and gyroscope bias with radix 11, $\mathbf{f}$, $\mathbf{J}$, and $\nabla\mathbf{f}$ with radix 14, β and ζ with radix 15, and Δt, in seconds, with radix 18. Intermediate products are computed in 32- or 64-bit arithmetic and saturated to 16 bits.

6.3 Reset Behavior

WIMS Reset behavior is the same for either software reset or power-on reset. On reset:

1. Drivers and modules are initialized.
2. A newline is printed to the serial interface.
3. Splash text and version information are printed to the serial interface by invoking the vers command.
4. Attempts to load configuration parameter from non-volatile memory (EEPROM) by invoking the load command. If an error occurs, or EEPROM is otherwise unavailable, default configuration parameters are loaded.
5. If the STARTUP_MODE_BIT_RUN bit is set in the run.smode configuration parameter:
    - A run is immediately initiated by invoking the run command. See Section 6.4: Run Behavior for details.
6. Until the device is shutdown:
    - The command prompt is printed to the serial interface, and the device enters the idle state while awaiting command input from serial interface. When a command delimiter is received, the input is processed and the command is executed.

Listing 1: Serial interface output on reset when STARTUP_MODE_BIT_RUN is not set.

```
# ================================================================================
#    _       ________  _______
#   | | /| / /  _/  |/  / __/  Wave-field Inertial Measurement System
#   | |/ |/ // // /|_/ /\ \     v2.01.00617b (RELEASE)
#   |__/|__/___/_/  /_/___/     A. Ekholm, WHOI
#
# ================================================================================
vers 2.01.00617b (RELEASE)
# Initializing...
# Loading Configuration...
>
```

6.4 Run Behavior

Typical output of a run with the default configuration parameters is shown below. With the default run options, `run.rmode` = 0, the configuration parameters and run information are not printed before the run. The spectral values shown are placeholders.

Listing 2: Typical run output.

```
> run;
# [OUT][WAVDRV] sampling...
# ------------------------------------------------------------------------
#   idx     freq      Cxy      Qzx      Qzy      Sxx      Syy      Szz
# - - - - - - - - - - - - - - - - - - - - - - - - - - - - - - - - - - - -
s[    0, 0.0000,       0,       0,       0,       0,       0,       0 ];
s[    1, 0.0195,       0,       0,       0,       0,       0,       0 ];
s[    2, 0.0391,       0,       0,       0,       0,       0,       0 ];
s[    3, 0.0586,       0,       0,       0,       0,       0,       0 ];
s[    4, 0.0781,       0,       0,       0,       0,       0,       0 ];
s[    5, 0.0977,       0,       0,       0,       0,       0,       0 ];
s[    6, 0.1172,       0,       0,       0,       0,       0,       0 ];
s[    7, 0.1367,       0,       0,       0,       0,       0,       0 ];
s[    8, 0.1563,       0,       0,       0,       0,       0,       0 ];
s[    9, 0.1758,       0,       0,       0,       0,       0,       0 ];
s[   10, 0.1953,       0,       0,       0,       0,       0,       0 ];
s[   11, 0.2148,       0,       0,       0,       0,       0,       0 ];
s[   12, 0.2344,       0,       0,       0,       0,       0,       0 ];
s[   13, 0.2539,       0,       0,       0,       0,       0,       0 ];
s[   14, 0.2734,       0,       0,       0,       0,       0,       0 ];
s[   15, 0.2930,       0,       0,       0,       0,       0,       0 ];
s[   16, 0.3125,       0,       0,       0,       0,       0,       0 ];
s[   17, 0.3320,       0,       0,       0,       0,       0,       0 ];
s[   18, 0.3516,       0,       0,       0,       0,       0,       0 ];
s[   19, 0.3711,       0,       0,       0,       0,       0,       0 ];
s[   20, 0.3906,       0,       0,       0,       0,       0,       0 ];
s[   21, 0.4102,       0,       0,       0,       0,       0,       0 ];
s[   22, 0.4297,       0,       0,       0,       0,       0,       0 ];
s[   23, 0.4492,       0,       0,       0,       0,       0,       0 ];
s[   24, 0.4688,       0,       0,       0,       0,       0,       0 ];
s[   25, 0.4883,       0,       0,       0,       0,       0,       0 ];
# ------------------------------------------------------------------------
# [OUT][WAVDRV] done sampling
>
```

6.4.1 Run Duration

The duration of a run is limited by time to reach the maximum number of samples, `wav.mxsam`. The duration, in seconds, to reach the maximum number of samples is

$$T_{max,sam} = \begin{cases} \texttt{wav.mxsam}/f_e & \texttt{wav.mxsam} > 0 \\ \infty & \texttt{wav.mxsam} = 0 \end{cases}, \tag{12}$$

where the effective sample rate, f_e is defined by the base sample rate, imu.srate, the sample rate divider, wav.srdiv, and the IMU clock frequency tolerance, Δf_{IMU}, by

$$f_e = \frac{\texttt{imu.srate} \times (1 + \Delta f_{IMU})}{\texttt{wav.srdiv} + 1} \qquad Hz. \tag{13}$$

In most cases, it is acceptable to assume an IMU clock frequency tolerance of $\Delta f_{IMU} = 0\%$.

In spectral output mode, the total run duration is limited by the time to reach the maximum number of segments. The time to reach the maximum number of segments, in seconds, is a function of the orientation filter settle time, wav.ostsc, segment length, wav.slen, and the number of segments, wav.mxseg, such that

$$T_{max,seg} = \begin{cases} \texttt{wav.ostsc} + \frac{(\texttt{wav.mxseg}+1)\times\texttt{wav.slen}}{2f_e} & \texttt{wav.mxseg} > 0 \\ \infty & \texttt{wav.mxseg} = 0 \end{cases}. \tag{14}$$

The total expected run time, in seconds, is then given by

$$T_{run} = T_{init} + \begin{cases} T_{max,sam} & \text{non-spectral output mode} \\ min\left(T_{max,sam},\ T_{max,seg}\right) & \text{spectral output mode} \end{cases}, \tag{15}$$

where the initialization time is $T_{init} \approx 2$ seconds, and the IMU clock frequency tolerance is assumed to be $\Delta f_{IMU} = 0\%$. The maximum and minimum possible run times can similarly calculated, assuming the worst case for the IMU frequency tolerance of $\Delta f_{IMU} = \pm 2\%$.

6.5 Low-power Shutdown

WIMS includes circuitry to provide low-power shutdown capability. During low-power shutdown, less than $0.1\mu A$ of quiescent current will be drawn by the device.

At any point while the state is idle, if the ENABLE pin is de-asserted for more than $100ms$, then the device will automatically power off by invoking the shutdown command.

The preferred procedure for low-power shutdown is:

1. Issue shutdown command.
2. Wait 100ms for buffer flushing and driver deinitialization.
3. De-assert ENABLE pin.
4. De-assert or pull-down all digital I/O pins for duration of shutdown.



7 Spectral Data Processing

WIMS reports power- and cross-spectral densities. Derived wave field parameters are computed shore-side from these spectra, as described in this section.

7.1 Naming Conventions

WIMS axis naming (subscripts x, y, and z) differ from NDBC naming conventions (subscripts 1, 2, and 3) for readability. WIMS naming conventions are as follow (with NDBC naming convention in parentheses):

x (= 2) east-west displacement, with x-axis pointing east

y (= 3) north-south displacement, with y-axis pointing north

z (= 1) wave elevation i.e. vertical displacement, with z-axis pointing upward

7.2 Spectra Frequencies

The frequency of each spectra bin is given by

$$f_n = \frac{n}{2N} f_e, \qquad n \in \{0, 1, \dots, N-1\}, \tag{16}$$

where N is the spectra length, equal to one half of the segment length, `wav.slen`, and f_e is the effective sample rate defined in Equation (13). Bin $n = 0$ is the DC (zero-frequency) bin of the Fourier transform. The bandwidth of each bin is given by

$$\Delta f_n = \frac{1}{2N} f_e. \tag{17}$$

> **NOTE:** *Firmware versions up to and including v2.01.00614b, and v1.x, label bin n with frequency $(n+1)f_e/2N$, one bin higher than the frequency of the spectral density it holds. Only the frequency labels are affected; the spectral values are unchanged. Spectra from these versions are processed shore-side with the frequencies of Equation (16). See Section 7.7.1: Decoding.*

The range of spectra bins reported is limited to the maximum, f_{max}, and minimum, f_{min}, bin frequencies specified by parameters `wav.fbmax` and `wav.fbmin`, respectively, such that frequencies of the reported bins satisfy the relationship

$$f_{min} \le \frac{n}{2N} f_e \le f_{max}, \tag{18}$$

where

$$f_{max} = \begin{cases} 10^{-3} \times \texttt{wav.fbmax} & \texttt{wav.fbmax} > 0 \\ \infty & \texttt{wav.fbmax} = 0 \end{cases} \tag{19}$$

and

$$f_{min} = 10^{-3} \times \texttt{wav.fbmin}. \tag{20}$$

Therefore, the indices of the reported frequency bins are

$$\hat{n} = \left\{ \left\lceil 2N \frac{f_{min}}{f_e} \right\rceil, \dots, min\left(N-1, \left\lfloor 2N \frac{f_{max}}{f_e} \right\rfloor\right) \right\}. \tag{21}$$

7.3 Scale Sensitivity

WIMS spectra are reported as counts: the auto-spectra, S_{xx}, S_{yy}, and S_{zz}, as `uint16`, saturated to the range $[0, 65535]$, and the cross-spectra, C_{xy}, Q_{zx}, and Q_{zy}, as `int16`, saturated to the range $[-32768, 32767]$. The spectral densities of each segment are saturated to these ranges before they are averaged, and the averages are saturated again. For the default configuration, the largest values, 65535 and 32767 counts, correspond to $0.47\ g^2/Hz$ and $0.23\ g^2/Hz$ (Equation (23)). To convert to scientific units, the counts are divided by the effective spectral sensitivity scale factor, G_s. The scale factor is a function of the accelerometer full-scale range, `imu.fsra`, the acceleration software gain, `wav.gaina`, the effective sample rate, f_e, defined in Equation (13), the segment length, `wav.slen`, and the Tukey window parameter, `wav.twalp`.

The base spectral sensitivity scale factor, the square of the number of accelerometer counts per g, is given by

$$G_{sb} = 2^{2r_a} = 2^{30-2log_2(\texttt{imu.fsra})} \qquad LSB^2/g^2, \tag{22}$$

where r_a is the acceleration radix defined in Equation (2).

The effective spectral sensitivity scale factor is given by

$$G_s = G_{sb} \times G_{sa}^2 \times \frac{U f_e^2}{2 \times \texttt{wav.slen}^2} \qquad LSB/\left(g^2/Hz\right), \tag{23}$$

where G_{sa} is the acceleration software gain, defined as

$$G_{sa} = \begin{cases} 2^{-3} \times \texttt{wav.gaina} & \texttt{wav.gaina} > 0 \\ 1 & \texttt{wav.gaina} = 0 \end{cases} \qquad g/g, \tag{24}$$

and U is the mean square of the Tukey window applied by the firmware. The window tapers L samples at each end of the segment with a half cosine, $w_j = \frac{1}{2}\left[1 - cos(\pi j/L)\right]$ for $j < L$, symmetrically at the other end, and $w_j = 1$ elsewhere, where

$$L = \left\lfloor \frac{(\texttt{wav.slen} - 1) \times \texttt{wav.twalp}}{256} \right\rceil \tag{25}$$

is rounded to the nearest integer, with halves rounded up. Its mean square is

$$U = \frac{1}{\texttt{wav.slen}} \sum_{j=0}^{\texttt{wav.slen}-1} w_j^2 = \begin{cases} 1 - \frac{5L/4+1}{\texttt{wav.slen}} & L > 0 \\ 1 & L = 0 \end{cases}. \tag{26}$$

The approximation $U \approx 1 - \frac{5}{8}\alpha$, with $\alpha = 2^{-7} \times \texttt{wav.twalp}$, exceeds the exact value by about $1/\texttt{wav.slen}$, 0.4% for the default segment length and window.

The last factor of Equation (23) arises because the complex FFT scales its output by $1/\texttt{wav.slen}$, the

firmware scales each product of Fourier amplitudes by $f_e/\texttt{wav.slen}$, the reported spectra are one-sided, and the window reduces the signal power by the factor U. The scale factor was verified by simulating the firmware processing of white noise of known spectral density, which agreed with Equation (23) to within the 1% statistical uncertainty of the simulation for effective sample rates of 2.5 and 5 Hz, segment lengths of 256 and 512, and `wav.twalp` of 0, 64, and 128. For the default configuration (`imu.fsra` $= 4$, `wav.gaina` $= 32$, $f_e = 5\ Hz$, `wav.slen` $= 256$, and `wav.twalp` $= 64$, so that $L = 64$ and $U = 0.68359$), $G_s = 140000\ LSB/(g^2/Hz)$. For $f_e = 2.5\ Hz$ and otherwise the same configuration, $G_s = 35000\ LSB/(g^2/Hz)$.

7.4 Converting from Acceleration to Displacement Spectra

WIMS natively reports acceleration cross- and power-spectral densities, in units of g^2/Hz. However, for the purpose of scientific analysis, cross- and power-spectral densities are desired in units of m^2/Hz.

The conversion follows from the Fourier representation of the motion. Let the displacement along one axis, $\eta(t)$, have Fourier amplitude $\hat{\eta}(f)$ at frequency f, so that the frequency component is $\hat{\eta}(f)e^{i2\pi ft}$. Differentiating twice with respect to time gives the acceleration, in m/s^2,

$$\hat{a}(f) = (i2\pi f)^2\hat{\eta}(f) = -(2\pi f)^2\hat{\eta}(f). \tag{27}$$

A spectral density is proportional to the expected product of a Fourier amplitude and the complex conjugate of another, $S_{pq}(f) \propto E[\hat{p}(f)\hat{q}^*(f)]$. Since the factor $-(2\pi f)^2$ is real and common to all axes, the acceleration and displacement spectral densities are related by

$$S_{accel,pq}(f) = (2\pi f)^4 S_{disp,pq}(f), \tag{28}$$

for the auto-spectra, S_{xx}, S_{yy}, and S_{zz}, and, with no change of phase, for the co- and quadrature spectra, C_{xy}, Q_{zx}, and Q_{zy}. WIMS reports acceleration in units of g, so that the acceleration in m/s^2 is g times the reported value and its spectral density is g^2 times the reported spectral density. Combining the two, at each bin frequency, f_n,

$$S_{disp}(f_n) = \frac{g^2}{(2\pi f_n)^4} \times S_{accel}(f_n) \qquad \frac{m^2}{Hz}, \tag{29}$$

where S_{accel} is in g^2/Hz and g is the acceleration due to gravity ($\approx 9.80665\ m/s^2$). The factor $(2\pi f_n)^{-4}$ amplifies low-frequency noise strongly, which is why the post-processing removes the lowest frequencies (Section 7.7.2: Post-Processing Steps). The bin at $f_n = 0$ has no displacement equivalent.

7.5 Directional Spectra

The directional wave spectrum is given by

$$S(f,\theta) = S_{zz}(f)D(f,\theta), \tag{30}$$

where S_{zz} is the vertical displacement (heave) power-spectral density and $D(f,\theta)$ is the directional spreading function, which is estimated from the first two pairs of directional Fourier coefficients as [5]

$$D(f,\theta) = \frac{1}{\pi}\left[\frac{1}{2} + r_1 cos(\theta - \theta_1) + r_2 cos\left(2[\theta - \theta_2]\right)\right]. \tag{31}$$

Because WIMS measures wave elevation and horizontal displacement, rather than surface slopes, the normalized directional Fourier coefficients are computed directly from the displacement spectra, without the wavenumber, as for other buoys that measure the three components of the wave orbital motion [6]:

$$a_1 = \frac{Q_{zx}}{\sqrt{S_{zz}(S_{xx}+S_{yy})}}, \quad b_1 = \frac{Q_{zy}}{\sqrt{S_{zz}(S_{xx}+S_{yy})}}, \quad a_2 = \frac{S_{xx}-S_{yy}}{S_{xx}+S_{yy}}, \quad b_2 = \frac{2C_{xy}}{S_{xx}+S_{yy}}, \tag{32}$$

where the x-axis points east and the y-axis points north. The conversion from acceleration to displacement spectra cancels in these ratios, so the coefficients may equally be computed from the acceleration spectra. The directional spreading parameters are

$$r_1 = \sqrt{a_1^2 + b_1^2} \qquad \text{and} \qquad r_2 = \sqrt{a_2^2 + b_2^2}, \tag{33}$$

both in the range $[0,1]$. The mean wave direction, θ_1, is given by

$$\theta_1 = arctan2(a_1, b_1), \tag{34}$$

where $arctan2$ is the two-input, four-quadrant arctangent function. The second-order coefficients, a_2 and b_2, depend only on the horizontal auto- and cross-spectra, which are unchanged when the direction of propagation is reversed. They therefore give only the principal axis,

$$\theta_2' = \frac{1}{2}arctan2(b_2, -a_2), \tag{35}$$

which is unique only modulo $180°$. The principal wave direction, θ_2, is taken as the end of this axis nearest the mean wave direction,

$$\theta_2 = \begin{cases} \theta_2' & \cos(\theta_2' - \theta_1) \geq 0 \\ \theta_2' + 180° & \cos(\theta_2' - \theta_1) < 0 \end{cases}. \tag{36}$$

This resolves the axis correctly when the waves at a frequency come predominantly from one direction.

When two wave systems at the same frequency propagate in opposite directions, or θ_1 is poorly defined (small r_1), the end of the axis chosen may be wrong.

> **NOTE:** *Wave directions are clockwise angles, and give the direction **toward** which the waves propagate, not the direction from which they come. Add 180° to θ_1 or θ_2 to obtain the direction from which the waves come. Both are reported in the range $[0^\circ, 360^\circ)$. The spectra reported by WIMS are referenced to magnetic north; the shore-side processing corrects the directions for the magnetic declination, so that the reported directions are referenced to true north (see Section 7.7.2: Post-Processing Steps).*

The direction convention follows from the definition of the quadrature spectra computed by the WIMS firmware, $Q_{zx} = \Im\{ZX^*\}$ and $Q_{zy} = \Im\{ZY^*\}$, where Z, X, and Y are the complex Fourier amplitudes of the earth-frame vertical (up), east, and north accelerations. For a wave propagating toward the east, for example, the horizontal displacement lags the elevation by 90°, so that $Q_{zx} > 0$, $Q_{zy} = 0$, and $\theta_1 = 90^\circ$.

7.6 Derived Wave Parameters

Spectral moments are given by [5]

$$m_i = \sum_{n=1}^{N-1} f_n^i S_{zz}(f_n) \Delta f_n, \qquad i \in \{0, 1, 2\}, \tag{37}$$

where f_n are the frequency bins and Δf_n is the bandwidth of each bin, defined in Equations (16) and (17), and S_{zz} is the vertical displacement spectral density. The DC bin, $n = 0$, is excluded, as the conversion from acceleration to displacement is undefined at $f_0 = 0$.

Significant wave height is defined as function of the zeroth moment by [5]

$$H_{m_0} = 4\sqrt{m_0}. \tag{38}$$

The peak, or dominant period, is given by [5]

$$T_p = \frac{1}{f_p}, \qquad max[S_{zz}(f)] = S_{zz}(f_p). \tag{39}$$

The average period is given by [5]

$$\bar{T} = \frac{m_0}{m_1}. \tag{40}$$

The zero-crossing period is given by [5]

$$T_0 = \sqrt{\frac{m_0}{m_2}}. \tag{41}$$

7.7 Shore-Side Data Validation and Post-Processing

The spectra reported by WIMS are relayed by the float controller in Iridium messages, decoded on shore, and then validated and post-processed by the `xmtps` data processing software (class `Wave`, method `PostProcess()`, in `FloatClasses.py`). This subsection describes the processing applied by that software. The numerical parameters given are those used by the current version of the software.

7.7.1 Decoding

Each of the six spectral components (S_{zz}, S_{yy}, S_{xx}, C_{xy}, Q_{zx}, and Q_{zy}) is sent in a separate wave message. The message header contains the segment length, N, the base sample rate, `imu.srate`, the sample rate divider, `wav.srdiv`, the accelerometer full-scale range, `imu.fsra`, the acceleration software gain, `wav.gaina`, and the index of the first bin in the message. Auto-spectra are sent as unsigned 16-bit counts and cross-spectra as signed 16-bit counts.

The decoder converts counts to acceleration spectral densities, in g^2/Hz, by dividing by the effective spectral sensitivity scale factor, G_s, defined in Equation (23), computed from the message header fields, and assigns each bin the frequency given by Equation (16), in which bin 0 is the DC bin. Bins that are not received are left undefined.

Some float firmware versions send only every other spectral bin, with the first half of the bins holding the spectrum at twice the bin spacing and the second half zero. For these, the decoder doubles the effective sample rate, so that the bin spacing is f_e/N and bin n has frequency nf_e/N.

7.7.2 Post-Processing Steps

The acceleration spectra of each dive are processed as follows. The spectra as received are retained alongside the processed spectra.

1. **Interpolation.** All six acceleration spectra are linearly interpolated onto a uniform frequency grid from 0.030 Hz to 1.250 Hz in steps of $\Delta f = 0.005$ Hz. Grid frequencies outside the band of received bins, or between undefined bins, are set to zero.

2. **Noise floor.** At grid frequencies where the vertical acceleration spectrum, S_{zz}, is below 0.0005 g^2/Hz, all six acceleration spectra are set to zero.

3. **Low-frequency response correction.** All six acceleration spectra are multiplied by an empirically determined cosine taper, $S'(f) = S(f)\,T(f)$, where

$$T(f) = \begin{cases} 0 & f < f_0 \\ \frac{1}{2}\left[1 - \cos\left(\frac{\pi(f-f_0)}{w}\right)\right] & f_0 \le f \le f_0 + w \\ 1 & f > f_0 + w \end{cases} \tag{42}$$

with the coefficients given in Table 13. The correction factor rises smoothly from 0.004 at the lowest grid frequency, 0.030 Hz, to 1 at $f_0 + w \approx 0.116$ Hz, above which the spectra are left unchanged, as shown in Figure 13. Because the noise floor and the correction scale all six spectra alike, they leave the directional coefficients, Equation (32), and the ratio of horizontal to vertical energy essentially unchanged (the coefficients are undefined where the spectra are zero), and r_1 does not exceed 1. Applied to the vertical spectrum only, as in earlier versions of the software, they inflated r_1 and that ratio wherever the correction is below 1 or S_{zz} was set to zero. The derivation of the coefficients is described in Section 7.8: Low-Frequency Response Correction.

Table 13: Low-frequency response correction coefficients.

Coefficient	Value	Unit
f_0	0.02622	Hz
w	0.08951	Hz

> **NOTE:** *The low-frequency response correction was determined for WIMS installed in ALAMO floats, and applies only to that platform. It may not be applicable to WIMS installed on other platforms, whose motion response, mounting, and noise differ.*

4. **Conversion to displacement.** All six spectra are converted from acceleration to displacement spectral densities, in m^2/Hz, as described in Section 7.4: Converting from Acceleration to Displacement Spectra.

5. **Smoothing.** Each displacement spectrum is smoothed with a centred three-point running mean. The ends of the spectrum are zero-padded.

6. **Validation.** The spectra of the dive are rejected if any of the criteria in Table 14 is met. When the spectra are rejected, all six displacement spectra are discarded, and no wave parameters are reported for that dive.

7. **Wave parameters.** The spectral moments, m_0, m_1, and m_2, are computed as in Section 7.6: Derived Wave Parameters, summing over the whole interpolated frequency grid with bin width $\Delta f = 0.005$ Hz. S_{zz} is never negative, so $m_0 \geq 0$; if $m_0 = 0$, the spectra are rejected. Otherwise, the significant wave height, H_{m_0}, the peak period, T_p, the average period, $\bar{T}$, and the zero-crossing period, T_0, are computed. The peak frequency is the grid frequency with the largest smoothed vertical displacement spectral density, so T_p is resolved to the 0.005 Hz grid spacing.

8. **Directional parameters.** The directional Fourier coefficients, a_1, b_1, a_2, and b_2, the spreading parameters, r_1 and r_2, and the mean and principal wave directions, θ_1 and θ_2, are computed at each frequency as described in Section 7.5: Directional Spectra. The bulk mean wave direction is the circular mean of θ_1 over 0.0625 Hz to 0.6 Hz, weighted by $\sqrt{S_{zz}}$. Since the WIMS firmware does not correct for the magnetic declination, the declination (east positive) from IGRF-14 [7], at the GPS fix at the end of the profile, is added to all directions, which are then referenced to true north; the declination applied is stored with the data. For a dive without a valid position, the most recent earlier valid position of the float is used; if there is none, the directions remain magnetic, as indicated in the data. Directions give the direction toward which the waves propagate, rounded to whole degrees in $[0, 360)$.

9. **Output.** The acceleration spectra stored are those of step 1, before the noise floor and the low-frequency response correction, which are applied in the conversion to displacement; the rejection criteria are evaluated on them. The processed data for each dive are stored with frequencies rounded to 0.001 Hz, acceleration spectra to 0.0001 g^2/Hz, displacement spectra to 0.001 m^2/Hz, directional coefficients to four decimal places, and directions to whole degrees. The data are then aggregated per float into wave parameter and wave spectra files.

Table 14: Spectra rejection criteria.

Criterion	Description
Low-frequency acceleration noise	Any interpolated acceleration auto-spectrum (S_{zz}, S_{yy}, or S_{xx}) exceeds 0.09 g^2/Hz at or below 0.05 Hz.
Acceleration out of range	Any interpolated acceleration auto-spectrum exceeds 0.3 g^2/Hz at any frequency.
Displacement out of range	Any smoothed displacement auto-spectrum exceeds 300 m^2/Hz, or the vertical displacement spectrum is undefined, at or above 0.0625 Hz.
No wave energy	The zeroth spectral moment, m_0, is zero.

7.8 Low-Frequency Response Correction

The coefficients of the low-frequency response correction, Equation (42), were determined by intercomparison of WIMS vertical acceleration spectra with colocated reference spectra during Hurricane Erin (2025) and Hurricane Lowell (2026). The correction is shown in Figure 13.

> **NOTE:** *The WIMS spectra used were from ALAMO floats deployed with firmware versions earlier than v2.01.00617b, which are the versions of the ALAMO floats deployed to date, with the configurations of Table 15. The correction applies to spectra from these floats. It has not been evaluated for firmware v2.01.00617b and later, whose trend removal for segment lengths of 512 and 1024, and default effective sample rate, differ (Section 12: Firmware Change Log), and should be verified for floats deployed with them.*

7.8.1 Data

The data sets are listed in Table 15. The NDBC spectra were obtained from the National Data Buoy Center, which processes them as described by [5]. The A-DWSD drifters are air-deployable versions of the Directional Wave Spectra Drifter [6]; their spectra and positions were obtained from the Lagrangian Drifter Laboratory of the Scripps Institution of Oceanography [8], [9]. A-DWSD spectra with zero energy, or whose significant wave height differs from the median of those of the same drifter within 3 hours before and after (at least two spectra) by more than a factor of $e^{0.5} \approx 1.65$, are excluded as outliers: 48 of the 3299 Erin spectra and 57 of the 17682 Lowell spectra. They are isolated increases, by factors of up to 18 and to significant wave heights of up to 48 m, that are not seen by the drifters nearby at the same time, and most have 10% to 50% of their energy below 0.05 Hz. The quality flag reported with the drifter data is not used, as its lower values are associated with high sea states rather than with these spectra. The storm tracks and wind radii are the best tracks of the National Hurricane Center [10], which for Hurricane Erin are those of its Tropical Cyclone Report [11]. The time and position of each WIMS spectrum are those of the profile position determined by the `xmtps` software, from the GPS fix at the end of the profile or, for the few profiles without one, from the Iridium position; spectra without either are not used. The positions are shown in Figures 11 and 12.

7.8.2 Method

1. **Colocation.** A WIMS spectrum and a reference spectrum are colocated if they are within the limits of Table 16, and their positions are in the same quadrant of the same storm (front or rear, right or left of its direction of motion), within 600 km of its center, or both more than 600 km from the center of every storm, so that both measured the same part of the wave field (Section 7.8.4:

Figure 11: Hurricane Erin and the intercomparison data sets: (a) best track of Hurricane Erin [11], with the position every 6 hours colored by Saffir-Simpson category, the area shown in (b) (rectangle), and NDBC buoy 41047 (star); (b) positions of the WIMS spectra, the A-DWSD drifter spectra, and NDBC buoy 41047, with the 220 km colocation radius around the buoy, the track of Hurricane Erin, and the extent of the 34, 50, and 64 kt winds (outlines) at the closest approach of the storm to the floats, over the GOES-19 band 13 infrared image of that hour (brightness temperature from 190 K, white, to 305 K, black) [12]; (c) distance of the ALAMO floats, of NDBC buoy 41047, and of the A-DWSD drifters (grey dots) from the center of the storm, with the mean radii of the 34, 50, and 64 kt winds, and the maximum sustained wind of the storm. Float 9302, which had no GPS fixes during the passage of the storm, is not shown in (c).

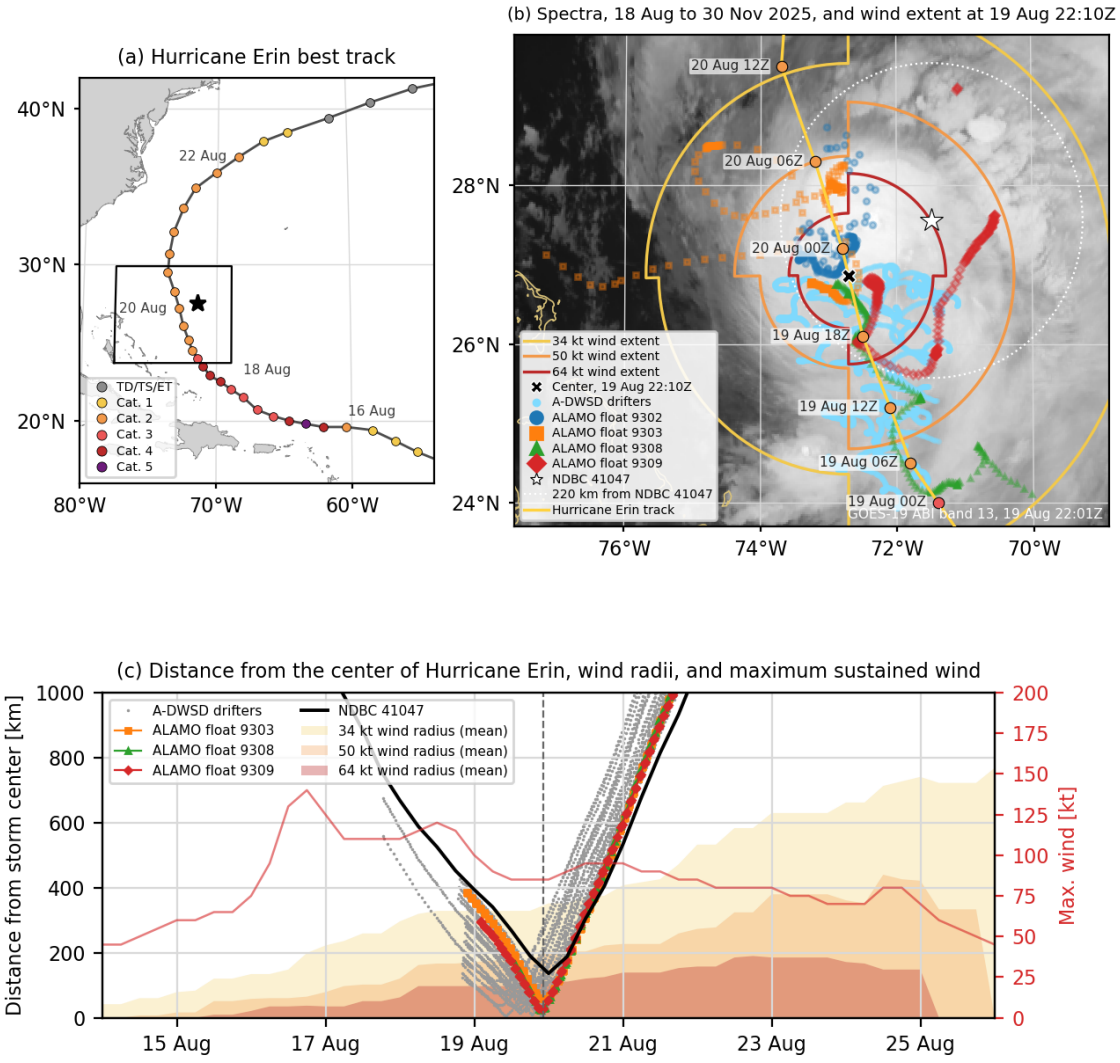


Figure 12: Hurricane Lowell and the intercomparison data sets: (a) best track of Hurricane Lowell [10], with the position every 6 hours colored by Saffir-Simpson category, and the area shown in (b) (rectangle); (b) positions of the WIMS spectra and the A-DWSD drifter spectra, with the track of Hurricane Lowell, labelled every 12 hours, and the extent of the 34, 50, and 64 kt winds (outlines) at the closest approach of the storm to the floats, over the GOES-18 band 13 infrared image of that hour (brightness temperature from 190 K, white, to 305 K, black) [12]; (c) distance of the ALAMO floats and of the A-DWSD drifters (grey dots) from the center of the storm, with the mean radii of the 34, 50, and 64 kt winds, and the maximum sustained wind of the storm.

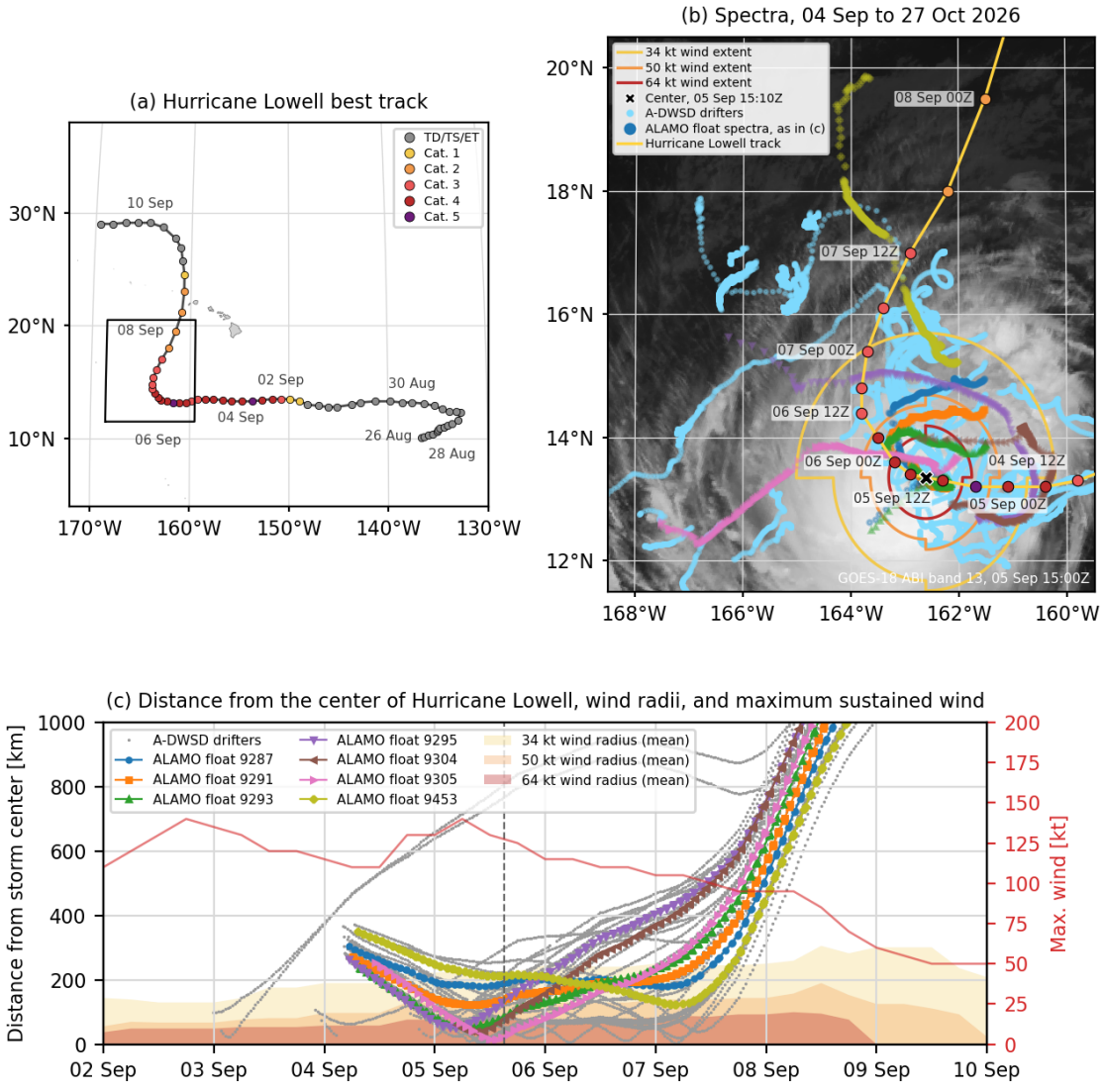


Table 15: Intercomparison data sets. The WIMS segment length was 256, except for floats 9287 and 9291 (512).

Data set	Period	Spectra	Sampling
Hurricane Erin			
WIMS floats 9302, 9303, 9308, and 9309	2025 Aug 18 – Nov 30	739	$f_e = 2.5$ Hz
NDBC buoy 41047 (27.557 N, 71.480 W)	2025 Aug 3 – Oct 30	3697	0.033 to 0.485 Hz, every 30 min
A-DWSD drifters (22)	2025 Aug 17 – Aug 24	3299	0.031 to 0.492 Hz, 0.0078 Hz spacing
Hurricane Lowell			
WIMS floats 9287, 9291, 9293, 9295, 9304, 9305, and 9453	2026 Sep 4 – Oct 31	2238	$f_e = 2.5$ Hz; 5 Hz (9287, 9291)
A-DWSD drifters (45)	2026 Sep 2 – Oct 28	17682	0.031 to 0.492 Hz, 0.0078 Hz spacing

Storm-Relative Position). The center and the direction of motion of the storm at the time of each spectrum are those of a cubic spline through the best track positions. The storms are all those of the NHC best tracks [10] of the Atlantic in 2025 and of the eastern and central Pacific in 2026, which include Hurricanes Humberto, Imelda and Melissa during the NDBC 41047 data of Erin. A WIMS spectrum may be colocated with more than one reference spectrum.

2. **Spectra.** The WIMS acceleration spectra, with the frequencies of Equation (16) and the scale factor of Equation (23), are processed as in steps 1 and 2 of Section 7.7.2: Post-Processing Steps, and spectra rejected by the acceleration criteria of Table 14 are excluded. The WIMS and reference spectra are interpolated onto a common grid from 0.040 Hz to 0.480 Hz in steps of 0.001 Hz, and the reference displacement spectra are converted to acceleration spectra (Section 7.4: Converting from Acceleration to Displacement Spectra).

3. **Per-bin scale factors.** At each grid frequency, the scale factor, $s(f)$, is the ratio of the mean reference to the mean WIMS acceleration spectral density of the colocated pairs. The ratio of the means is not biased by the decorrelation of spectra measured apart, unlike a regression through the origin, and is less sensitive to the few outliers than the median ratio.

4. **Correction fit.** The cosine taper, Equation (42), is fitted by non-linear least squares to the per-bin scale factors of all three data sets combined, up to 0.15 Hz.

5. **Evaluation.** The significant wave height of each pair is computed from the displacement spectra over the common grid, with and without the correction.

Table 16: Colocation criteria and colocated pairs in the same storm quadrant or both more than 600 km from the center of the storm, after rejection of WIMS spectra and of the A-DWSD outliers.

Data set	Time limit	Distance limit	Pairs	WIMS spectra	Median distance
Erin, NDBC 41047	30 min	220 km	791	440	158 km
Erin, A-DWSD	60 min	50 km	873	126	34 km
Lowell, A-DWSD	60 min	50 km	9674	613	27 km

7.8.3 Results

The fitted coefficients are those of Table 13, with a root-mean-square residual of 0.051. The per-bin scale factors are small at the lowest frequencies, where WIMS acceleration noise, amplified by the conversion to displacement, exceeds the wave signal, and rise to about one at 0.11 Hz (Figure 13). From 0.06 Hz to 0.1 Hz, the scale factors of the A-DWSD drifters of the two storms agree closely, and the median ratio of NDBC 41047 is only slightly higher, but its ratio of the means reaches about 1.3 near 0.09 Hz. Because the ratio of the means is dominated by the pairs of highest energy, this excess comes from a minority of pairs, and it is consistent with the location of the buoy relative to the storm: in the highest sea states, the buoy was in the right quadrants of the storm, up to 220 km from the floats, where the median ratio of WIMS to NDBC significant wave height is 0.82 to 0.91 (Section 7.8.4: Storm-Relative Position). The platforms are not expected to contribute much in this band, as waves 160 m to 430 m long are long compared with both the buoy and the float; their different responses appear above about 0.12 Hz (Section 7.8.6: Limitations). Below 0.055 Hz, where the wave signal is weak in both spectra, the ratio of the means of the Lowell drifters remains at about 0.15 to 0.25, while those of the Erin data sets fall to 0.1 and below, and the median ratios are 0.1 to 0.2 for the drifters and near zero for the NDBC buoy. In this range, the scale factors depend on the noise floors and sensitivities of the WIMS and reference sensors, and on the amount of long-period swell, which differed between the storms.

The differences of the colocated vertical acceleration spectra, without and with the correction, are shown in Figures 14 to 16. With the correction, the median difference from the A-DWSD drifters is within $0.0030\ g^2/Hz$ from 0.06 Hz to 0.12 Hz, and that from the NDBC buoy within $0.0003\ g^2/Hz$. Above about 0.12 Hz, the WIMS spectral densities are increasingly lower than those of the A-DWSD drifters, and higher than those of the NDBC buoy (Section 7.8.6: Limitations).

The significant wave heights of the colocated pairs are compared in Table 17 and Figure 17. With the correction, the mean WIMS significant wave height agrees with that of the A-DWSD drifters to within 1.6% for both storms, and the median ratios are 1.01 for both. Relative to the NDBC buoy, the mean ratio is 0.94, but the median ratio is 1.00: the difference is in the highest sea states, when the buoy was on the right side of the storm.

Figure 13: Per-bin scale factors, reference / WIMS, of the three data sets, as (a) the ratio of the means, with that of all data sets combined, and (b) the median ratio, and the adopted correction factor, $T(f)$.

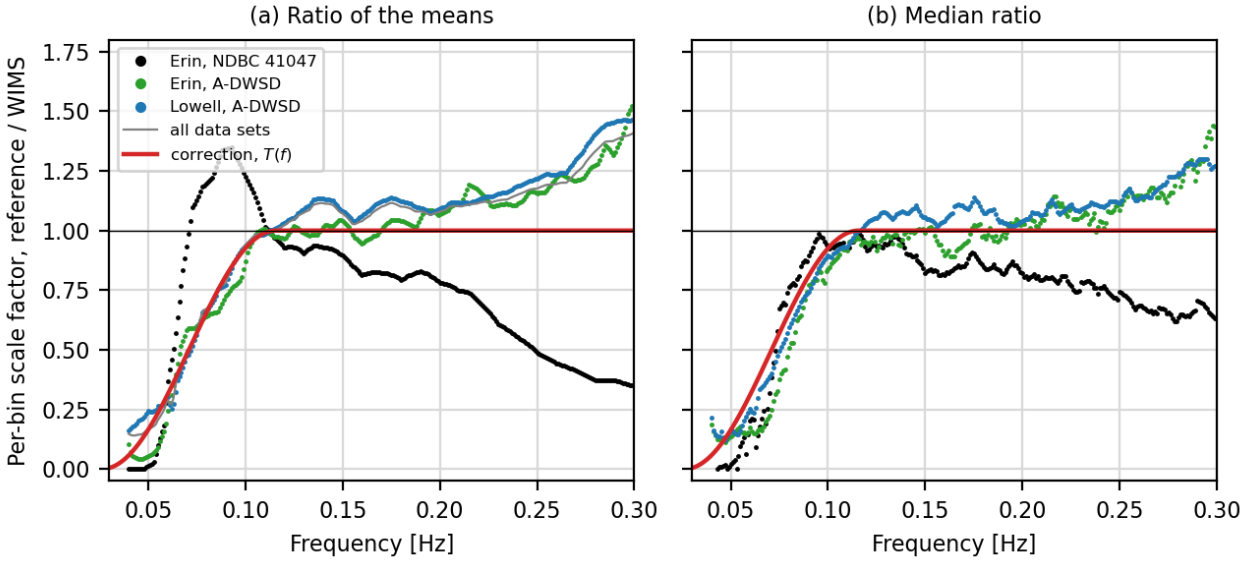


Figure 14: Colocated NDBC 41047 during Hurricane Erin: difference of each pair of vertical acceleration spectra, WIMS minus NDBC, without and with the correction, as the median and interquartile range, and the mean.

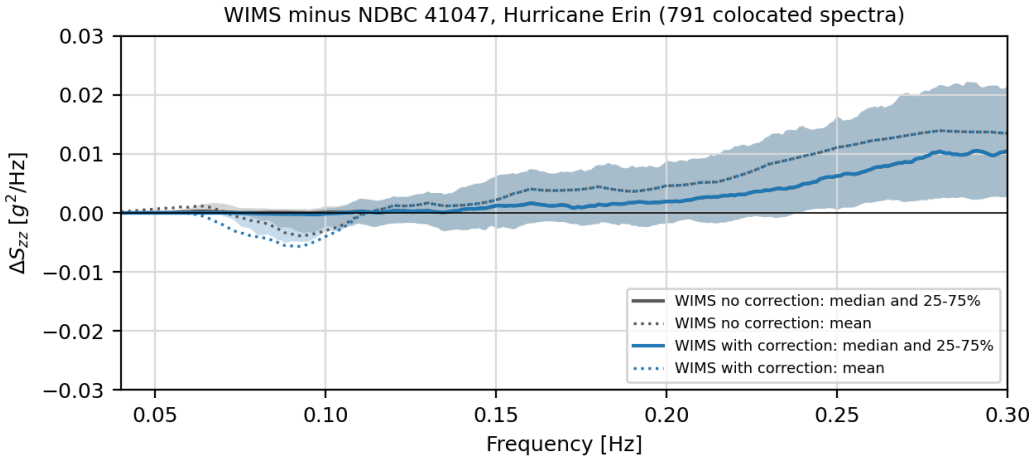


Figure 15: Colocated A-DWSD drifters during Hurricane Erin: difference of each pair of vertical acceleration spectra, WIMS minus A-DWSD, without and with the correction, as the median and interquartile range, and the mean.

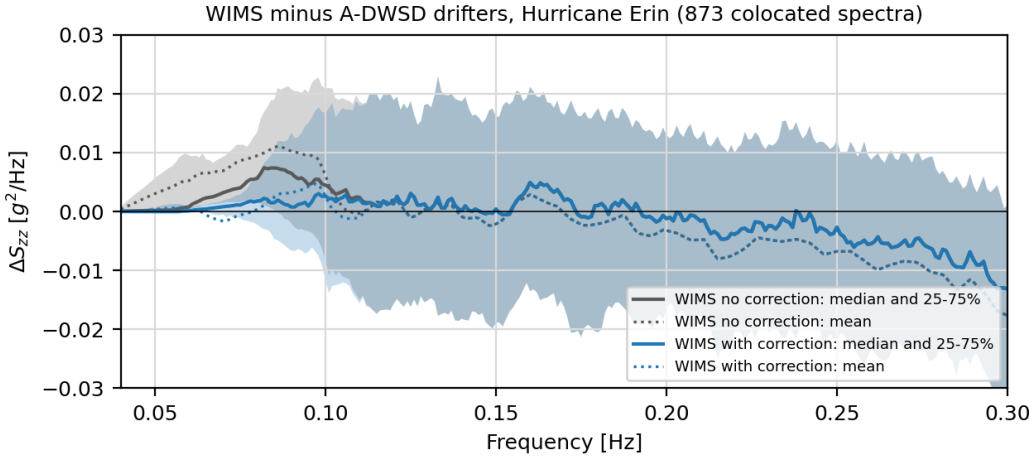


Figure 16: Colocated A-DWSD drifters during Hurricane Lowell: difference of each pair of vertical acceleration spectra, WIMS minus A-DWSD, without and with the correction, as the median and interquartile range, and the mean.

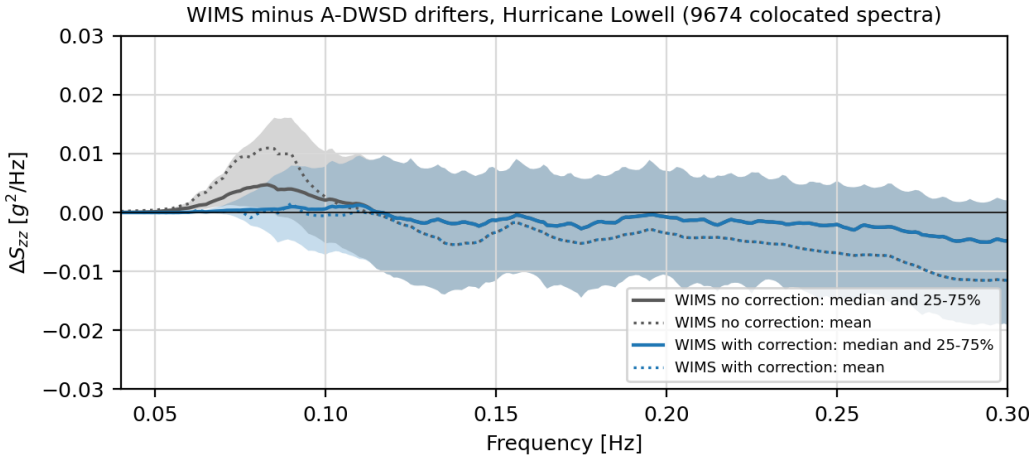
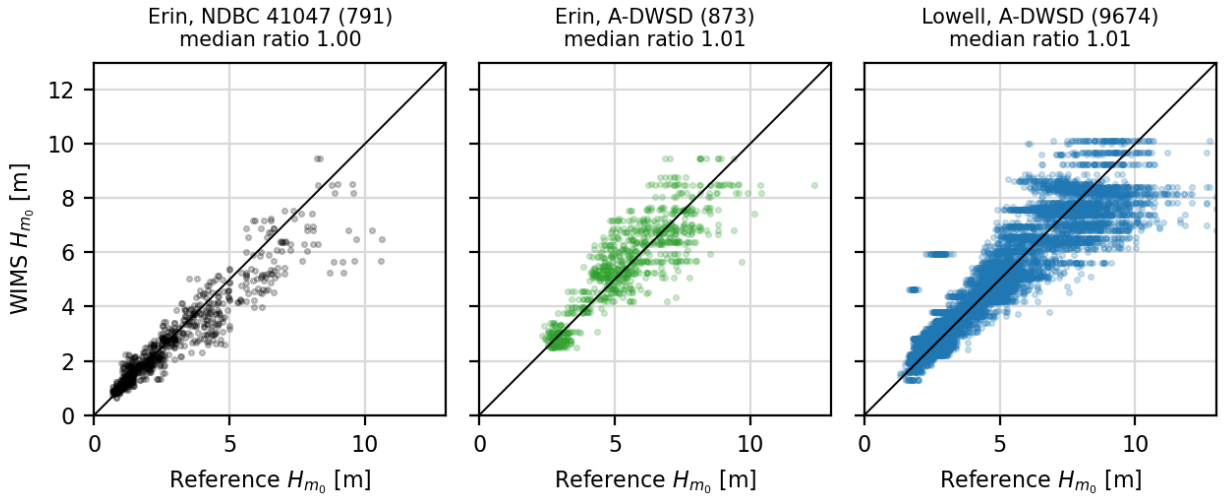


Table 17: Significant wave height of colocated WIMS and reference spectra, from 0.04 Hz to 0.48 Hz. Bias and RMS are of the WIMS minus the reference value. The ratio is that of the mean values; the median ratio is $\exp(\text{median}(\ln(H_{m0,\text{WIMS}}/H_{m0,\text{ref}})))$.

Data set	Correction	Pairs	Bias [m]	RMS [m]	Ratio	Median ratio
Erin, NDBC 41047	none	791	+0.26	0.91	1.09	1.11
	adopted	791	-0.18	0.73	0.94	1.00
Erin, A-DWSD	none	873	+1.17	1.77	1.22	1.19
	adopted	873	+0.09	0.90	1.02	1.01
Lowell, A-DWSD	none	9674	+0.69	1.37	1.14	1.13
	adopted	9674	-0.01	0.90	1.00	1.01

Figure 17: Significant wave height of colocated WIMS and reference spectra, with the adopted correction. The horizontal rows of points are WIMS spectra colocated with several drifters.



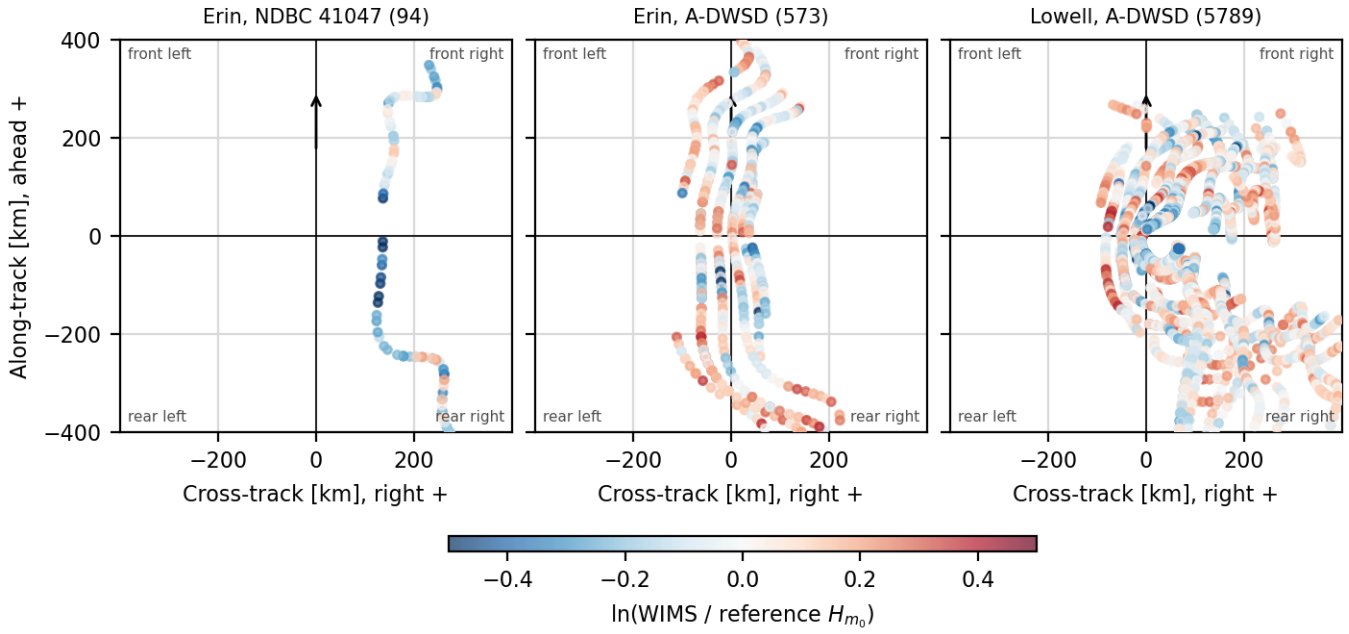
7.8.4 Storm-Relative Position

The colocated spectra are up to 50 km (A-DWSD) and 220 km (NDBC) apart, in wave fields that vary strongly around the storm, and the waves are highest to the right of the track (in the northern hemisphere). Table 18 and Figure 18 give the agreement by the quadrant of the storm, relative to its direction of motion on the cubic spline through the best track positions, in which the reference was, for references within 600 km of the center of the storm.

Table 18: Median ratio of WIMS to reference significant wave height, with the adopted correction, by the storm quadrant of the WIMS and reference positions, with the number of pairs. Quadrants are within 600 km of the center of the storm. The 33 NDBC 41047 pairs in the same quadrant of Hurricane Imelda or Melissa, not shown, have a median ratio of 0.90.

Data set	Front left	Front right	Rear left	Rear right	Outside
Erin, NDBC 41047	–	0.91 (42)	–	0.82 (58)	1.03 (658)
Erin, A-DWSD	1.02 (132)	0.97 (190)	1.14 (110)	1.03 (235)	1.00 (206)
Lowell, A-DWSD	1.02 (164)	1.00 (3023)	0.98 (295)	1.00 (2726)	1.03 (3466)

Figure 18: Storm-relative positions of the references within 400 km of the center of the storm, along and across its track (cubic spline through the best track positions), colored by the logarithm of the ratio of WIMS to reference significant wave height, with the adopted correction, with the number of pairs. The arrow is the direction of motion of the storm.



NDBC buoy 41047 was only on the right side of Hurricane Erin, 130 km to 350 km from the track, where

the colocated WIMS floats, up to 220 km away in a different part of the wave field of the storm, read 9% to 18% lower than the buoy. Outside the storm, WIMS agrees with the buoy (median ratio 1.03). The A-DWSD drifters, which were closer to the floats, agree with WIMS to within about 5% in most quadrants of both storms. The low NDBC ratios are therefore attributed to the separation of the buoy and the floats across the storm, not to the measurements. For this reason the correction is fitted to the per-bin scale factors of all three data sets combined, 93% of whose pairs are A-DWSD pairs, and not to the NDBC buoy alone. Consistently, the A-DWSD significant wave height is 11% lower than that of the NDBC buoy for the 380 pairs of A-DWSD and NDBC spectra within 30 minutes and 100 km of each other.

The corrected significant wave heights and the mean wave directions of the swell and of the wind waves of all the WIMS spectra of the two storms, not only those colocated with a reference, are shown in the same storm-relative frame in Figures 19 to 21. The swell and the wind waves are separated at 0.10 Hz (10 s), within the band of the bulk mean wave direction, 0.06 Hz to 0.25 Hz (Section 7.9: Wave Direction Validation). Near the center of the storm, wind waves longer than 10 s are counted as swell.

Figure 19: Storm-relative positions of the WIMS spectra within 400 km of the center of the storm, along and across its track, colored by the WIMS significant wave height, with the adopted correction. The arrow is the direction of motion of the storm.

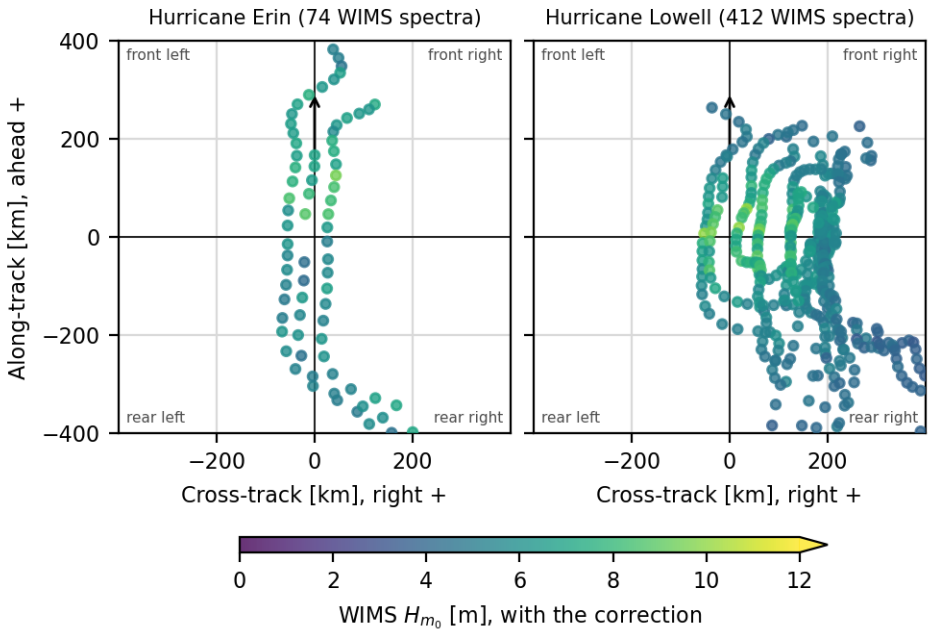


Figure 20: Storm-relative positions of the WIMS spectra within 400 km of the center of the storm, along and across its track, colored by the WIMS mean swell direction, 0.06 Hz to 0.10 Hz, toward which the waves propagate, relative to the direction of motion of the storm (up).

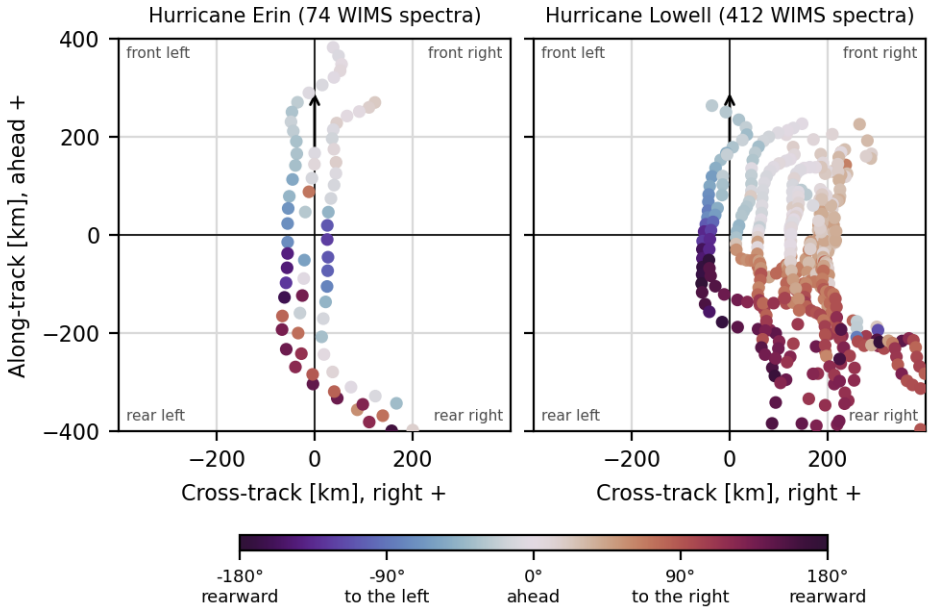
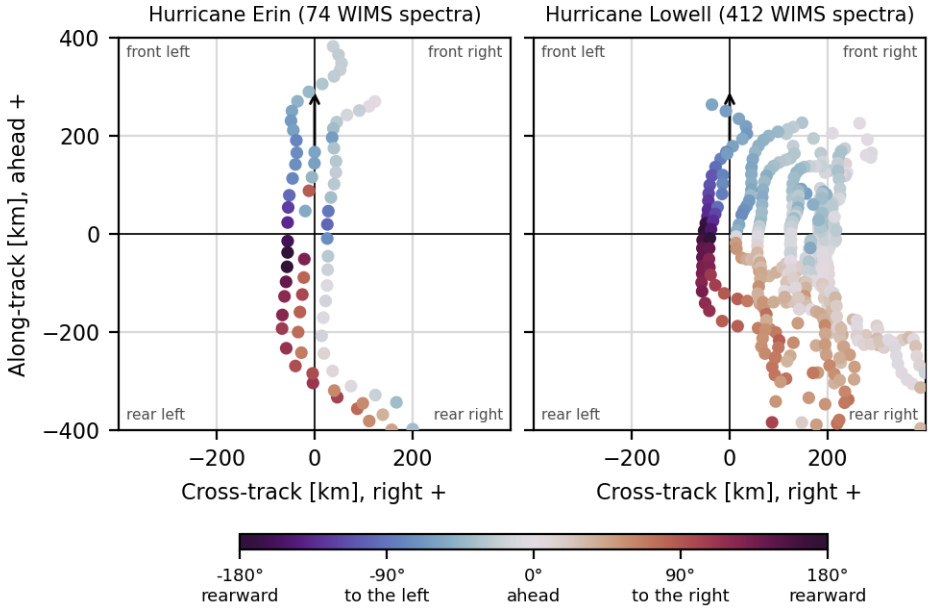


Figure 21: Storm-relative positions of the WIMS spectra within 400 km of the center of the storm, along and across its track, colored by the WIMS mean wind-wave direction, 0.10 Hz to 0.25 Hz, toward which the waves propagate, relative to the direction of motion of the storm (up).



7.8.5 Rejection Criteria Evaluation

The rejection criteria of Table 14 were evaluated with the adopted correction, for all the WIMS spectra of both storms, including the rejected ones, against all three data sets. For each criterion, Table 19 gives the spectra rejected and the agreement of the kept and dropped pairs, as the percentage of outliers, pairs whose significant wave height ratio is outside 0.61 to 1.65 ($|\ln(H_{m0,\mathrm{WIMS}}/H_{m0,\mathrm{ref}})| > 0.5$).

Table 19: Evaluation of rejection criteria, for the 2977 WIMS spectra of both storms and their 11699 colocated pairs with all three data sets, in the same storm quadrant or both outside the storm, without the A-DWSD outliers. Low-frequency criteria are the maximum acceleration spectral density at or below 0.05 Hz, for the axes given.

Criterion	Spectra rejected	Kept outliers	Dropped outliers	Dropped median ratio
None	0 (0%)	2.4%	–	–
Current criteria (Table 14)	98 (3.3%)	0.4%	55%	2.00
Low-frequency, vertical only, $> 0.09\ g^2/Hz$	28 (0.9%)	1.9%	75%	2.71
Low-frequency, horizontal only, $> 0.09\ g^2/Hz$	89 (3.0%)	1.0%	59%	2.20
Current criteria, low-frequency $> 0.05\ g^2/Hz$	147 (4.9%)	0.3%	42%	1.43
Current criteria, low-frequency $> 0.07\ g^2/Hz$	119 (4.0%)	0.4%	51%	1.70
Low-frequency, all axes, $> 0.12\ g^2/Hz$	70 (2.4%)	1.0%	63%	2.24
Low-frequency, all axes, $> 0.2\ g^2/Hz$	38 (1.3%)	1.8%	66%	2.55
Current criteria and $\lvert\ln K\rvert > 0.5$	675 (22.7%)	0.2%	21%	1.17

The evaluation shows that:

- The current criteria are effective. They reject 3.3% of the spectra, more than half of whose pairs are outliers, with WIMS significant wave heights twice those of the references (median), and reduce the outliers of the kept pairs from 2.4% to 0.4%. The low-frequency noise criterion makes most of the rejections, mainly through the horizontal axes; the acceleration and displacement limits and the zeroth moment criterion add a few.
- Thresholds of $0.05\ g^2/Hz$ to $0.12\ g^2/Hz$ give similar agreement for the kept pairs. A threshold of $0.05\ g^2/Hz$ slightly reduces the outliers, but rejects 50% more spectra, half of them of float 9308,

and 88% of the pairs of the additional spectra are not outliers. The threshold of $0.09\ g^2/Hz$ is retained.

- A check on the ratio of horizontal to vertical displacement energy from 0.07 Hz to 0.30 Hz, $K = \sum(S_{xx} + S_{yy})/\sum S_{zz}$, which is one for linear waves in deep water, reduces the outliers further, but rejects nearly a quarter of the spectra, most of which agree with the references. It is not adopted.

7.8.6 Limitations

- The correction is fitted only up to 0.15 Hz, and is 1 above $f_0 + w \approx 0.116$ Hz. Above about 0.12 Hz, the WIMS vertical spectral densities are lower than those of the A-DWSD drifters and higher than those of the NDBC buoy, increasingly with frequency (Figure 13). These differences are likely due to the different sizes of the platforms, which respond differently to the shorter waves: the A-DWSD drifter is a small surface follower, the NDBC buoy a large hull, and the ALAMO float probably behaves more like a spar buoy for these waves. They are not attributed to WIMS, and the correction does not model them.

- Below about 0.055 Hz, the scale factors of the two storms differ, 0.1 and below for Erin and 0.15 to 0.25 for Lowell (Figure 13), and the fitted correction, 0.004 at 0.030 Hz and 0.16 at 0.050 Hz, lies between them. The correction is least certain there, which matters most for spectra with much of their energy below 0.06 Hz, such as long-period swell with peak periods longer than about 17 s.

- Floats 9287 and 9291, with a segment length of 512, ran firmware with the trend removal error corrected in v2.01.00617b, which left most of the linear trend in each segment. The power of the remaining trend is almost entirely below 0.055 Hz, where it adds to the WIMS spectra of these two floats; its effect on the Lowell scale factors below 0.055 Hz has not been evaluated separately.

- The colocated spectra are measured apart in wave fields that vary strongly around the storms, which accounts for most of the scatter in Figure 17 (Section 7.8.4: Storm-Relative Position).

- The coefficients of Table 13 were fitted to the 11338 colocated pairs, without the A-DWSD outliers, in the same quadrant of the same storm, of all the storms active during the deployments, or both more than 600 km from the center of every storm. Fitted to all 12047 pairs without the outliers, the coefficients are $f_0 = 0.02410$ Hz and $w = 0.09296$ Hz, and the correction factor differs by at most 0.016, below 0.06 Hz, with the significant wave height statistics of each data set within 0.01 m in bias and RMS, and 0.003 in median ratio. The A-DWSD outliers affect the correction more: although only 0.3% of the pairs, they raise the scale factors below about 0.07 Hz, because the ratio of the means is dominated by the pairs of highest energy. With them, the coefficients are $f_0 = 0.02035$ Hz and $w = 0.09764$ Hz for the pairs in the same quadrant, and

$f_0 = 0.01671$ Hz and $w = 0.10308$ Hz for all pairs; revisions 3.20 and earlier used $f_0 = 0.01445$ Hz and $w = 0.10457$ Hz, fitted to all pairs with the outliers.

- The correction is fitted to the vertical spectrum only, and applied to all six spectra alike (Section 7.7.2: Post-Processing Steps). Whether the horizontal spectra need a correction of their own has not been determined. The correction does not change the directional Fourier coefficients, which are compared with those of the reference instruments in Section 7.9.1: Directional Fourier Coefficients and Spreading Parameters.
- All WIMS data used were from WIMS installed in ALAMO floats. The correction may not be applicable to other platforms.

7.9 Wave Direction Validation

The WIMS wave directions were validated against NDBC buoy 41047 and the A-DWSD drifters during Hurricane Erin, and against the A-DWSD drifters during Hurricane Lowell, with the colocations of Table 16 and the adopted correction. The WIMS mean wave directions, θ_1 (Equation (34)), are processed as in Section 7.7.2: Post-Processing Steps, and referenced to true north. The reference directions, the NDBC mean wave direction, α_1, and the A-DWSD direction $\arctan 2(b_1, a_1)$, are directions from which the waves come, referenced to true north, and $180°$ was added to both. The A-DWSD convention reproduces the dominant wave direction reported by the drifters to within $0.1°$ for both storms.

Only pairs whose WIMS and reference positions were in the same quadrant of the storm (front or rear, right or left of its direction of motion), within 600 km of the center, or both more than 600 km from the center, were used, as in Section 7.8.4: Storm-Relative Position, so that both measured the same part of the wave field; the pairs with the positions in different quadrants are excluded. The bulk mean wave direction of each pair, from 0.06 Hz to 0.25 Hz, is the circular mean of θ_1, weighted by the vertical displacement spectral density. The differences are summarized in Table 20, given by storm quadrant, and for the pairs outside the storm, in Table 21, and shown in Figure 22. The bias is the circular mean of the difference, WIMS minus reference.

Table 20: WIMS bulk mean wave direction, 0.06 Hz to 0.25 Hz, compared with the reference directions, for the pairs in the same storm quadrant or both outside the storm.

Data set	Pairs	Bias	Median |difference|	Within $30°$
Erin, NDBC 41047	791	$+11°$	$27°$	54%
Erin, A-DWSD	873	$-6°$	$22°$	61%
Lowell, A-DWSD	9674	$-2°$	$13°$	79%

The validation shows that:

- The direction convention is correct: an error in the convention or in the sign of the quadrature spectra would give differences of about $180°$.
- Relative to the A-DWSD drifters, which were closest to the floats (median distance 27 km to 34 km), the bias is $-2°$ for Lowell and $-6°$ for Erin, and the median difference at each frequency is within about $7°$ of zero from 0.07 Hz to 0.25 Hz. For Lowell, half of the bulk directions differ by less than $13°$, and 79% by less than $30°$.
- The agreement depends on the storm quadrant (Table 21). It is best in the front right quadrant of Lowell, where most of the pairs are: half of the bulk directions differ by less than $7°$, and 95% by less than $30°$. The largest biases, $-38°$ (Erin, rear right) and $+30°$ (Lowell, rear left), are in the rear quadrants, where the wave field is the most complex. Pairs whose positions are in different

Table 21: WIMS bulk mean wave direction, 0.06 Hz to 0.25 Hz, compared with the reference directions, by the storm quadrant of both positions, and for the pairs with both positions outside the storm (more than 600 km from the center).

Data set	Storm quadrant	Pairs	Bias	Median |difference|	Within 30°
Erin, NDBC 41047	Front right	42	−14°	12°	90%
	Rear right	58	+5°	39°	29%
	Outside	658	+14°	26°	55%
Erin, A-DWSD	Front left	132	+14°	10°	76%
	Front right	190	+14°	16°	85%
	Rear left	110	−3°	22°	64%
	Rear right	235	−38°	45°	36%
	Outside	206	−8°	23°	58%
Lowell, A-DWSD	Front left	164	−11°	16°	76%
	Front right	3023	+3°	7°	95%
	Rear left	295	+30°	33°	46%
	Rear right	2726	−4°	18°	74%
	Outside	3466	−8°	17°	71%

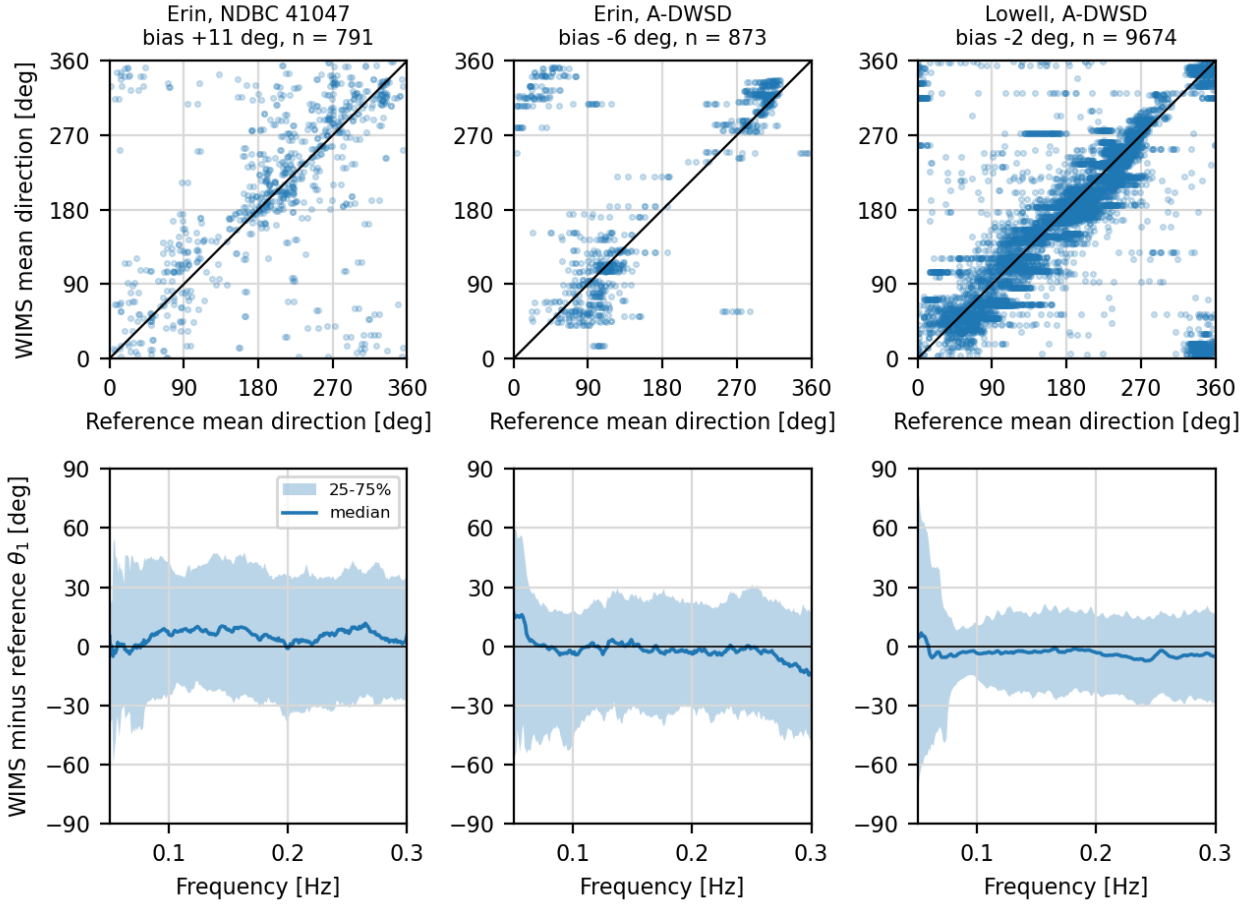
quadrants agree poorly (median absolute difference 38° to 61°), and are not used. Outside the storm, the median absolute difference is 17° (Lowell) to 26° (Erin, NDBC 41047).

- Of the 916 NDBC 41047 pairs, 791 are used: 100 in the same quadrant of Erin, 33 in the same quadrant of Imelda or Melissa, and 658 with both positions more than 600 km from the center of every storm (median distance 158 km). Their bias is +11°, with a median difference at each frequency of about +5° to +12° from 0.1 Hz to 0.27 Hz, and half of the bulk directions differ by more than 27°. The 100 pairs in the storm, in its right quadrants, have a bias of −14° (front right) and +5° (rear right). The pairs were measured up to 220 km apart, in the rapidly changing wave field of the hurricane or far from it.

7.9.1 Directional Fourier Coefficients and Spreading Parameters

The directional Fourier coefficients, a_1, b_1, a_2, and b_2, of the Longuet-Higgins formulation of the directional spectrum [13], and the spreading parameters, r_1 and r_2 (Section 7.5: Directional Spectra), were compared between WIMS and the A-DWSD drifters during Hurricanes Erin and Lowell, NDBC buoy 41047 during Hurricane Erin, with the pairs of this section, and the NDBC buoys, with the pairs of Section 7.10: NDBC Buoy Intercomparison.

Figure 22: WIMS and reference bulk mean wave directions, 0.06 Hz to 0.25 Hz, toward which the waves propagate, referenced to true north, for the pairs in the same storm quadrant or both outside the storm (top), and the difference of the mean wave directions, θ_1, at each frequency, with the median and interquartile range (bottom).



- **Processing.** The WIMS spectra are processed as in Section 7.7.2: Post-Processing Steps, and the coefficients computed with Equation (32). The A-DWSD coefficients are those reported by the drifters, and the NDBC coefficients are computed from the reported mean and principal directions, α_1 and α_2, and spreading parameters, r_1 and r_2. The reference coefficients are interpolated onto the WIMS frequency grid, and only bins at which both spectra are defined and positive are compared.

- **Convention.** All coefficients are compared in the NDBC convention [5], in which α is the direction from which the waves come, clockwise from true north, and $a_1 = r_1 \cos \alpha_1$, $b_1 = r_1 \sin \alpha_1$, $a_2 = r_2 \cos 2\alpha_2$, and $b_2 = r_2 \sin 2\alpha_2$. The WIMS coefficients are converted with $\alpha_1 = \theta_1 + D + 180°$ and $2\alpha_2 = 2\theta_2' + 2D$, where D is the magnetic declination of the dive, which leaves r_1 and r_2 unchanged. For each data set, the median difference between α_2 and α_1 at the spectral peak is $1°$

to $2°$ for the references and $6°$ to $10°$ for WIMS, against $23°$ to $88°$ for the other sign conventions of a_2 and b_2, which confirms the conversion.

- **Bulk values.** The coefficients of each instrument are averaged over 0.0625 Hz to 0.3 Hz, weighted by its own vertical displacement spectrum, and the bulk spreading parameters, directions, and circular spread, $\sqrt{2(1-r_1)}$, are computed from the averaged coefficients. These bulk directions are averaged over a wider band, and from the coefficients, so they differ slightly from those of Table 20.

Table 22: WIMS bulk directional coefficients and parameters, 0.0625 Hz to 0.3 Hz, compared with the reference instruments: bias (WIMS minus reference) / RMS difference / correlation coefficient for the coefficients, and bias / RMS difference / median absolute difference for the directions. Directions are from which the waves come; principal direction differences are modulo 180°. The spread is the bulk circular spread, $\sqrt{2(1-r_1)}$.

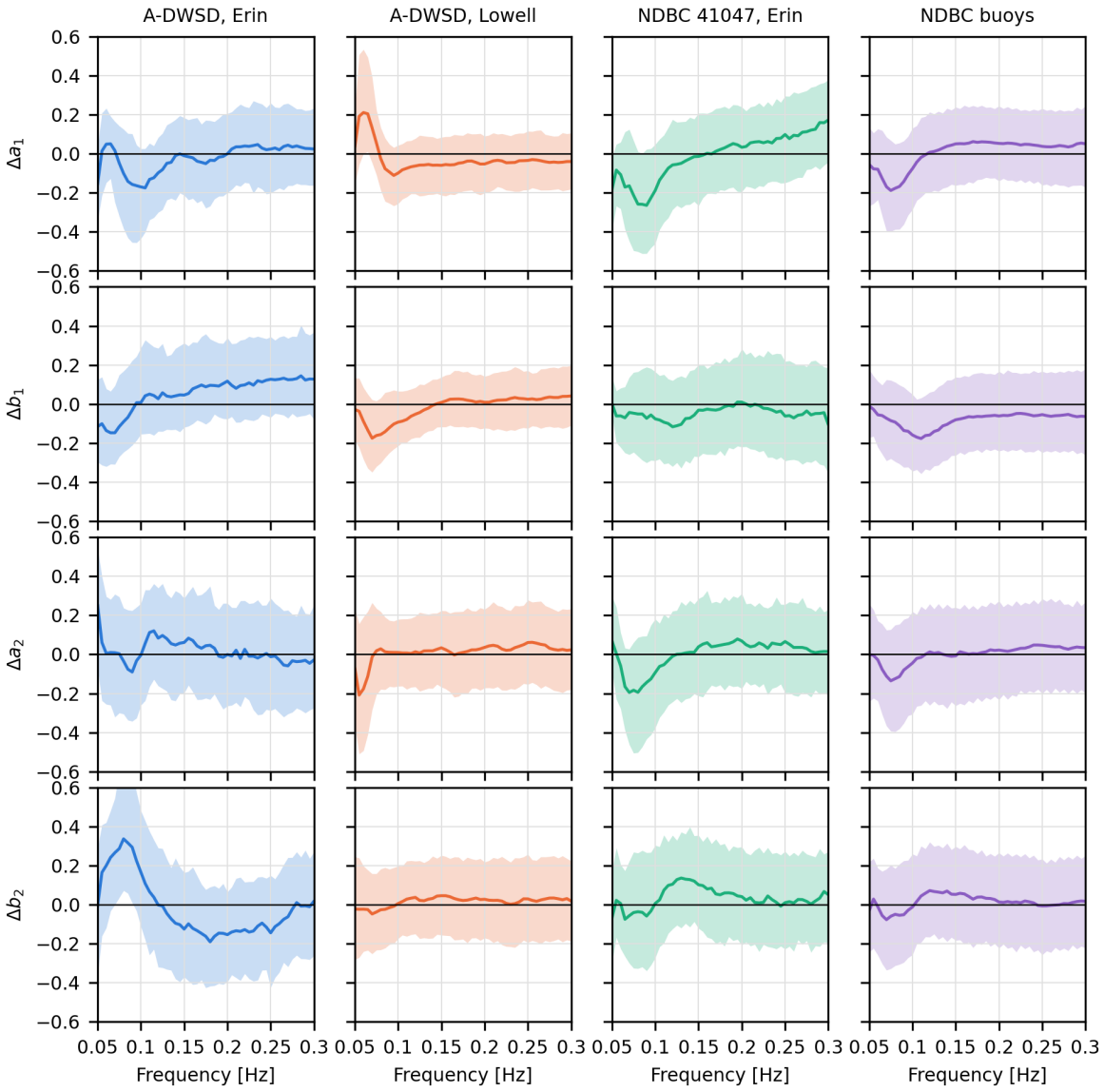
	A-DWSD, Erin	A-DWSD, Lowell	NDBC 41047, Erin	NDBC buoys
Pairs (WIMS spectra)	873 (117)	9674 (599)	791 (404)	3939 (2730)
Median separation	34 km	27 km	158 km	163 km
a_1	−0.05 / 0.23 / 0.76	−0.05 / 0.18 / 0.87	−0.12 / 0.35 / 0.74	0.00 / 0.29 / 0.80
b_1	+0.07 / 0.30 / 0.84	−0.06 / 0.17 / 0.94	−0.06 / 0.30 / 0.71	−0.09 / 0.29 / 0.76
a_2	+0.04 / 0.23 / 0.33	+0.01 / 0.18 / 0.88	−0.06 / 0.31 / 0.38	−0.01 / 0.28 / 0.48
b_2	+0.12 / 0.28 / 0.43	0.00 / 0.19 / 0.61	+0.02 / 0.31 / 0.47	+0.01 / 0.27 / 0.50
r_1	−0.12 / 0.18 / 0.72	−0.12 / 0.17 / 0.81	−0.24 / 0.31 / 0.45	−0.18 / 0.25 / 0.51
r_2	−0.10 / 0.21 / 0.37	−0.04 / 0.16 / 0.50	−0.19 / 0.28 / 0.35	−0.12 / 0.22 / 0.24
r_1, median ratio	0.83	0.78	0.67	0.77
r_2, median ratio	0.72	0.90	0.54	0.70
Spread, WIMS / ref.	56° / 48°	60° / 53°	63° / 48°	57° / 46°
Mean dir., α_1	−7.4° / 45° / 22°	−5.2° / 31° / 13°	+9.6° / 55° / 25°	+2.8° / 47° / 19°
Principal dir., α_2	+3.0° / 38° / 24°	+0.5° / 23° / 9°	−0.2° / 43° / 27°	−1.5° / 38° / 22°

Table 23: Median ratio of WIMS to reference r_1 / r_2, at each frequency bin, by frequency band.

Band	A-DWSD, Erin	A-DWSD, Lowell	NDBC 41047, Erin	NDBC buoys
0.05 to 0.08 Hz	0.80 / 0.69	0.62 / 0.67	0.66 / 0.80	0.64 / 0.84
0.08 to 0.12 Hz	0.80 / 0.68	0.77 / 0.89	0.64 / 0.69	0.66 / 0.74
0.12 to 0.20 Hz	0.87 / 0.75	0.92 / 0.98	0.72 / 0.79	0.80 / 0.82
0.20 to 0.30 Hz	0.86 / 0.76	0.99 / 1.03	0.71 / 0.96	0.82 / 0.94

The results are given in Tables 22 and 23 and shown in Figures 23 to 26. The intercomparison shows that:

Figure 23: Differences of the directional Fourier coefficients, WIMS minus reference, in the NDBC convention, against frequency: median (line) and interquartile range (shading), for each reference data set.



- **Spreading.** The WIMS spreading parameters are lower than those of all four references: the median ratio of the bulk r_1 is 0.67 to 0.83, and that of r_2 0.54 to 0.90, so the directional distributions measured by WIMS are broader, with a circular spread 7° to 15° larger. The deficit is largest at low frequencies: against the Lowell drifters, which agree best, the median ratio of r_1 is 0.62 from 0.05 Hz to 0.08 Hz and rises to 0.92 to 0.99 above 0.12 Hz, and against the NDBC buoys it is 0.64 to 0.66 below 0.12 Hz and 0.80 to 0.82 above.

- **First-order coefficients.** The biases of a_1 and b_1 are within 0.07 of zero against the drifters, with

Figure 24: Differences of the spreading parameters, r_1 and r_2, WIMS minus reference, against frequency: median (line) and interquartile range (shading), for each reference data set.

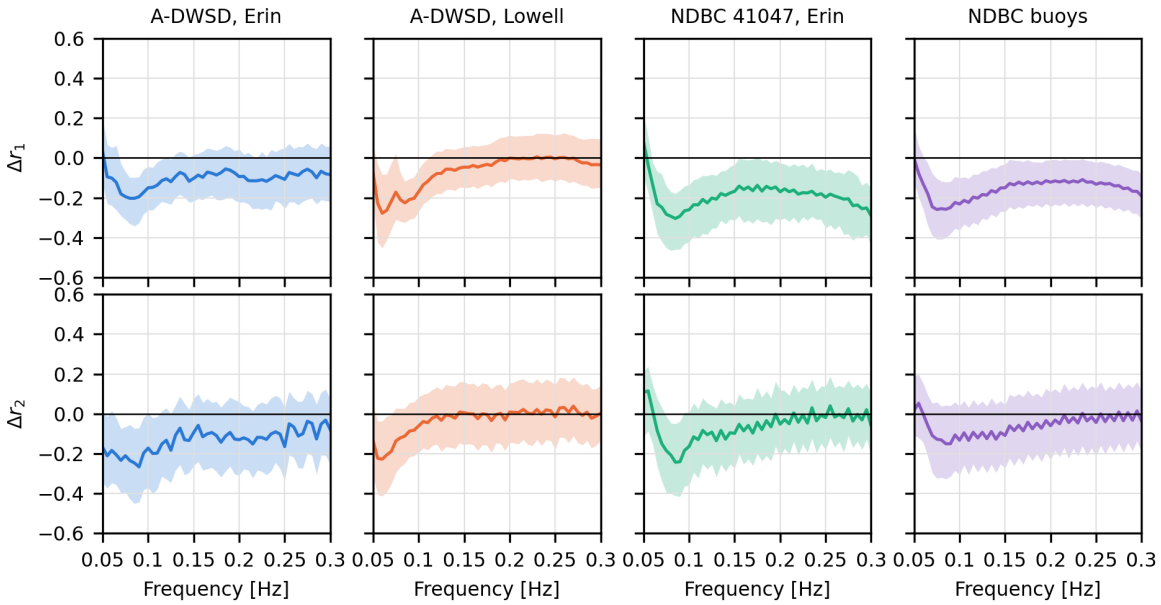
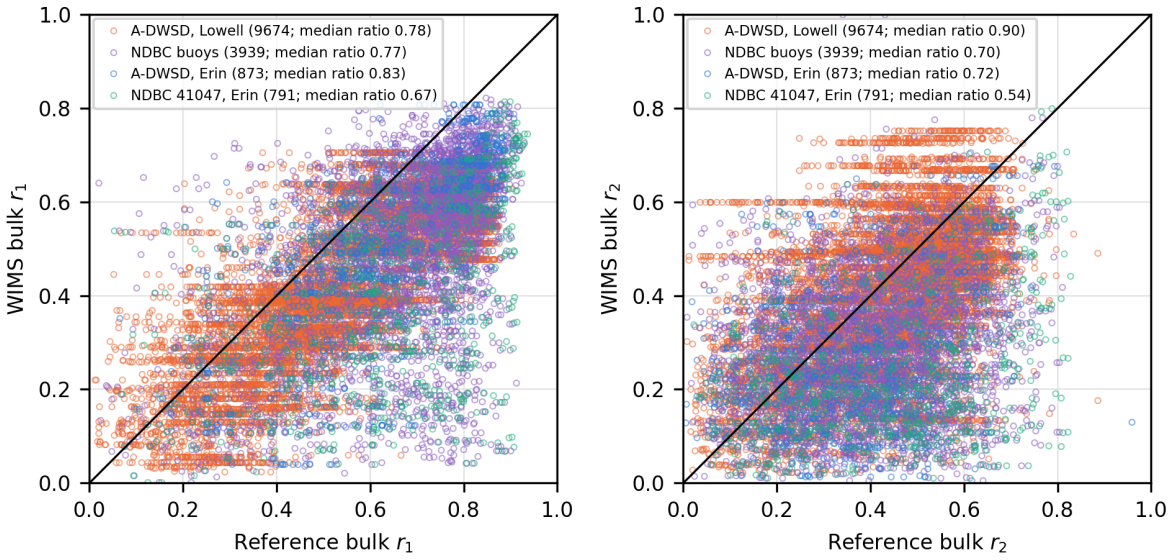
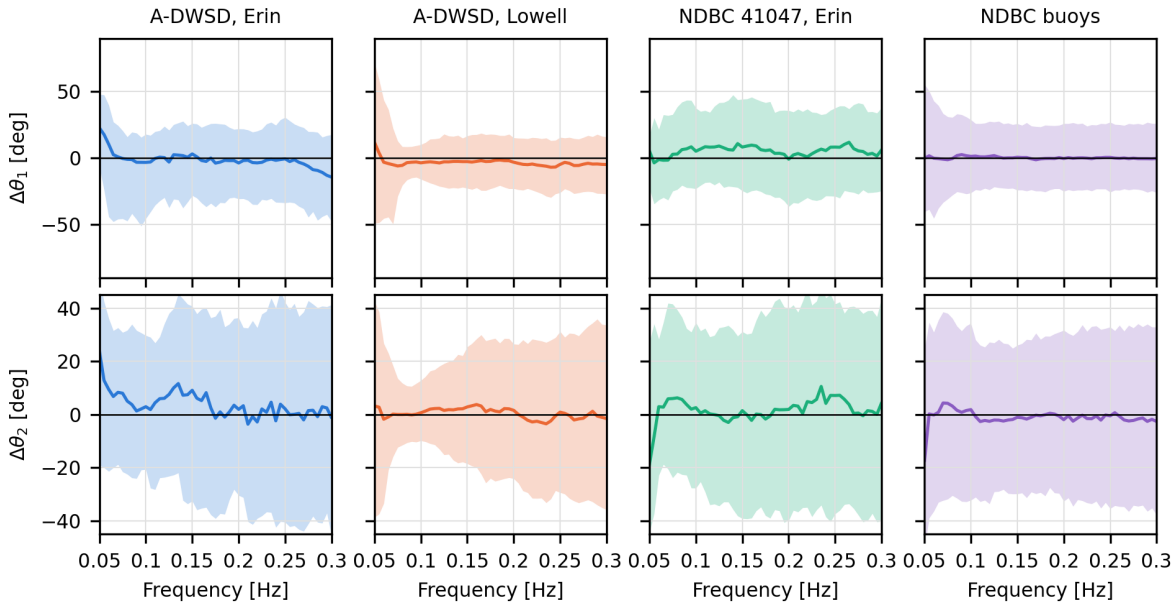


Figure 25: Bulk r_1 (a) and r_2 (b), 0.0625 Hz to 0.3 Hz, WIMS against the reference instruments, with the number of pairs and the median ratio of each data set. Horizontal rows of points are WIMS spectra colocated with several references.



correlations of 0.76 to 0.94, highest for Lowell. The larger biases against the NDBC buoys, -0.12 in a_1 against NDBC 41047 and -0.09 in b_1 against the NDBC buoys, are mostly the shrinkage toward zero that the low r_1 implies.

Figure 26: Differences of the mean direction, α_1, and of the principal direction, α_2 (modulo 180°), WIMS minus reference, against frequency: median (line) and interquartile range (shading), for each reference data set.



- **Second-order coefficients.** a_2 and b_2 agree less well, with correlations of 0.33 to 0.88, the best again for Lowell. Their biases are within 0.12 of zero, and are consistent with the low r_2.
- **Directions.** The bulk mean direction has a bias of $-7.4°$ to $+9.6°$, with a median absolute difference of $13°$ (Lowell) to $25°$ (NDBC 41047), as found in Table 20. The bulk principal direction agrees within $3°$ on average.

Limitations:

- The instruments are 27 km to 163 km apart (medians) and measure different parts of the wave field; the references also have errors of their own. Both add to the differences, and decorrelation of the wave field lowers the correlations, but does not explain a consistent deficit of r_1 and r_2 against all four references.
- The cause of the low WIMS spreading parameters has not been determined. Any horizontal acceleration that is not coherent with the vertical, such as noise or motion of the float other than its following of the waves, reduces r_1, and the orientation filter may also contribute. The low-frequency response correction does not affect the coefficients, as it scales all six spectra alike (Section 7.7.2: Post-Processing Steps).
- The pairs are not independent: a WIMS spectrum is colocated with several drifters, and a float near a buoy for several days produces many pairs.

- Most of the NDBC 41047 pairs (658 of 791) have both positions more than 600 km from the center of every storm (Table 21).

7.10 NDBC Buoy Intercomparison

The post-processed WIMS significant wave heights and wave directions were compared with those of 15 NDBC buoys in water deeper than 50 m in the western North Atlantic, the Caribbean Sea, and the Gulf of Mexico [5], with WIMS spectra from 21 ALAMO floats from August 2020 to July 2026. The pairs include 790 of the 914 pairs at NDBC buoy 41047 during Hurricane Erin, from August to November 2025: those with the WIMS spectrum and the buoy in the same quadrant of the same storm, within 600 km of its center (98 pairs of Erin and 37 of Imelda and Melissa), or both more than 600 km from the center of every storm (655 pairs), as in Section 7.9: Wave Direction Validation. The 124 pairs in different quadrants or storms are excluded. The same selection of the NDBC 41047 pairs is used to fit the low-frequency response correction (Section 7.8: Low-Frequency Response Correction), so the included pairs, marked in Table 25, are not an independent test of the correction. The floats, the buoys they were colocated with, and the periods of their colocated pairs are listed in Table 25, and the buoy positions in Table 24.

7.10.1 Method

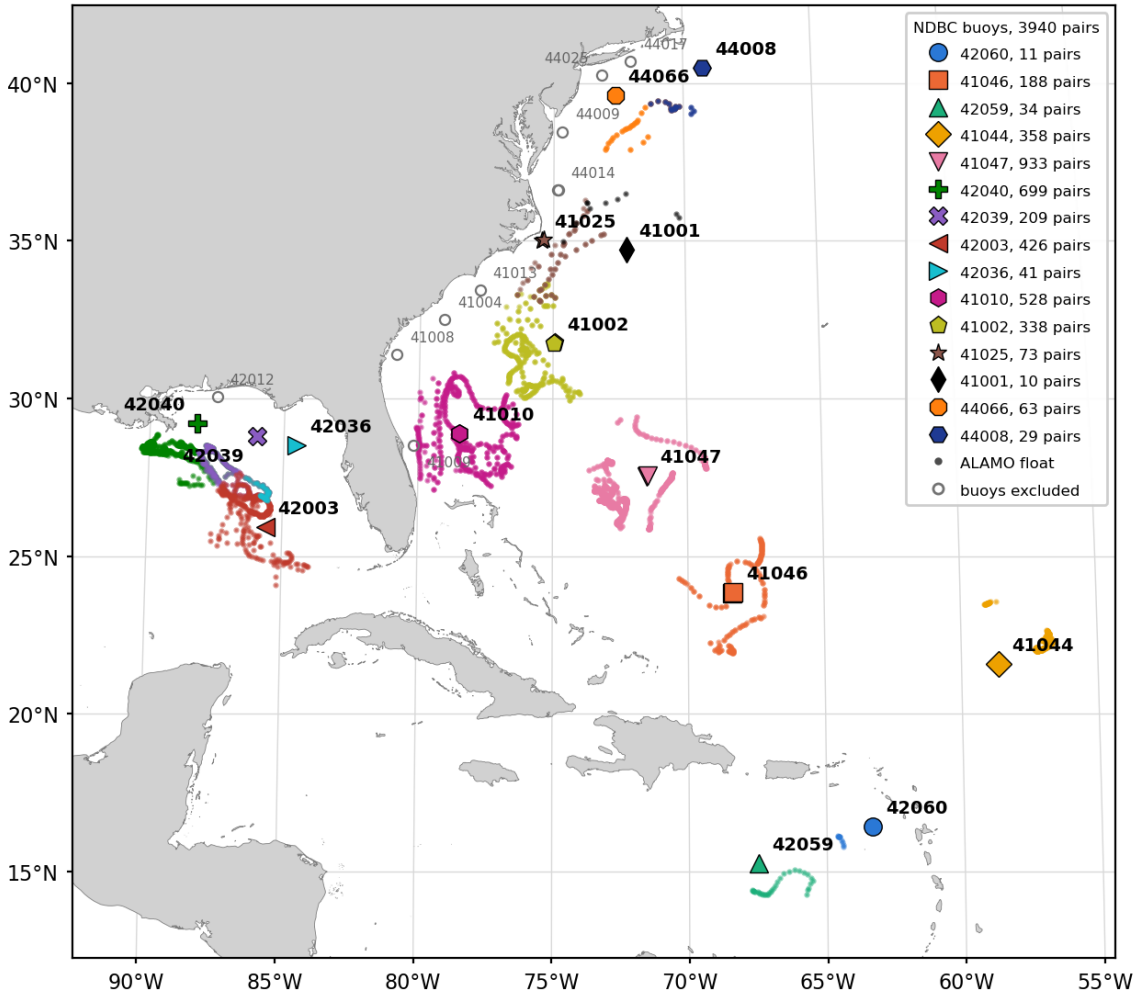
The WIMS spectra are those of all ALAMO floats with WIMS, except floats 9298 and 9310 (configuration errors). The NDBC buoys are found among all NDBC stations, including stations no longer reporting, from the deployment histories of the NDBC station metadata, and their spectral and directional data are taken from the NDBC historical archive. The position of a buoy is that of its deployment in effect at the time of each NDBC spectrum (Table 24).

WIMS and NDBC spectra within 30 minutes and 220 km of each other are colocated, if the WIMS spectrum is in water deeper than 50 m, from the ETOPO 2022 bathymetry [14] at the position of the WIMS spectrum (Section 7.8.1: Data). This excludes 200 pairs, mainly of float 9290 on the Texas shelf. The WIMS spectra are processed as in Section 7.7.2: Post-Processing Steps, including the low-frequency response correction; rejected spectra, and spectra without the full set of auto- and cross-spectra, are excluded. Significant wave heights are computed from 0.040 Hz to 0.480 Hz, and the bulk mean wave directions from 0.06 Hz to 0.25 Hz, as in Sections 7.8.2 and 7.9. The median ratio is $\exp(\mathrm{median}(\ln(H_{m0,\mathrm{WIMS}}/H_{m0,\mathrm{NDBC}})))$, and the direction bias is the circular mean of the difference, WIMS minus NDBC.

The buoys used are in water deeper than 50 m, from the water depths of the NDBC station pages. The depths of Table 24 are those of the ETOPO 2022 bathymetry at each deployment position; at the current positions they agree with the NDBC depths to within 4%, and the 2021 to 2025 position of NDBC 41025 is 48 m deep:

- Eleven are in deep water, 192 m to 5553 m deep. NDBC 42040, at 192 m on the continental slope, is in deep water for waves above 0.064 Hz.
- Four are on the outer continental shelf, 53 m to 77 m deep: NDBC 41025, 42036, 44008, and

Figure 27: The NDBC buoys at their deployment positions during the colocated pairs, with their number of colocated pairs, the ALAMO float positions of the colocated WIMS spectra, in the color of their buoy, and the excluded buoys in water shallower than 50 m.



44066.

- NDBC 42019 and 42020, 85 m and 86 m deep off Texas, have no pairs with WIMS spectra in water deeper than 50 m.

The buoys in water shallower than 50 m are excluded:

- NDBC 41004, 41008, 41009, 41013, 42012, 44009, 44014, 44017, and 44025, 16 m to 49 m deep.
- They are up to about 200 km from the floats in deep water.
- Their median significant wave height ratio, 1.36 (945 pairs), reflects the different wave fields rather than the measurements.

The buoys and the float positions of the colocated pairs are shown in Figure 27.

Table 24: NDBC buoys: location, deployments in effect during the colocated pairs, from the NDBC station metadata, with the position of each deployment, the water depth at that position from the ETOPO 2022 bathymetry [14], and the period and number of the colocated pairs. Deployments at the same position are combined.

NDBC buoy	Location	Deployment	Position	Depth	Colocated pairs	Pairs
41001	East Hatteras, 150 NM E of Cape Hatteras, NC	2022 Mar 2 – 2025 May 15	34.703 N, 72.242 W	4501 m	2022 May 14 – Dec 7	10
41002	South Hatteras, 225 NM S of Cape Hatteras, NC	2021 Jun 7 – 2025 Apr 27	31.759 N, 74.936 W	3783 m	2021 Oct 24 – 2025 Apr 24	153
		2025 Apr 27 – present	31.743 N, 74.955 W	3692 m	2025 Apr 27 – 2026 Feb 13	185
41010	Canaveral East, 120 NM E of Cape Canaveral, FL	2018 Feb 28 – 2024 May 1	28.878 N, 78.485 W	900 m	2021 Oct 17 – 2022 Nov 22	63
		2024 May 1 – 2026 May 28	28.880 N, 78.480 W	900 m	2024 Oct 6 – 2025 Jul 31	465
41025	Diamond Shoals, NC	2021 Jul 3 – 2025 May 6	35.010 N, 75.454 W	48 m	2021 Oct 25 – 2024 Dec 16	47
		2025 May 6 – present	35.026 N, 75.380 W	63 m	2026 Jan 19 – Feb 8	26
41044	NE St Martin, 330 NM NE of St Martin	2018 Mar 25 – present	21.582 N, 58.630 W	5486 m	2020 Sep 17 – Oct 24	358
41046	East Bahamas, 335 NM E of San Salvador, Bahamas	2017 Apr 4 – 2023 May 4	23.822 N, 68.384 W	5551 m	2020 Aug 20 – Aug 24	48
		2025 Apr 21 – present	23.840 N, 68.340 W	5560 m	2025 Nov 27 – 2026 May 4	140
41047[1]	NE Bahamas, 350 NM ENE of Nassau, Bahamas	2017 Apr 8 – 2021 Jun 5	27.514 N, 71.494 W	5328 m	2020 Sep 27 – Oct 3	97
		2025 Apr 25 – present	27.557 N, 71.480 W	5328 m	2025 Aug 18 – 2026 Jul 28	836
42003	East Gulf, 208 NM W of Naples, FL	2018 Feb 25 – 2022 Aug 6	25.925 N, 85.615 W	3264 m	2021 Aug 30 – Nov 30	426
42036	West Tampa, 112 NM WNW of Tampa, FL	2021 Apr 17 – 2025 Mar 14	28.500 N, 84.508 W	51 m	2021 Sep 23 – Oct 14	41
42039	Pensacola, 115 NM SSE of Pensacola, FL	2021 Apr 17 – 2026 Mar 23	28.787 N, 86.007 W	286 m	2021 Aug 29 – Nov 11	209
42040	Luke Offshore Test Platform, 63 NM S of Dauphin Island, AL	2021 Apr 16 – present	29.207 N, 88.237 W	200 m	2021 Aug 12 – Dec 5	699
42059	Eastern Caribbean Sea, 180 NM SSW of Ponce, PR	2016 May 19 – 2021 May 24	15.252 N, 67.483 W	4781 m	2020 Sep 7 – Oct 18	34
42060	Caribbean Valley, 63 NM WSW of Montserrat	2020 Apr 13 – 2026 May 6	16.434 N, 63.329 W	1476 m	2020 Aug 10 – Aug 19	11
44008	Nantucket, 54 NM SE of Nantucket, MA	2021 Jun 23 – 2025 May 9	40.496 N, 69.250 W	73 m	2022 Dec 21 – 2023 Jan 5	29
44066	Texas Tower 4, 75 NM E of Long Beach, NJ	2019 May 8 – present	39.618 N, 72.644 W	77 m	2022 Dec 13 – 2023 Jan 22	63

[1] NDBC 41047 data from August to November 2025, colocated with floats 9302, 9303, 9308, and 9309 during Hurricane Erin, were used to calculate the low-frequency response correction (Section 7.8: Low-Frequency Response Correction); only the pairs with the WIMS spectrum and the buoy in the same storm quadrant, or both more than 600 km from the center of the storm, are included.

7.10.2 Results

The results are summarized by float and buoy in Table 25, by sea state in Table 26, and shown in Figure 28.

Table 25: WIMS compared with NDBC buoys, by ALAMO float and NDBC buoy, in order of the first colocated pair, with the period of the colocated pairs.

				Median	H_{m0}		Mean wave direction		
Float	NDBC buoy	Period	Pairs	distance	Bias	Median ratio	Bias	Median |diff.|	Within 30°
9239	42060	2020 Aug 10 – Aug 19	11	137 km	+0.07 m	0.99	−2°	7°	100%
9245	41046	2020 Aug 20 – Aug 24	48	183 km	-0.17 m	0.88	+1°	7°	100%
9239	42059	2020 Sep 7 – Oct 18	34	109 km	+0.03 m	1.04	−6°	12°	88%
9248	41044	2020 Sep 17 – Sep 22	68	199 km	+0.40 m	1.09	−10°	71°	25%
9246	41044	2020 Sep 17 – Oct 14	254	178 km	+0.01 m	0.98	+1°	14°	76%
9249	41044	2020 Sep 18 – Sep 20	10	213 km	+0.75 m	1.09	−61°	54°	30%
9245	41047	2020 Sep 27 – Oct 3	97	217 km	+0.26 m	1.20	−6°	8°	100%
9271	41044	2020 Oct 21 – Oct 24	25	216 km	+0.18 m	1.11	−42°	46°	24%
9267	41044	2020 Oct 22 – Oct 22	1	219 km	+0.72 m	1.38	−22°	22°	100%
9300	42040	2021 Aug 12 – Aug 29	19	215 km	-0.23 m	1.14	+8°	6°	89%
9290	42040	2021 Aug 27 – Dec 5	173	107 km	+0.20 m	1.24	−9°	16°	71%
9288	42040	2021 Aug 27 – Sep 14	85	92 km	+0.16 m	1.00	−1°	35°	42%
9285	42040	2021 Aug 29 – Sep 9	79	159 km	-0.18 m	0.91	+12°	15°	68%
9290	42039	2021 Aug 29 – Nov 11	107	177 km	+0.13 m	1.12	−6°	22°	65%
9300	42003	2021 Aug 30 – Nov 30	44	166 km	+0.27 m	1.32	−24°	31°	48%
9288	42039	2021 Sep 3 – Sep 25	25	202 km	+0.11 m	1.13	−11°	50°	36%
9283	42040	2021 Sep 5 – Oct 14	247	183 km	+0.09 m	1.13	+10°	22°	61%
9282	42040	2021 Sep 7 – Sep 13	96	166 km	+0.19 m	1.16	−9°	12°	84%
9285	42039	2021 Sep 7 – Sep 21	29	202 km	+0.06 m	1.10	−8°	16°	72%
9288	42003	2021 Sep 8 – Oct 1	35	122 km	+0.19 m	1.12	+24°	50°	29%
9285	42003	2021 Sep 10 – Oct 9	53	141 km	+0.15 m	1.23	−1°	17°	66%
9282	42039	2021 Sep 12 – Sep 28	48	210 km	+0.36 m	1.51	+4°	23°	60%
9282	42003	2021 Sep 13 – Oct 5	252	66 km	+0.14 m	1.11	+11°	12°	83%

Float	NDBC buoy	Period	Pairs	Median distance	H_{m0}		Mean wave direction		
					Bias	Median ratio	Bias	Median |diff.|	Within 30°
9282	42036	2021 Sep 23 – Sep 26	16	217 km	+0.35 m	1.68	−41°	22°	56%
9290	42003	2021 Oct 2 – Oct 14	42	133 km	+0.08 m	1.07	−5°	10°	88%
9290	42036	2021 Oct 6 – Oct 14	25	195 km	+0.04 m	1.05	−24°	25°	52%
9288	41010	2021 Oct 17 – Oct 19	6	147 km	+0.56 m	1.37	−1°	38°	33%
9288	41002	2021 Oct 24 – Oct 24	1	215 km	+0.13 m	1.15	−55°	55°	0%
9288	41025	2021 Oct 25 – Oct 28	9	124 km	+1.31 m	1.48	−7°	54°	11%
9282	41010	2021 Oct 28 – Nov 21	47	153 km	-0.03 m	0.96	−5°	14°	70%
9300	41010	2022 Apr 13 – Apr 17	5	91 km	-0.27 m	0.78	−1°	7°	100%
9300	41002	2022 May 4 – May 11	7	198 km	+0.06 m	1.08	+16°	16°	100%
9300	41001	2022 May 14 – Jul 24	8	199 km	+0.17 m	1.14	+1°	12°	75%
9301	41010	2022 Nov 17 – Nov 22	5	169 km	+0.24 m	1.17	−30°	23°	60%
9301	41002	2022 Nov 27 – Dec 2	2	201 km	-0.09 m	0.94	+40°	40°	0%
9301	41001	2022 Dec 7 – Dec 7	2	213 km	+0.31 m	1.20	−12°	12°	100%
9301	44066	2022 Dec 13 – 2023 Jan 22	63	160 km	+0.31 m	1.25	+1°	21°	63%
9301	44008	2022 Dec 21 – 2023 Jan 5	29	169 km	+0.05 m	0.99	+2°	17°	72%
9292	41010	2024 Oct 6 – Oct 9	10	152 km	+0.22 m	1.10	−19°	19°	70%
9292	41002	2024 Oct 13 – Oct 14	4	217 km	+0.18 m	1.13	+49°	49°	50%
9292	41025	2024 Oct 14 – Oct 17	14	117 km	+0.42 m	1.54	−24°	26°	57%
9297	41010	2024 Oct 18 – 2025 Jul 31	430	151 km	+0.02 m	1.02	−4°	19°	70%
9297	41002	2024 Nov 10 – 2025 Jun 6	212	168 km	-0.06 m	0.99	+16°	27°	53%
9296	41010	2024 Nov 24 – Dec 1	25	130 km	-0.20 m	0.79	−3°	19°	84%
9296	41002	2024 Dec 7 – Dec 11	15	193 km	+0.43 m	1.35	+1°	8°	87%
9296	41025	2024 Dec 10 – Dec 16	24	130 km	+0.48 m	1.27	+4°	33°	46%
9303	41047[1]	2025 Aug 18 – Oct 15	218	160 km	-0.28 m	0.95	+11°	17°	74%
9309	41047[1]	2025 Aug 19 – Oct 27	280	122 km	-0.39 m	0.95	0°	35°	44%
9308	41047[1]	2025 Aug 19 – Sep 17	102	161 km	-0.18 m	0.99	+19°	34°	47%
9302	41047[1]	2025 Aug 30 – Oct 29	190	176 km	-0.07 m	1.02	+25°	30°	49%
9308	41046	2025 Nov 27 – 2026 May 4	140	121 km	+0.12 m	1.10	+1°	15°	73%

Float	NDBC buoy	Period	Pairs	Median distance	H_{m0}		Mean wave direction		
					Bias	Median ratio	Bias	Median |diff.|	Within 30°
9302	41002	2025 Dec 29 – 2026 Feb 13	69	116 km	-0.03 m	1.01	−11°	37°	35%
9303	41002	2026 Jan 14 – Jan 30	28	159 km	+0.10 m	1.09	+32°	29°	54%
9303	41025	2026 Jan 19 – Feb 8	26	194 km	+1.16 m	1.49	−2°	27°	62%
9303	41047	2026 Jun 5 – Jul 28	46	166 km	+0.17 m	1.15	+12°	15°	70%
All		2020 Aug 10 – 2026 Jul 28	3940	163 km	+0.04 m	1.05	+2°	20°	65%
All		within 100 km	619	76 km	+0.08 m	1.05	+3°	18°	68%

[1] NDBC 41047 data from August to November 2025, colocated with floats 9302, 9303, 9308, and 9309 during Hurricane Erin, were used to calculate the low-frequency response correction (Section 7.8: Low-Frequency Response Correction); only the pairs with the WIMS spectrum and the buoy in the same storm quadrant, or both more than 600 km from the center of the storm, are included.

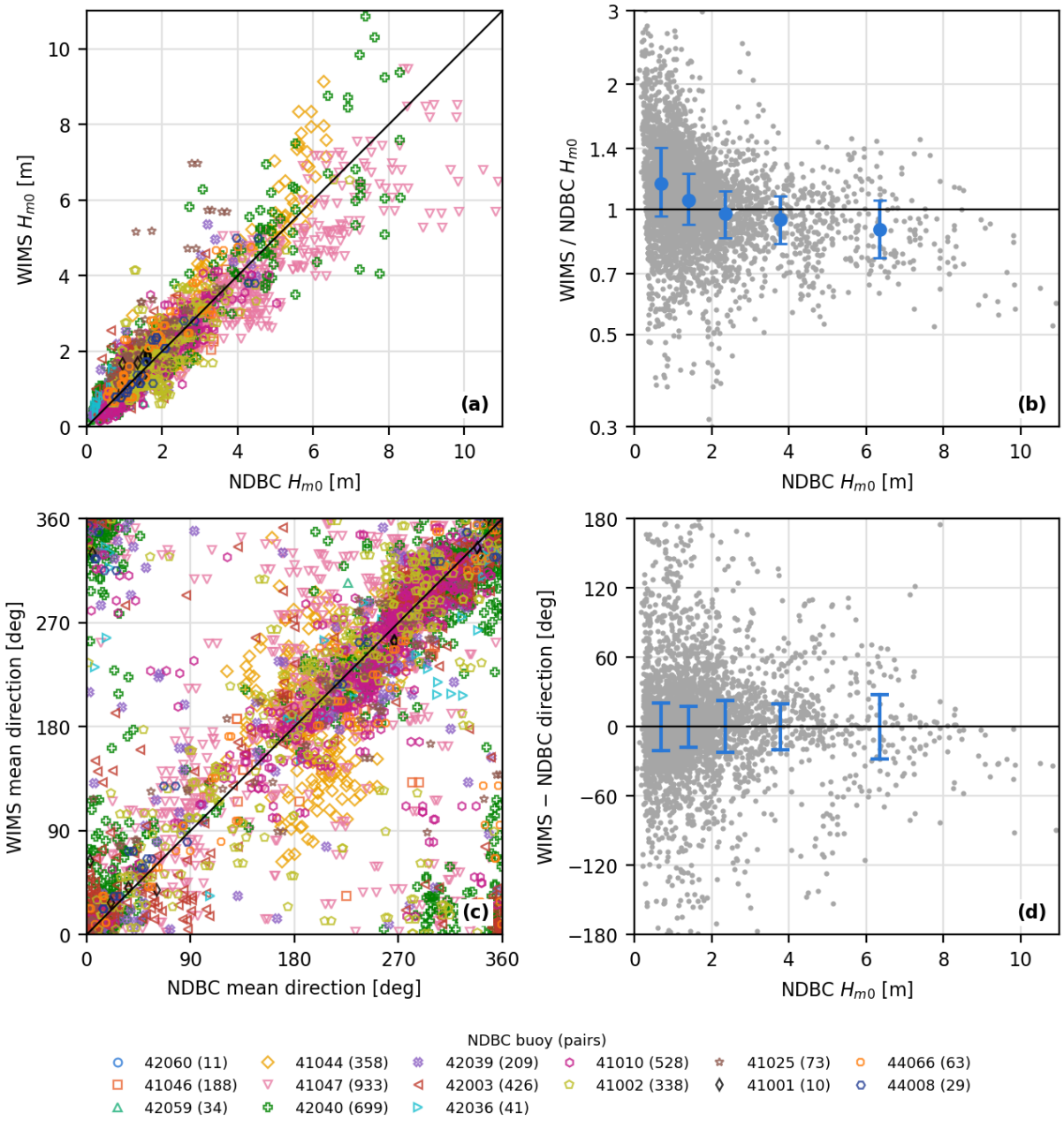
Table 26: WIMS compared with NDBC buoys, by NDBC significant wave height.

NDBC H_{m0}	Pairs	H_{m0} bias	H_{m0} median ratio	Direction median |diff.|	Within 30°
0 to 1 m	1313	+0.13 m	1.15	21°	63%
1 to 2 m	1565	+0.11 m	1.05	18°	68%
2 to 3 m	524	-0.04 m	0.98	22°	62%
3 to 5 m	347	-0.18 m	0.95	20°	66%
Above 5 m	191	-0.61 m	0.89	28°	52%

The intercomparison shows that:

- The WIMS significant wave height is 5% higher than that of the NDBC buoys overall (median ratio 1.05, bias $+0.04$ m), and 5% higher within 100 km (median ratio 1.05). It is 15% higher below 1 m, 5% higher from 1 m to 2 m, agrees from 2 m to 3 m (median ratio 0.98), and is 5% lower from 3 m to 5 m (0.95). Without the 790 Erin pairs at NDBC 41047, the median ratio is 1.07 (bias $+0.11$ m, 3150 pairs); the Erin pairs alone have a median ratio of 0.98 (bias -0.25 m). This is consistent with the higher WIMS vertical spectral densities above about 0.12 Hz (Section 7.8.6: Limitations), where more of the energy of lower sea states is. Above 5 m, the median ratio is 0.89, from 191 pairs, 121 of them the Erin pairs at NDBC 41047, in the right quadrants of the storm or far from it (Section 7.8.4: Storm-Relative Position).
- The wave directions agree without a significant bias ($+2°$), with a median absolute difference of $18°$ to $22°$ up to 5 m and $28°$ above 5 m, compared with $27°$ for the colocations at NDBC 41047

Figure 28: WIMS compared with NDBC buoys: significant wave heights, by buoy, with the number of pairs (a); ratio of significant wave heights against the NDBC significant wave height, with the median and interquartile range in 0–1, 1–2, 2–3, 3–5, and above 5 m bins (b); bulk mean wave directions, 0.06 Hz to 0.25 Hz, toward which the waves propagate, referenced to true north (c); and difference of the bulk mean wave directions, with ± the median absolute difference in the same bins (d).



during Hurricane Erin (Section 7.9: Wave Direction Validation). Of the 3933 pairs with directions, 298 (8%) differ by more than 90°, 219 of them below 2 m, attributed mainly to different wave

systems at the two positions in low sea states.

- The WIMS directional spreading parameters are lower than those of the buoys, with median ratios of the bulk r_1 and r_2 of 0.77 and 0.70, and the directional Fourier coefficients agree with those of the buoys with correlations of 0.48 to 0.80 (Section 7.9.1: Directional Fourier Coefficients and Spreading Parameters).

- The largest wave height differences are at buoys on the outer continental shelf, with the floats in deeper water: median ratios of 1.42 at NDBC 41025, off the U.S. East Coast, and 1.25 and 1.24 at NDBC 44066 and 42036. The deep-water buoys have median ratios of 0.99 to 1.20, the highest at NDBC 42039 and 42003 in the Gulf of Mexico (1.20 and 1.14).

- The largest direction differences, of the combinations with at least 20 pairs, are for floats 9248 and 9271 at NDBC 41044 (median 71° and 46°), and float 9288 at NDBC 42003 and 42039 (50°).

7.10.3 Tropical Cyclones

The colocated pairs measured during Atlantic tropical cyclones, with both the float and the buoy within 600 km of the center of a tropical or subtropical storm, at the best track position interpolated linearly in time (HURDAT2 [15] and the NHC best tracks [10]), are listed by storm in Table 27. They are the pairs of Section 7.10.1, in water deeper than 50 m; the 57 pairs of Hurricane Ida at the shelf buoy NDBC 42012 (27 m), and all the pairs of Hurricane Milton (2024), at NDBC 41004 and 41008, are in shallower water and are not included. The pairs at NDBC 41047 during Hurricanes Erin, Humberto, Imelda, and Melissa are part of the Erin data set used to fit the low-frequency response correction (Section 7.8: Low-Frequency Response Correction).
The comparison shows that:

- The floats came within 27 km to 52 km of the centers of the strongest storms, Teddy (2020), Ida (2021), Erin (2025), and Melissa (2025), and measured significant wave heights of up to 10.9 m (Ida); the buoys came within 46 km to 240 km.

- In the storms not used in the fit, the WIMS significant wave height is 7% higher than that of the buoys (median ratio 1.07, 199 pairs). It is 14% higher in Teddy, where the floats were 36 km to 110 km from the center and the buoy, NDBC 41044, 240 km, and 5% higher in Ida (113 pairs), where it is 13% higher when the float was nearer the center and 7% lower when the buoy was.

- At NDBC 41047, the WIMS significant wave height is 19% lower during Erin and 16% lower during Imelda, when the buoy was on the right side of the storms (Section 7.8.4: Storm-Relative Position), and 17% higher during Melissa, when the float, 52 km from the center, was nearer it than the buoy in 16 of the 17 pairs.

Table 27: Colocated WIMS and NDBC pairs during tropical cyclones, with both instruments within 600 km of the center of the storm: Saffir-Simpson peak of the storm, floats and buoys, number of pairs (in the same storm quadrant), closest approach of the float and of the buoy to the center, largest WIMS and NDBC significant wave height, median ratio of WIMS to NDBC significant wave height (same quadrant), and median absolute difference of the bulk mean wave direction (same quadrant).

Storm	Peak	Floats	Buoys	Pairs	Closest [km]	Max. H_{m0} [m]	H_{m0} ratio	$\lvert\Delta\theta\rvert$
Josephine (2020)	TS	9239	42060	1 (1)	475 / 388	1.7 / 1.2	1.44 (1.44)	24° (24°)
Teddy (2020)	Cat. 4	9246, 9248, 9249	41044	60 (58)	36 / 240	9.1 / 6.3	1.14 (1.13)	49° (50°)
Ida (2021)	Cat. 4	9285, 9288, 9290, 9300	42039, 42040	113 (94)	46 / 152	10.9 / 8.3	1.05 (1.02)	19° (18°)
Mindy (2021)	TS	9282, 9283, 9285	42039, 42040	15 (12)	129 / 86	2.1 / 1.5	0.83 (0.67)	6° (7°)
Nicholas (2021)	Cat. 1	9283	42040	6 (6)	322 / 437	2.3 / 1.6	1.41 (1.41)	44° (44°)
Chantal (2025)	TS	9297	41010	4 (2)	446 / 273	1.3 / 1.7	0.79 (0.77)	29° (12°)
Erin (2025)[1]	Cat. 5	9303, 9308, 9309	41047	164 (96)	27 / 137	9.5 / 11.9	0.81 (0.85)	41° (28°)
Humberto (2025)[1]	Cat. 5	9302, 9303	41047	4 (4)	490 / 354	3.0 / 3.5	1.04 (1.04)	67° (67°)
Imelda (2025)[1]	Cat. 1	9302, 9303, 9309	41047	44 (38)	284 / 304	5.0 / 6.5	0.84 (0.87)	36° (40°)
Melissa (2025)[1]	Cat. 5	9302	41047	17 (2)	52 / 46	7.7 / 10.3	1.17 (0.97)	58° (18°)

[1] Pairs of the Erin data set used to fit the low-frequency response correction, not an independent test.

- The mean wave directions differ by $19°$ (median) in Ida, and by $36°$ to $58°$ in Teddy, Erin, Imelda, and Melissa, in the rotating wave fields of the storms with the instruments up to 220 km apart.
- As in Section 7.8.4: Storm-Relative Position, the differences depend on the positions of the two instruments in the wave field of the storm: the logarithm of the significant wave height ratio is correlated with the difference of their distances from the center in Ida (0.59) and Melissa (0.70), but not in Teddy (0.00) or Erin (-0.18), where the buoy was on the right side of the storm. The pairs measure different parts of the storm wave field and are not a measure of the WIMS accuracy.

7.10.4 Limitations

- Most pairs are at a few combinations of float and buoy: 9297 at NDBC 41010 (430 of 3940 pairs), the four floats at NDBC 41047 during Hurricane Erin (790), 9246 at NDBC 41044 (254), 9282 at NDBC 42003 (252), and 9283 at NDBC 42040 (247).
- The median significant wave height ratio of the floats with at least 40 pairs ranges from 0.95 (9309, 280 pairs) to 1.16 (9282, 459 pairs, and 9290, 347 pairs).
- The buoys on the outer continental shelf, 53 m to 77 m deep, measure waves modified by the shelf, while the floats are up to 220 km away in deeper water.

- The floats deployed in 2020 sampled at an effective rate of 4 Hz (2 Hz for part of float 9245), while the correction was fitted to floats at 2.5 Hz and 5 Hz. Their median ratio, 1.03 (548 pairs), is within the range of the other floats.
- The pairs are not independent: a float near a buoy for several days produces many pairs.
- The colocated measurements are up to 220 km apart (median 163 km), which accounts for much of the scatter.

8 Serial Interface

Serial interface commands may be entered any time while WIMS is in the idle state. When WIMS enters the idle state, the command prompt string is printed, preceded by a line delimiter.

8.1 Special Characters and Strings

Table 28: Serial interface special characters and strings.

Type	ASCII	Hex	Description
Command prompt	'>',<SP>	0x3E20	String printed when WIMS enters the idle state to indicate that it is ready to accept a command.
Comment delimiter	'#',<SP>	0x2320	String printed at the start of comment messages, indicating that the remainder of the current line (until the next newline sequence) is a comment.
Command terminators	<ETX> <EOT> <LF> <CR> <ETB> ';'	0x03 0x04 0x0A 0x0D 0x17 0x3B	Characters received by WIMS that indicate the end of a command input (after a command prompt). When any of these characters are received and the preceding input is zero-length or entirely whitespace, then WIMS will respond by clearing the input buffer, then returning a line terminator followed by the command prompt. Otherwise, when any of these characters are received at the end of a non-zero length command input, WIMS sends the message delimiter followed by a line terminator, then processes the command. Upon completion of processing the command, WIMS will enter the idle state, indicated by sending the command prompt. These characters are not echoed to the serial interface when received.
Escape characters	<NUL> <BS> <CAN> <ESC> <DEL>	0x00 0x08 0x18 0x1B 0x7F	Characters received by WIMS that cancel command input. If any of these character are received, WIMS will respond by clearing the input buffer, then returning a line terminator followed by the command prompt. These characters are not echoed to the serial interface when received.
Line terminator	<LF>	0x0A	Newline (linefeed) character printed at the end of a line. All output from WIMS is immediately terminated with a line terminator, except for the command prompt.
Message delimiter	';'	0x3B	Character indicating the end of a message. Multiple messages and message delimiters may appear on the same line in some output modes.



8.2 Serial Interface Commands

Table 29: Serial interface commands.

Command	No. Args	Description	Sec. (Pg.)
`baud`	1	Set serial interface data rate	8.2.1 (90)
`get`	1	Get current configuration parameter value	8.2.2 (90)
`help`	0	Prints a verbose description of available commands	8.2.3 (91)
`load`	0 - 1	Load configuration parameters from non-volatile memory, or load default configuration parameter values	8.2.4 (91)
`mcal`	0	Run magnetometer calibration routine	8.2.5 (92)
`mst`	0	Run magnetometer self-test	8.2.6 (93)
`read`	0 - 1	Read stored spectra	8.2.7 (93)
`reset`	0	Request microcontroller software reset	8.2.8 (94)
`run`	0	Initiate a run	8.2.9 (95)
`runinfo`	0 - 1	Print detailed run information	8.2.10 (95)
`save`	0	Save current configuration parameters to non-volatile memory.	8.2.11 (97)
`set`	2	Set configuration parameter value	8.2.12 (97)
`shutdown`	0	Enter STOP mode	8.2.13 (98)
`sleep`	0	Enter SLEEP mode	8.2.14 (98)
`vers`	0	Print firmware version information	8.2.15 (98)

8.2.1 baud

Set the serial data rate.

Usage:

```
baud RATE;
```

Set the serial data rate to `RATE`, in baud. The valid range for the data rate is 9600 to 460800 baud. Upon entering this command, the serial data rate is changed immediately. On reset, the serial data rate will always be set to the default value of 115200 baud.

> **NOTE:** *Changing the data rate re-initializes the serial interface, which also resets `log.level` to its default value.*

8.2.2 get

Get current configuration parameter value.

Usage:

```
get INDEX|NAME|"all";
```

Get configuration parameter value by index or name, or get all parameter values using the keyword "all". The values of the parameters returned by this command are those that currently stored in RAM, and do not reflect the values stored in non-volatile memory (EEPROM).

Listing 3: Command example: "get" by parameter index.

```
> get 36;
param 36 wav.omode = 5       #            Output mode
>
```

Listing 4: Command example: "get" by parameter name.

```
> get wav.omode;
param 36 wav.omode = 5       #            Output mode
>
```

Listing 5: Command example: "get all" configuration parameters.

```
> get all;
param  0 brd.leds  = 0       #            LEDs enable
param  1 cal.acofx = -171    # [counts]   Accelerometer cal. offset, X
param  2 cal.acofy = -155    # [counts]   Accelerometer cal. offset, Y
param  3 cal.acofz = -1537   # [counts]   Accelerometer cal. offset, Z
param  4 cal.acscx = -9      # [2^-14]    Accelerometer cal. scale, X
param  5 cal.acscy = -31     # [2^-14]    Accelerometer cal. scale, Y
param  6 cal.acscz = -147    # [2^-14]    Accelerometer cal. scale, Z
```

```
param  7 cal.gcofx = -507    # [counts]   Gyroscope cal. offset, X
param  8 cal.gcofy = -136    # [counts]   Gyroscope cal. offset, Y
param  9 cal.gcofz = 68      # [counts]   Gyroscope cal. offset, Z
param 10 cal.gcscx = 0       # [2^-14]    Gyroscope cal. scale, X
param 11 cal.gcscy = 0       # [2^-14]    Gyroscope cal. scale, Y
param 12 cal.gcscz = 0       # [2^-14]    Gyroscope cal. scale, Z
param 13 cal.mcofx = 0       # [counts]   Magnetometer cal. offset, X
param 14 cal.mcofy = 0       # [counts]   Magnetometer cal. offset, Y
param 15 cal.mcofz = 0       # [counts]   Magnetometer cal. offset, Z
param 16 cal.mcscx = 0       # [2^-14]    Magnetometer cal. scale, X
param 17 cal.mcscy = 0       # [2^-14]    Magnetometer cal. scale, Y
param 18 cal.mcscz = 0       # [2^-14]    Magnetometer cal. scale, Z
param 19 imu.dlpf  = 24      # [Hz]       Digital LPF cutoff frequency
param 20 imu.fsra  = 4       # [+/-g]     Accelerometer full-scale range
param 21 imu.fsrg  = 500     # [+/-deg/s] Gyroscope full-scale range
param 22 imu.srate = 45      # [Hz]       Sample rate
param 23 log.level = 2       #            Log message output level
param 24 run.rmode = 2       #            Run options bitmask
param 25 run.smode = 0       #            Startup options bitmask
param 26 serialnum = 0       #            Device serial number
param 27 wav.afilt = 10      #            Accelerometer filter select
param 28 wav.fbmax = 500     # [mHz]      Spectra max. frequency
param 29 wav.fbmin = 0       # [mHz]      Spectra min. frequency
param 30 wav.gaina = 32      # [2^-3]     Accelerometer static gain
param 31 wav.mxsam = 32768   # [samples]  Maximum samples
param 32 wav.mxseg = 7       # [segments] Maximum segments
param 33 wav.nfwax = 0       #            Normally forward axis
param 34 wav.nupax = 2       #            Normally up axis
param 35 wav.obeta = 1343    # [2^-15]    Orientation filter beta
param 36 wav.omode = 5       #            Output mode
param 37 wav.ostsc = 180     # [sec]      Orientation filter settle time
param 38 wav.ozeta = 163     # [2^-15]    Orientation filter zeta
param 39 wav.slen  = 256     # [samples]  Segment length
param 40 wav.smode = 2       #            Sample mode
param 41 wav.srdiv = 8       # [+1 Hz/Hz] Sample rate divider
param 42 wav.twalp = 64      # [2^-7]     Tukey window function alpha
>
```

8.2.3 help

Print help text.

Usage:

```
help;
```

Prints a verbose description of available commands.

8.2.4 load

Load configuration parameters from non-volatile memory.

Usage:

```
load ["default"];
```

Attempts to load configuration parameter values from EEPROM. If EEPROM is not available, an error occurs, or saved hash is invalid, then default configuration parameters are loaded. If the "default" keyword is specified, then default configuration parameter values are loaded. Loading the default values does not change `log.level` or `brd.leds`.

> **NOTE:** *If the saved hash is invalid, the default configuration parameter values are also immediately saved to EEPROM, overwriting all stored values, including calibration coefficients. Record calibration coefficients separately so they can be restored.*

Listing 6: Command example: "load" configuration.

```
> load;
# Loading Configuration...
>
```

8.2.5 mcal

Run magnetometer calibration routine.

Usage:

```
mcal;
```

Initializes the IMU driver and wave module runtime data. Sets the IMU configuration from current parameters, and enables buffered continuous sampling. Reads and processes individual packets from the IMU until interrupted by user input. The magnetometer samples are filtered with the filter selected by `wav.afilt` and downsampled by `wav.srdiv` + 1. Each downsampled sample is printed as `NNNNNNN r[AX AY AZ;GX GY GZ;MX MY MZ]; m[FX FY FZ];`, where `NNNNNNN` is the sample number, `r[...]` holds the uncalibrated accelerometer, gyroscope, and magnetometer counts of the most recent IMU sample, and `m[...]` holds the filtered magnetometer counts.

Samples received during the orientation filter settle time, `wav.ostsc`, are not used. From the remaining samples, the minimum and maximum filtered magnetometer counts of each axis are found. When the routine is interrupted, the following lines are printed:

- `mcal 1 X Y Z min` – minimum counts.
- `mcal 2 X Y Z max` – maximum counts.

- `mcal 3 X Y Z offs` – offsets, the midpoints of the minimum and maximum counts.
- `mcal 4 X Y Z scale` – half ranges, half of the difference of the maximum and minimum counts.
- `mcal 5 X Y Z scale adj` – scale coefficients, in units of 2^{-14}, that scale each axis to the largest half range.

The offsets and scale coefficients are applied to the `cal.mcof[A] and cal.mcsc[A]` parameters in RAM. They are not saved to EEPROM; use the save command to save them. See Section 6.1.3: Magnetometer Calibration.

8.2.6 mst

Run magnetometer self-test.

Usage:

```
mst;
```

Initializes ICM-20948 driver and enters bypass mode to communicate with the AK09916 magnetometer directly. Puts the magnetometer in self test mode and reads results. In self test mode, the magnetometer generates an internal magnetic field. Results are bounds checked and pass/fail is printed.

Listing 7: Command example: "mst".

```
> mst;
# ------------------------------------------------------------------------
# MAGNETOMETER SELF-TEST RESULTS
# - - - - - - - - - - - - - - - - - - - - - - - - - - - - - - - - - - - - -
# mag self test  (-200 <= Hx <=  200):     +3 PASS
# mag self test  (-200 <= Hy <=  200):     -3 PASS
# mag self test (-1000 <= Hz <= -200):   -403 PASS
# ------------------------------------------------------------------------
>
```

8.2.7 read

Read stored spectral data.

Usage:

```
read [INDEX];
```

Reads stored segment-averaged co- and quadrature-spectral densities from a previous run. If optional index is not provided, or index value is 0, then all 6 spectra will be printed. Otherwise, individual spectra may be printed by index:

0: all

1: Cxy (co-spectral density of east-north axes)

2: Qzx (quadrature spectral density of vertical-east axes)

3: Qzy (quadrature spectral density of vertical-north axes)

4: Sxx (power spectral density of east axis)

5: Syy (power spectral density of north axis)

6: Szz (power spectral density of vertical axis)

Listing 8: Command example: "read" stored spectral data.

```
> read;
# ------------------------------------------------------------------------------
#   idx     freq      Cxy      Qzx      Qzy      Sxx      Syy      Szz
# - - - - - - - - - - - - - - - - - - - - - - - - - - - - - - - - - - - - - - -
s[    0, 0.0000,       0,       0,       0,       0,       0,       0 ];
s[    1, 0.0195,       0,       0,       0,       0,       0,       0 ];
s[    2, 0.0391,       0,       0,       0,       0,       0,       0 ];
s[    3, 0.0586,       0,       0,       0,       0,       0,       0 ];
s[    4, 0.0781,       0,       0,       0,       0,       0,       0 ];
s[    5, 0.0977,       0,       0,       0,       0,       0,       0 ];
s[    6, 0.1172,       0,       0,       0,       0,       0,       0 ];
s[    7, 0.1367,       0,       0,       0,       0,       0,       0 ];
s[    8, 0.1563,       0,       0,       0,       0,       0,       0 ];
s[    9, 0.1758,       0,       0,       0,       0,       0,       0 ];
s[   10, 0.1953,       0,       0,       0,       0,       0,       0 ];
s[   11, 0.2148,       0,       0,       0,       0,       0,       0 ];
s[   12, 0.2344,       0,       0,       0,       0,       0,       0 ];
s[   13, 0.2539,       0,       0,       0,       0,       0,       0 ];
s[   14, 0.2734,       0,       0,       0,       0,       0,       0 ];
s[   15, 0.2930,       0,       0,       0,       0,       0,       0 ];
s[   16, 0.3125,       0,       0,       0,       0,       0,       0 ];
s[   17, 0.3320,       0,       0,       0,       0,       0,       0 ];
s[   18, 0.3516,       0,       0,       0,       0,       0,       0 ];
s[   19, 0.3711,       0,       0,       0,       0,       0,       0 ];
s[   20, 0.3906,       0,       0,       0,       0,       0,       0 ];
s[   21, 0.4102,       0,       0,       0,       0,       0,       0 ];
s[   22, 0.4297,       0,       0,       0,       0,       0,       0 ];
s[   23, 0.4492,       0,       0,       0,       0,       0,       0 ];
s[   24, 0.4688,       0,       0,       0,       0,       0,       0 ];
s[   25, 0.4883,       0,       0,       0,       0,       0,       0 ];
# ------------------------------------------------------------------------------
```

8.2.8 reset

Request microcontroller software reset.

Usage:



```
reset;
```

Flushes user comms, deinitializes drivers and modules, and then initiates a system reset request to reset the microcontroller. The behavior of the software reset is identical to power-on reset.

Listing 9: Command example: "reset" microcontroller.

```
> reset;
# reset...

# ============================================================================
#    _       ________  _______
#   | | /| / /  _/  |/  / __/  Wave-field Inertial Measurement System
#   | |/ |/ // // /|_/ /\ \     v2.01.00617b (RELEASE)
#   |__/|__/___/_/  /_/___/     A. Ekholm, WHOI
#
# ============================================================================
vers 2.01.00617b (RELEASE)
# Initializing...
# Loading Configuration...
>
```

8.2.9 run

Initiate a run.

Usage:

```
run;
```

Initializes the IMU driver and wave module runtime data. Sets the IMU configuration from current parameters, and enables buffered continuous sampling. Reads and processes individual packets from the IMU until either the run is complete or interrupted by user input. See Section 6.4: Run Behavior;

8.2.10 runinfo

Print run information.

Usage:

```
runinfo [VERBOSE];
```

Prints the expected duration of a run and related sampling and spectral information for the current configuration. If `VERBOSE` is non-zero, a formatted summary is printed before the run information line. If `VERBOSE` is omitted, the summary is printed when `log.level` is 2 or greater.

The run information line, `runinfo [T, SRATE, DIV, FSRA, GAINA, SLEN];`, contains the following fields:

- `T` – maximum total run time, in seconds, including the initialization time and the maximum IMU clock error of $+2\%$, or `inf` if the run duration is unlimited.
- `SRATE` – base sample rate, `imu.srate`, in Hz.
- `DIV` – sample rate divider plus one, `wav.srdiv` + 1.
- `FSRA` – accelerometer full-scale range, `imu.fsra`, in $\pm g$.
- `GAINA` – accelerometer software gain, `wav.gaina`, in units of 2^{-3}.
- `SLEN` – segment length, `wav.slen`, in samples.

Listing 10: Command example: print non-verbose "runinfo".

```
> runinfo 0;
runinfo [394, 45, 9, 4, 32, 256];
>
```

Listing 11: Command example: print verbose "runinfo".

```
> runinfo 1;
# ------------------------------------------------------------------------------
# Run Info
# ------------------------------------------------------------------------------
#             base sample rate:         45 [Hz]
#          sample rate divider:          9 [Hz/Hz]
#        effective sample rate:     5.0000 [Hz]
# - - - - - - - - - - - - - - - - - - - - - - - - - - - - - - - - - - - - - - -
#                 max. samples:      32768
#   time to reach max. samples:     109:13 [mm:ss]
# - - - - - - - - - - - - - - - - - - - - - - - - - - - - - - - - - - - - - - -
#      accel. full-scale range:       +/-4 [g]
#         accel. software gain:        4.0 [g/g]
#       gyro. full-scale range:     +/-500 [dps]
# - - - - - - - - - - - - - - - - - - - - - - - - - - - - - - - - - - - - - - -
#                  output mode:          5 (WAVE_OUTPUT_MODE_SPECTRA_FULL)
# - - - - - - - - - - - - - - - - - - - - - - - - - - - - - - - - - - - - - - -
#           filter settle time:      03:00 [mm:ss]
# - - - - - - - - - - - - - - - - - - - - - - - - - - - - - - - - - - - - - - -
#               segment length:        256
#             segment duration:      00:51 [mm:ss]
#              segment overlap:         50 [%]
#                max. segments:          7
#  time to reach max. segments:      06:24 [mm:ss]
# - - - - - - - - - - - - - - - - - - - - - - - - - - - - - - - - - - - - - - -
#               spectra length:        128
#        spectra bin bandwidth:     0.0195 [Hz]
#        spectra max. bin freq:     2.4805 [Hz]
# - - - - - - - - - - - - - - - - - - - - - - - - - - - - - - - - - - - - - - -
```




```
#       min. reported bin freq:    0.0000 [Hz]
#        min. reported bin idx:         0
#       max. reported bin freq:    0.5000 [Hz]
#        max. reported bin idx:        25
#    no. spectra bins reported:        26
# - - - - - - - - - - - - - - - - - - - - - - - - - - - - - - - - - - - - - - - -
#            expected run time:     06:26 [mm:ss]
#         max. IMU clock error:      +/-2 [%]
#          max. total run time:     06:34 [mm:ss]
# ------------------------------------------------------------------------------
runinfo [394, 45, 9, 4, 32, 256];
>
```

8.2.11 save

Save current configuration parameters to non-volatile memory.

Usage:

```
save;
```

Attempts to save the current configuration parameter values and a computed hash of the parameter values to EEPROM. If EEPROM is not available, an error message is printed and the configuration parameter values in RAM are unchanged.

8.2.12 set

Set a configuration parameter value.

Usage:

```
set INDEX|NAME VALUE;
```

Set a configuration parameter value by its specified name or index.

Listing 12: Command example: "set" a parameter value by name.

```
> set wav.omode 0;
param 36 wav.omode = 0       #            Output mode
>
```

Listing 13: Command example: "set" a parameter value by index.

```
> set 36 5;
param 36 wav.omode = 5       #            Output mode
>
```

8.2.13 shutdown

Enter STOP mode.

Usage:

```
shutdown;
```

Flushes user comms buffers, deinitializes drivers and modules, and then enters STOP mode. This command is used as part of the low-power shutdown sequence. See Section 6.5: Low-power Shutdown.

Listing 14: Command example: "shutdown".

```
>  shutdown;
# Shutdown...
```

8.2.14 sleep

Enter SLEEP mode.

Usage:

```
sleep;
```

Flushes user comms buffers, deinitializes drivers and modules, and then enters low-power SLEEP mode. There is currently no method for waking the device from SLEEP mode.

8.2.15 vers

Print firmware version information.

Usage:

```
vers;
```

Prints splash text and firmware version string.

Listing 15: Command example: "vers".

```
> vers;
# ================================================================================
#    _       ________  _______
#   | | /| / /  _/  |/  / __/  Wave-field Inertial Measurement System
#   | |/ |/ // // /|_/ /\ \     v2.01.00617b (RELEASE)
#   |__/|__/___/_/  /_/___/     A. Ekholm, WHOI
#
# ================================================================================
vers 2.01.00617b (RELEASE)
>
```

8.3 Output Message Formats

All output from WIMS is delimited by a newline character

8.3.1 Comment Lines

Comment lines start with a pound character ('#', 0x23) and have an associated log level. During operation, only comment lines with a log level less than or equal to the value of the parameter `log.level` will be printed. Comment lines are intended for human readability only and can be safely ignored during automated processing WIMS data. Log messages are comment lines of the form `# [TAG][MODULE] message`, where `TAG` is the log tag of Table 36; for example, `# [OUT][WAVDRV] sampling...`.

8.3.2 Run Output Records

During a run, one record is printed per downsampled sample, or per spectral bin at the end of the run, depending on the output mode, `wav.omode`. Each record is terminated by a semicolon and a newline. The record formats are:

- `wav.omode = 0`, raw counts: `NNNN; tSSS.MMM; r[AX AY AZ;GX GY GZ;MX MY MZ];`, where `NNNN` is the sample number, `SSS.MMM` is the time since the first sample in seconds and milliseconds, and `r[...]` holds the calibrated accelerometer, gyroscope, and magnetometer counts in the sensor frame, after axis remapping (see `wav.nupax`).
- `wav.omode = 1`, orientation filter: the raw counts record, followed by `w[...]`, the bias-corrected angular rates and the gyroscope bias estimates, in rad/s with radix 11, `f[...]`, the orientation filter objective function, `q[Q0 Q1 Q2 Q3]`, the sensor- to earth-frame rotation quaternion with radix 14, and `a[...]`, the earth-frame acceleration.
- `wav.omode = 2`, earth-frame acceleration: `NNNNNNN a[AE AN AU]; q[Q0 Q1 Q2 Q3];`, where `a[...]` holds the east, north, and up accelerations, in accelerometer counts, and `q[...]` is the rotation quaternion with radix 14.
- `wav.omode = 3`, Euler angles: `NNNNNNN e[PSI THETA PHI]; q[Q0 Q1 Q2 Q3];`, where `e[...]` holds the angles $\psi = atan2(q_0q_3 + q_1q_2,\ q_0^2 + q_1^2 - 1/2)$, $\theta = asin(2q_0q_1 + 2q_2q_3)$, and $\phi = atan2(q_0q_2 + q_1q_3,\ q_0^2 + q_3^2 - 1/2)$, in binary radians ($2^{15}$ binary radians $= 180°$).
- `wav.omode = 4`, vertical spectra: at the end of the run, `Szz [ V V ... V ];`, the averaged vertical acceleration power-spectral densities of the reported bins, in counts, in order of increasing frequency, without bin indices or frequencies.
- `wav.omode = 5`, full spectra: at the end of the run, one record per reported bin, `s[ IDX, FREQ, CXY, QZX, QZY, SXX, SYY, SZZ ];`, where `IDX` is the bin index, n, `FREQ` is the bin frequency, f_n, in Hz, and the spectral densities are in counts (see Section 7.3: Scale Sensitivity).

The accelerometer counts of a full-scale range of `imu.fsra` $= R$ are $2^{15}/R$ counts per g.

8.3.3 Error Messages and Status Codes

Errors and warnings are reported as comment lines with the `ERR` and `WRN` log tags, which are printed at all log levels of `log.level` of 0 or greater, and 1 or greater, respectively. Messages from the command interface have the form `# [ERR] message`, and messages from the firmware modules have the form `# [ERR] [MODULE] message`, where `MODULE` identifies the module: `WAVDRV`, the wave module; `ICMDRV`, the ICM-20948 IMU driver; `OFLMOD`, the orientation filter; `EEPROM`, the configuration memory; and `AT24CDRV`, the EEPROM device driver. In the tables below, *N* is a decimal number, *NN* and *NNNNNNNN* are hexadecimal numbers, and *cmd* is the name of the function that reports the error.

Many messages include a hexadecimal status code. The status codes are listed in Table 30. Their meaning depends on the module that reports them.

Table 30: Status codes.

Code	Meaning
`0x00`	Success.
`0x01`	General error. The driver or module operation failed.
`0x02`	Null pointer (IMU driver, orientation filter, and wave module).
`0x03`	Invalid value or state (IMU driver, orientation filter, and wave module); null pointer (other modules).
`0x04`	The IMU sensors are disabled (IMU driver and wave module); overflow (other modules).
`0x05`	Timeout.
`0x06`	Invalid input.
`0x10`	I2C transfer failed. In I2C read failures of the IMU driver, the low bits give the cause: `0x11`, no acknowledge (NACK); `0x12`, bus error; `0x13`, arbitration lost. Null pointer (circular buffer and FIR filter).
`0x11`	I2C transfer not acknowledged (EEPROM).
`0x20`	Buffer empty (circular buffer and FIR filter).
`0x21`	Buffer full (circular buffer and FIR filter).

Table 31: Command interface error messages.

Message	Meaning and action
`# [ERR] invalid cmd`	The command is not recognized. Check the spelling; see help.
`# [ERR] cmd not implemented`	The command is recognized but not implemented in this firmware version.
`# [ERR] cmd buf ovflw`	The command line is too long and was discarded.
`# [ERR] cmd arg ovflw`	The command has too many arguments and was discarded.
`# [ERR] not enough arguments`, `# [ERR] too many arguments`, `# [ERR]` *cmd*`: not enough arguments.`, `# [ERR]` *cmd*`: too may arguments.`	The number of command arguments is wrong. See the command usage.
`# [ERR] Invalid argument.`, `# [ERR] invalid spectra:` *arg*	An argument value is not valid, for example a read index other than 0 to 6.
`# [ERR]` *cmd*`: param not found`, `# [ERR]` *cmd*`: param bad idx,` *N*	No configuration parameter has the given name or index. Use `get all` to list the parameters.
`# [ERR]` *cmd*`: set baud, invalid rate`, `# [ERR]` *cmd*`: set baud, invalid arg`	The baud rate is not a number in the range 9600 to 460800.
`# [ERR]` *cmd*`: fail, set fail`, `# [ERR]` *cmd*`: get cfg param fail, stat = 0x`*NNNNNNNN*	Setting or getting a parameter failed, for example because the value was rejected by the wave module (see `param set fail` below).
Other messages of the form `# [ERR]` *cmd*`: ... null ...` or `zero len name`	Internal errors in the configuration parameter table. These should not occur; report them.

NOTE: *A serial receive error (noise or overrun) can leave the serial interface unresponsive until the device is reset, and a fault on the IMU I2C bus during a run can stop the device until it is reset. Neither is reported by an error message. Provide a means to reset or power-cycle WIMS from the host.*

Table 32: Configuration memory error messages.

Message	Meaning and action
`# [WRN] Configuration hash mismatch.`	The configuration stored in EEPROM is not valid, for example after a firmware update that changed the configuration parameters. The default configuration is loaded and saved, overwriting the stored calibration coefficients. See load.
`# [ERR] EEPROM read error.`, `# [ERR] load cfg fail, code 0x`*NNNNNNNN*	The configuration could not be read from EEPROM. The default configuration is loaded.
`# [ERR] EEPROM Unavailable. Cannot save configuration.`, `# [ERR] save cfg fail, code 0x`*NNNNNNNN*	The configuration could not be saved. The configuration in RAM is unchanged. Check the EEPROM supply and I2C bus.
`# [ERR] EEPROM memory size insufficient.`, `# [ERR] EEPROM allocated parameter memory size insufficient.`	The EEPROM is too small for the configuration. These should not occur with the WIMS v5.02 hardware.
`# [ERR][EEPROM] init fail code = 0x`*NNNNNNNN*`, deinit fail code`	The EEPROM driver could not be initialized or deinitialized; the code is a status code of Table 30.
`# [ERR][AT24CDRV] ...`	Errors of the AT24C512C EEPROM device driver, for example I2C transfer failures.



Table 33: Run error messages.

Message	Meaning and action
`# [ERR][WAVDRV] init fail - init imu fail code = 0x`*NN*`, # [ERR][WAVDRV] reset fail - init mpu fail code = 0x`*NN*	The IMU could not be initialized at the start of a run or magnetometer calibration; the run is not started. Check the IMU supply and I2C bus, and see the `ICMDRV` messages printed before it.
`# [ERR][WAVDRV] init rt dat fail code = 0x`*NNNNNNNN*`, # [ERR][WAVDRV] init rt fail invalid slen = `*N*	The run data could not be initialized, for example because of an invalid segment length. The run is not started.
`# [ERR][WAVDRV] fifo rd pckt fail code 0x`*NN*`, # [ERR][WAVDRV] fifo proc pckt pop fail code 0x`*NN*	An IMU FIFO packet could not be read. The run is ended, and the spectra of the completed segments are printed.
`# [ERR][WAVDRV] fifo decode packet exit code 0x`*NN*`, # [ERR][WAVDRV] fifo proc pckt fail code 0x`*NN*	An IMU FIFO packet could not be decoded or processed. The run is ended.
`# [ERR][WAVDRV] invalid sample mode, # [ERR][WAVDRV] invalid output mode`	`wav.smode` or `wav.omode` is not valid. Set a valid value.
`# [ERR][WAVDRV] invalid omode, invalid smode, invalid nupax, invalid nfwax, invalid filt, # [ERR][WAVDRV] param set fail - invalid param`	A set command gave a parameter value that is not valid. The parameter is unchanged.
`# [WRN][WAVDRV] invalid afilt: `*N*`, # [WRN][WAVDRV] setting afilt = 0`	The selected acceleration filter is not valid; filtering is disabled (`wav.afilt = 0`).

Table 34: IMU error messages.

Message	Meaning and action
`# [WRN][ICMDRV] fifo overflow`	The IMU FIFO overflowed because samples were not read in time. The FIFO is reset and the samples it held are lost, leaving a gap in the time series.
`# [WRN][ICMDRV] fifo pckt dcde:` *N* `extra bytes`	An IMU FIFO packet was longer than expected; the extra bytes are ignored.
`# [ERR][ICMDRV] dev wai fail id = 0x`*NN*, `# [ERR][ICMDRV] soft reset failed code = 0x`*NN*	The IMU did not respond with the expected device identifier, or could not be reset. Check the IMU supply and I2C bus.
`# [ERR][ICMDRV] [I2C] ...`	An I2C transfer with the IMU failed. The code is a status code of the IMU driver: `0x10`, transfer failed; `0x11`, not acknowledged after retries.
`# [ERR][ICMDRV] mag init fail code = 0x`*NN*, `set bypass fail code`, `mag self test fail code`	The magnetometer could not be initialized or tested; see mst.
`# [ERR][OFLMOD] init fail null oflt`, `reset fail null oflt`	Internal error of the orientation filter. This should not occur; report it.

9 Configuration Parameters

Table 35: Configuration parameters.

Idx.	Parameter	Type	Default	Valid Range/Values	Unit	Description	Sec. (Pg.)
0	brd.leds	bool	0	{0, 1}	-	Enable board LEDs.	9.1 (108)
1	cal.acofx	int16	0	[-32768, 32767]	counts	Accelerometer calibration coefficient: offset, X-channel	9.2 (108)
2	cal.acofy	int16	0	[-32768, 32767]	counts	Accelerometer calibration coefficient: offset, y-channel	9.2 (108)
3	cal.acofz	int16	0	[-32768, 32767]	counts	Accelerometer calibration coefficient: offset, z-channel	9.2 (108)
4	cal.acscx	int16	0	[-32768, 32767]	2^{-14}	Accelerometer calibration coefficient: scale, X-channel	9.2 (108)
5	cal.acscy	int16	0	[-32768, 32767]	2^{-14}	Accelerometer calibration coefficient: scale, y-channel	9.2 (108)
6	cal.acscz	int16	0	[-32768, 32767]	2^{-14}	Accelerometer calibration coefficient: scale, z-channel	9.2 (108)
7	cal.gcofx	int16	0	[-32768, 32767]	counts	Gyroscope calibration coefficient: offset, X-channel	9.3 (109)
8	cal.gcofy	int16	0	[-32768, 32767]	counts	Gyroscope calibration coefficient: offset, y-channel	9.3 (109)
9	cal.gcofz	int16	0	[-32768, 32767]	counts	Gyroscope calibration coefficient: offset, z-channel	9.3 (109)
10	cal.gcscx	int16	0	[-32768, 32767]	2^{-14}	Gyroscope calibration coefficient: scale, X-channel	9.3 (109)
11	cal.gcscy	int16	0	[-32768, 32767]	2^{-14}	Gyroscope calibration coefficient: scale, y-channel	9.3 (109)
12	cal.gcscz	int16	0	[-32768, 32767]	2^{-14}	Gyroscope calibration coefficient: scale, z-channel	9.3 (109)
13	cal.mcofx	int16	0	[-32768, 32767]	counts	Magnetometer calibration coefficient: offset, X-channel	9.4 (110)
14	cal.mcofy	int16	0	[-32768, 32767]	counts	Magnetometer calibration coefficient: offset, y-channel	9.4 (110)
15	cal.mcofz	int16	0	[-32768, 32767]	counts	Magnetometer calibration coefficient: offset, z-channel	9.4 (110)

Continued on next page...

Table 35: Configuration parameters (continued).

Idx.	Parameter	Type	Default	Valid Range/Values	Unit	Description	Sec. (Pg.)
16	`cal.mcscx`	int16	0	[-32768, 32767]	2^{-14}	Magnetometer calibration coefficient: scale, X-channel	9.4 (110)
17	`cal.mcscy`	int16	0	[-32768, 32767]	2^{-14}	Magnetometer calibration coefficient: scale, y-channel	9.4 (110)
18	`cal.mcscz`	int16	0	[-32768, 32767]	2^{-14}	Magnetometer calibration coefficient: scale, z-channel	9.4 (110)
19	`imu.dlpf`	uint8	24	{6, 12, 24}	Hz	IMU digital low-pass filter cutoff frequency	9.5 (110)
20	`imu.fsra`	uint8	4	{2, 4, 8, 16}	$\pm g$	IMU accelerometer full-scale range	9.6 (111)
21	`imu.fsrg`	uint16	500	{250, 500, 1000, 2000}	$\pm dps$	IMU gyroscope full-scale range	9.7 (111)
22	`imu.srate`	uint16	45	{5, 9, 15, 25, 45, 75, 125}	Hz	IMU base sample rate	9.8 (111)
23	`log.level`	uint8	2	[0, 7]	-	Log message output level	9.9 (112)
24	`run.rmode`	uint16	0	-	-	Run options bitmask	9.10 (112)
25	`run.smode`	uint16	0	-	-	Startup options bitmask	9.11 (113)
26	`serialnum`	uint16	0	-	-	WIMS serial number	9.12 (113)
27	`wav.afilt`	uint8	10	[0, 11]	-	Acceleration low-pass filter	9.13 (114)
28	`wav.fbmax`	uint16	500 (0.500)	[0, 10000]	$10^{-3}Hz$	Max. spectra frequency bin	9.14 (115)
29	`wav.fbmin`	uint16	0 (0.000)	[0, 10000]	$10^{-3}Hz$	Min. spectra frequency bin	9.15 (115)
30	`wav.gaina`	uint8	32 (4.0)	[0, 255]	$2^{-3}g/g$	Accelerometer software gain	9.16 (115)
31	`wav.mxsam`	uint16	32768	[0, 65535]	samples	Maximum samples	9.17 (116)
32	`wav.mxseg`	uint16	7	[0, 65535]	segments	Maximum segments	9.18 (116)

Continued on next page...



Table 35: Configuration parameters (continued).

Idx.	Parameter	Type	Default	Valid Range/Values	Unit	Description	Sec. (Pg.)
33	wav.nfwax	uint8	0	[0, 6]	-	Normally forward axis	9.19 (116)
34	wav.nupax	uint8	2	[0, 6]	-	Normally up axis	9.20 (116)
35	wav.obeta	uint16	1343 (0.041)	[0, 32768]	2^{-15}	Orientation filter beta	9.21 (117)
36	wav.omode	uint8	5	[0, 5]	-	Output mode	9.22 (117)
37	wav.ostsc	uint16	180	[60, 600]	seconds	Orientation filter settle time	9.23 (119)
38	wav.ozeta	uint16	163 (0.005)	[0, 32768]	2^{-15}	Orientation filter zeta	9.24 (120)
39	wav.slen	uint16	256	{64, 128, 256, 512, 1024}	samples	Segment length	9.25 (120)
40	wav.smode	uint8	2	[0, 2]	-	Sample mode	9.26 (120)
41	wav.srdiv	uint8	8	[0, 254]	$(+1)\ Hz/Hz$	Sample rate divider	9.27 (120)
42	wav.twalp	uint8	64 (0.500)	[0, 128]	2^{-7}	Tukey window function alpha	9.28 (121)

9.1 brd.leds

Idx.	Parameter	Type	Default	Valid Range/Values	Unit	Description
0	brd.leds	bool	0	{0, 1}	-	Enable board LEDs.

This parameter controls the operation of the board indicator LEDs. If set to zero, LEDs will be disabled. Otherwise, LEDs will be enabled. The indicator LED sequence is determined by the current state and repeats at an interval of 8 seconds.

9.2 cal.acof[A] and cal.acsc[A]

Idx.	Parameter	Type	Default	Valid Range/Values	Unit	Description
1	cal.acofx	int16	0	[-32768, 32767]	counts	Accelerometer calibration coefficient: offset, X-channel
2	cal.acofy	int16	0	[-32768, 32767]	counts	Accelerometer calibration coefficient: offset, y-channel
3	cal.acofz	int16	0	[-32768, 32767]	counts	Accelerometer calibration coefficient: offset, z-channel
4	cal.acscx	int16	0	[-32768, 32767]	2^{-14}	Accelerometer calibration coefficient: scale, X-channel
5	cal.acscy	int16	0	[-32768, 32767]	2^{-14}	Accelerometer calibration coefficient: scale, y-channel
6	cal.acscz	int16	0	[-32768, 32767]	2^{-14}	Accelerometer calibration coefficient: scale, z-channel

These parameters set the scale and offset corrections for accelerometer data. For more information on accelerometer calibration, see Section 6.1.1: Accelerometer Calibration. The corrections are applied to the raw measured acceleration of each axis, such that the corrected acceleration, $\hat{a}$, is given by

$$\hat{a} = \frac{\left(a - 2^{(r_a - 14)} a_o\right) \times \left(2^{14} + a_g\right)}{2^{14}}, \tag{43}$$

where a_o is the offset correction, a_g is the scale correction, and the acceleration radix, r_a, is given by Equation (2).

9.3 cal.gcof[A] and cal.gcsc[A]

Idx.	Parameter	Type	Default	Valid Range/Values	Unit	Description
7	cal.gcofx	int16	0	[-32768, 32767]	counts	Gyroscope calibration coefficient: offset, X-channel
8	cal.gcofy	int16	0	[-32768, 32767]	counts	Gyroscope calibration coefficient: offset, y-channel
9	cal.gcofz	int16	0	[-32768, 32767]	counts	Gyroscope calibration coefficient: offset, z-channel
10	cal.gcscx	int16	0	[-32768, 32767]	2^{-14}	Gyroscope calibration coefficient: scale, X-channel
11	cal.gcscy	int16	0	[-32768, 32767]	2^{-14}	Gyroscope calibration coefficient: scale, y-channel
12	cal.gcscz	int16	0	[-32768, 32767]	2^{-14}	Gyroscope calibration coefficient: scale, z-channel

These parameters set the scale and offset corrections for gyroscope data. For more information on gyroscope calibration, see Section 6.1.2: Gyroscope Calibration. The corrections are applied to the raw measured angular rate of each axis, such that the corrected angular rate, $\hat{\omega}$, is given by

$$\hat{\omega} = \frac{(\omega - \omega_o) \times \left(2^{14} + \omega_g\right)}{2^{14}}, \tag{44}$$

where ω_o is the offset correction and ω_g is the scale correction.

9.4 cal.mcof[A] and cal.mcsc[A]

Idx.	Parameter	Type	Default	Valid Range/Values	Unit	Description
13	`cal.mcofx`	int16	0	[-32768, 32767]	counts	Magnetometer calibration coefficient: offset, X-channel
14	`cal.mcofy`	int16	0	[-32768, 32767]	counts	Magnetometer calibration coefficient: offset, y-channel
15	`cal.mcofz`	int16	0	[-32768, 32767]	counts	Magnetometer calibration coefficient: offset, z-channel
16	`cal.mcscx`	int16	0	[-32768, 32767]	2^{-14}	Magnetometer calibration coefficient: scale, X-channel
17	`cal.mcscy`	int16	0	[-32768, 32767]	2^{-14}	Magnetometer calibration coefficient: scale, y-channel
18	`cal.mcscz`	int16	0	[-32768, 32767]	2^{-14}	Magnetometer calibration coefficient: scale, z-channel

These parameters set the scale and offset corrections for magnetometer data. For more information on magnetometer calibration, see Section 6.1.3: Magnetometer Calibration. The corrections are applied to the raw measured magnetism of each axis, such that the corrected magnetism, $\hat{H}$, is given by

$$\hat{H} = \frac{(H - H_o) \times \left(2^{14} + H_g\right)}{2^{14}}, \tag{45}$$

where H_o is the offset correction and H_g is the scale correction.

9.5 imu.dlpf

Idx.	Parameter	Type	Default	Valid Range/Values	Unit	Description
19	`imu.dlpf`	uint8	24	{6, 12, 24}	Hz	IMU digital low-pass filter cutoff frequency

This parameter sets the cutoff frequency of the IMU's onboard digital low-pass filter (DLPF). The accelerometer and gyroscope filters are configured separately, each to the highest available cutoff frequency that does not exceed this parameter, or to 6 Hz if this parameter is less than 6 Hz. The available accelerometer cutoff frequencies are 6, 12, 24, 50, 111, and 246 Hz, and the available gyroscope cutoff frequencies are 6, 12, 24, 51, 120, 152, and 197 Hz. Values of 6, 12, and 24 Hz select the same cutoff frequency for both sensors.

> **NOTE:** *For spectral output modes, it is recommended that this parameter be set to* $24Hz$.

9.6 imu.fsra

Idx.	Parameter	Type	Default	Valid Range/Values	Unit	Description
20	`imu.fsra`	uint8	4	{2, 4, 8, 16}	$\pm g$	IMU accelerometer full-scale range

This parameter set the full-scale range of the accelerometer. The available ranges are $\pm 2, \pm 4, \pm 8$, and $\pm 16g$. This parameter affect the spectra scale sensitivity (see Section 7.3: Scale Sensitivity).

> **NOTE:** *For spectral output modes, it is recommended that this parameter be set to* $\pm 4g$.

9.7 imu.fsrg

Idx.	Parameter	Type	Default	Range	Unit	Description
21	`imu.fsrg`	uint16	500	{250,500,1000,2000}	$\pm dps$	IMU gyroscope full-scale range

This parameter set the full-scale range of the gyroscope. The available ranges are $\pm 250, \pm 500, \pm 1000$, and $\pm 2000 dps$.

> **NOTE:** *For spectral output modes, this parameter must always be set to* $\pm 500 dps$.

9.8 imu.srate

Idx.	Parameter	Type	Default	Range	Unit	Description
22	`imu.srate`	uint16	45	{5, 9, 15, 25, 45, 75, 125}	Hz	IMU base sample rate

This parameter sets the IMU sample rate. This is the rate at which the orientation filter is updated.

The IMU derives its sample rate from a 1125 Hz base rate using an integer divider, so the sample rate applied is $\lfloor 1125/\lfloor 1125/\texttt{imu.srate} \rfloor \rfloor$ Hz. Values of `imu.srate` are limited to the range 5 to 225 Hz. The listed values are applied exactly. Other values are rounded; for example, 50 Hz results in a sample rate of 51 Hz.

The IMU sample rate affects effective sample rate, f_e, defined in Equation (13), which in turn affects the run duration (see Section 6.4.1: Run Duration) and the spectra frequencies (see Section 7.2: Spectra Frequencies).

> **NOTE:** *For spectral output modes, it is recommended that this parameter be set to the default, $45Hz$, with `wav.srdiv` $= 8$, the default, for an effective sample rate of $5Hz$.*

9.9 log.level

Idx.	Parameter	Type	Default	Valid Range/Values	Unit	Description
23	`log.level`	uint8	2	[0, 7]	-	Log message output level

This enumerated parameter sets the verbosity of serial interface log message output. The enumerated log level values are shown in Table 36. The default log level is 2 for release builds and 3 for debug builds.

Table 36: Serial interface log levels.

Value	Log Tag	Log Level
`log.level = 0`	`ERR`	Error messages only
`log.level = 1`	`WRN`	Errors and warnings
`log.level = 2`	`OUT`	Standard output
`log.level = 3`	`INF`	Standard output plus additional informational messages
`log.level = 4`	`DBG`	Debug output (debug builds only)
`log.level = 5`	`TR1`	Debug trace level 1 output (debug builds only)
`log.level = 6`	`TR2`	Debug trace level 2 output (debug builds only)
`log.level = 7`	`TR3`	Debug trace level 3 output (debug builds only)

9.10 run.rmode

Idx.	Parameter	Type	Default	Valid Range/Values	Unit	Description
24	`run.rmode`	uint16	0	-	-	Run options bitmask

The parameter sets the run mode bitmask options. These options affect the behavior of WIMS at the start of a run (see Section 6.4: Run Behavior). The bitmask options are shown in Table 37.



Table 37: Run mode (`run.rmode`) bitmask.

15	14	13	12	11	10	9	8	7	6	5	4	3	2	1	0
RESERVED													CONT	RUNINFO	GETALL

Option	Description
GETALL	Invoke the "get all" command before initiating the run. See Section 8.2.2: get.
RUNINFO	Invoke the "runinfo" command before initiating the run. See Section 8.2.10: runinfo.
CONT	Run continuously by immediately starting a new run after completing a run. The GETALL and RUNINFO options apply only to the first run. Continuous running stops when any character is received on the serial interface.

9.11 run.smode

Idx.	Parameter	Type	Default	Valid Range/Values	Unit	Description
25	`run.smode`	uint16	0	-	-	Startup options bitmask

The parameter sets the start mode bitmask options. These options affect the behavior of WIMS after a reset (see Section 6.3: Reset Behavior). The bitmask options are shown in Table 38.

Table 38: Start mode (`run.smode`) bitmask.

15	14	13	12	11	10	9	8	7	6	5	4	3	2	1	0
RESERVED															RUN

Option	Description
RUN	WIMS will immediately initiate a run after reset by invoking the "run" command.

9.12 serialnum

Idx.	Parameter	Type	Default	Valid Range/Values	Unit	Description
26	`serialnum`	uint16	0	-	-	WIMS serial number

The parameter sets the serial number which uniquely identifies the WIMS module.

9.13 wav.afilt

Idx.	Parameter	Type	Default	Valid Range/Values	Unit	Description
27	`wav.afilt`	uint8	10	[0, 11]	-	Acceleration low-pass filter

This enumerated parameter sets the acceleration finite-impulse response (FIR) low-pass filter (LPF). The filter options are shown in Table 39. Setting `wav.afilt = 0` disables FIR filtering, and acceleration data is instead filtered by a rolling average filter with width `wav.srdiv` + 1.

> **NOTE:** *For spectral output modes, it is recommended that this parameter be set to 10.*

Table 39: Acceleration finite-impulse response FIR LPF characteristics for base sample rate, `imu.srate` = 45 Hz.

Value	Order	Passband [Hz]	Passband Ripple [dB]	-3dB Corner [Hz]	Stopband [Hz]	Stopband Atten. [dB]	Group Delay [seconds]
`wav.afilt = 0`[1]	8	-	-	2.227	4.050	> 12	0.089
`wav.afilt = 1`	62	0.375	< 0.008	1.138	2.500	> 59	0.689
`wav.afilt = 2`	62	2.250	< 0.005	3.317	5.000	> 63	0.689
`wav.afilt = 3`	126	0.500	< 0.005	1.038	1.875	> 63	1.400
`wav.afilt = 4`	126	1.000	< 0.004	1.590	2.500	> 68	1.400
`wav.afilt = 5`	126	2.500	< 0.008	2.982	3.750	> 61	1.400
`wav.afilt = 6`	254	0.500	< 0.004	0.795	1.250	> 64	2.822
`wav.afilt = 7`	254	1.000	< 0.002	1.353	1.875	> 66	2.822
`wav.afilt = 8`	254	1.625	< 0.004	1.978	2.500	> 68	2.822
`wav.afilt = 9`	510	0.250	< 0.005	0.397	0.625	> 61	5.667
`wav.afilt = 10`	510	0.875	< 0.006	1.023	1.250	> 62	5.667
`wav.afilt = 11`	510	2.125	< 0.005	2.274	2.500	> 62	5.667

[1] For `wav.srdiv` = 8.

9.14 wav.fbmax

Idx.	Parameter	Type	Default	Valid Range/Values	Unit	Description
28	`wav.fbmax`	uint16	500	[0, 10000]	mHz	Max. spectra frequency bin

This parameter sets the maximum reported spectra frequency bin (see Section 7.2: Spectra Frequencies).

> **NOTE:** *For spectral output modes, it is recommended that this parameter be set to* $500mHz$.

9.15 wav.fbmin

Idx.	Parameter	Type	Default	Valid Range/Values	Unit	Description
29	`wav.fbmin`	uint16	0	[0, 10000]	mHz	Min. spectra frequency bin

This parameter sets the minimum reported spectra frequency bin (see Section 7.2: Spectra Frequencies).

> **NOTE:** *For spectral output modes, it is recommended that this parameter be set to* $0mHz$.

9.16 wav.gaina

Idx.	Parameter	Type	Default	Valid Range/Values	Unit	Description
30	`wav.gaina`	uint8	32 (4.000)	[0, 255]	$2^{-3}g/g$	Accelerometer software gain

This parameter sets the software gain for acceleration in spectral output modes. The gain is applied after the segment mean is removed and before trend removal. The software gain affects spectra scale sensitivity (see Section 7.3: Scale Sensitivity). Setting this parameter to 0 disables the software gain, which is then equivalent to a gain of 1 (`wav.gaina` $= 8$).

> **NOTE:** *For spectral output modes it is recommended for this parameter to be set 32 (*$4.000g/g$*).*

9.17 wav.mxsam

Idx.	Parameter	Type	Default	Valid Range/Values	Unit	Description
31	wav.mxsam	uint16	32768	[0, 65535]	samples	Maximum samples

This parameter sets the maximum number of samples collected during a run (after downsampling). Setting this value to zero allows an infinite number of samples. The maximum number of samples affects the run duration (see Section 6.4.1: Run Duration).

9.18 wav.mxseg

Idx.	Parameter	Type	Default	Valid Range/Values	Unit	Description
32	wav.mxseg	uint16	7	[0, 65535]	segments	Maximum segments

This parameter sets the maximum number of segments during a run in spectral output modes. The maximum number of segments affects the run duration (see Section 6.4.1: Run Duration).

9.19 wav.nfwax

Idx.	Parameter	Type	Default	Valid Range/Values	Unit	Description
33	wav.nfwax	uint8	0	[0, 6]	-	Normally forward axis

This enumerated parameter sets the normally-forward facing axis based on the mounting orientation of the device. The enumerated values are shown in Table 40. Equivalent orientation representation for combinations for wav.nfwax and wav.nupax are shown in Table 41. By setting this parameter appropriately, azimuth estimates can be correctly referenced to the forward direction of the host platform.

9.20 wav.nupax

Idx.	Parameter	Type	Default	Valid Range/Values	Unit	Description
34	wav.nupax	uint8	2	[0, 6]	-	Normally up axis

This enumerated parameter sets the normally-upward facing axis based on the mounting orientation of the device. The enumerated values are shown in Table 40. Equivalent orientation representation

Table 40: Axis enumeration for `wav.nfwax` and `wav.nupax`.

Value	Axis
0	None
1	Positive Z-axis.
2	Positive Y-axis.
3	Positive X-axis.
4	Negative Z-axis.
5	Negative Y-axis.
6	Negative X-axis.

for combinations for `wav.nfwax` and `wav.nupax` are shown in Table 41. By setting this parameter appropriately, the maximum initial orientation filter settle time can be significantly reduced.

9.21 wav.obeta

Idx.	Parameter	Type	Default	Valid Range/Values	Unit	Description
35	`wav.obeta`	uint16	1343 (0.041)	[0, 32768]	2^{-15}	Orientation filter beta

This parameter sets the orientation filter beta parameter (see Section 6.2: Orientation Filter), which is the primary tunable parameter that controls the relative contributions of the angular rate data from the gyroscope and gradient descent toward the reference vector (from acceleration and magnetism).

> **NOTE:** *This parameter has been tuned based on the work of Madgwick et al [3] and should not normally be changed from the default value.*

9.22 wav.omode

Idx.	Parameter	Type	Default	Valid Range/Values	Unit	Description
36	`wav.omode`	uint8	5	[0, 5]	-	Output mode

This parameter sets the WIMS output mode. The available output modes are shown in Table 42.

The output record format of each mode is described in Section 8.3: Output Message Formats.

Table 41: Equivalent orientation representation for combinations for `wav.nfwax` and `wav.nupax`.

Idx.	Axis			Tait-Bryan Angles			Quaternion ($\times 2^{14}$)			
	Upward (Z)	Forward (Y)	Right (X)	ψ (yaw)	θ (pitch)	ϕ (roll)	q_0	q_1	q_2	q_3
1	z	y	x	0	0	0	16384	0	0	0
2	-y	z	x	-90	-90	-90	11585	-11585	0	0
	-y	z	x	0	-90	0	11585	-11585	0	0
	-y	z	x	90	-90	90	11585	-11585	0	0
	-y	z	x	180	-90	180	11585	-11585	0	0
3	-z	-y	x	180	0	180	0	-16384	0	0
4	y	-z	x	90	90	-90	11585	11585	0	0
	y	-z	x	0	90	0	11585	11585	0	0
	y	-z	x	-90	90	90	11585	11585	0	0
	y	-z	x	180	90	180	-11585	-11585	0	0
5	-z	x	y	180	0	-90	0	11585	11585	0
6	x	z	y	-90	0	-90	8192	-8192	-8192	-8192
7	z	-x	y	0	0	-90	11585	0	0	-11585
8	-x	-z	y	90	0	-90	8192	8192	8192	-8192
9	y	x	z	180	90	-90	8192	8192	8192	8192
	y	x	z	90	90	0	8192	8192	8192	8192
	y	x	z	0	90	90	8192	8192	8192	8192
	y	x	z	-90	90	180	8192	8192	8192	8192
10	-x	y	z	90	0	0	11585	0	11585	0
11	-y	-x	z	0	-90	-90	8192	-8192	8192	-8192
	-y	-x	z	90	-90	0	8192	-8192	8192	-8192
	-y	-x	z	180	-90	90	8192	-8192	8192	-8192
	-y	-x	z	-90	-90	180	-8192	8192	-8192	8192
12	x	-y	z	-90	0	180	0	11585	0	11585
13	-z	y	-x	180	0	0	0	0	16384	0
14	y	z	-x	-90	90	-90	0	0	-11585	-11585
	y	z	-x	180	90	0	0	0	11585	11585
	y	z	-x	90	90	90	0	0	11585	11585
	y	z	-x	0	90	180	0	0	11585	11585
15	z	-y	-x	0	0	180	0	0	0	16384
16	-y	-z	-x	90	-90	-90	0	0	11585	-11585
	-y	-z	-x	180	-90	0	0	0	11585	-11585
	-y	-z	-x	-90	-90	90	0	0	-11585	11585
	-y	-z	-x	0	-90	180	0	0	-11585	11585
17	z	x	-y	0	0	90	11585	0	0	11585
18	-x	z	-y	90	0	90	8192	-8192	8192	8192
19	-z	-x	-y	180	0	90	0	-11585	11585	0
20	x	-z	-y	-90	0	90	8192	8192	-8192	8192
21	-y	x	-z	180	-90	-90	-8192	8192	8192	-8192
	-y	x	-z	-90	-90	0	8192	-8192	-8192	8192
	-y	x	-z	0	-90	90	8192	-8192	-8192	8192
	-y	x	-z	90	-90	180	8192	-8192	-8192	8192
22	x	y	-z	-90	0	0	11585	0	-11585	0
23	y	-x	-z	0	90	-90	8192	8192	-8192	-8192
	y	-x	-z	-90	90	0	8192	8192	-8192	-8192
	y	-x	-z	180	90	90	-8192	-8192	8192	8192
	y	-x	-z	90	90	180	-8192	-8192	8192	8192
24	-x	-y	-z	90	0	180	0	-11585	0	11585

Table 42: Output modes.

Value	Mode
`wav.omode = 0`	Raw output mode. Read raw accelerometer, gyroscope, and magnetometer samples.
`wav.omode = 1`	Orientation filter output mode. Read raw accelerometer, gyroscope, and magnetometer samples. Prints intermediate values from orientation filter and orientation estimates.
`wav.omode = 2`	Earth-frame acceleration mode. Read out acceleration in earth-fixed coordinates, referenced to magnetic north.
`wav.omode = 3`	Euler angles mode. Reports the Euler angles ψ, θ, and ϕ of the orientation estimate, in binary radians, referenced to magnetic north.
`wav.omode = 4`	Vertical spectral output mode. Reports the power-spectral density of the earth-frame vertical acceleration only.
`wav.omode = 5`	Full (directional) spectral output mode. Reports six spectra necessary for reconstruction of directional wave-field properties.

9.23 wav.ostsc

Idx.	Parameter	Type	Default	Valid Range/Values	Unit	Description
37	`wav.ostsc`	uint16	180	[60, 600]	seconds	Orientation filter settle time

This parameter sets the orientation filter settle time, in seconds. When in spectral output modes, this is the duration allotted to allow the orientation filter to converge before spectral signal processing begins. This parameter affects the run duration in spectral output modes (see Section 6.4.1: Run Duration).

9.24 wav.ozeta

Idx.	Parameter	Type	Default	Valid Range/Values	Unit	Description
38	wav.ozeta	uint16	163 (0.005)	[0, 32768]	2^{-15}	Orientation filter zeta

This parameter set the orientation filter zeta parameter. This parameter sets the rate of convergence of the dynamic gyroscope bias correction (see Section 6.2: Orientation Filter). If set to zero, the dynamic gyroscope bias correction is disabled.

9.25 wav.slen

Idx.	Parameter	Type	Default	Valid Range/Values	Unit	Description
39	wav.slen	uint16	256	{64, 128, 256, 512, 1024}	samples	Segment length

This parameter sets the segment length for spectral processing. In spectral output modes, this parameter affects both the run duration (see Section 6.4.1: Run Duration) and the spectra frequency bins (see Section 7.2: Spectra Frequencies).

9.26 wav.smode

Idx.	Parameter	Type	Default	Valid Range/Values	Unit	Description
40	wav.smode	uint8	2	[0, 2]	-	Sample mode

This parameter sets the sample mode. The sample mode determines the method in which samples are retrieved from the IMU. The sample modes are shown in Table 43.

> **NOTE:** *It is not recommended that this parameter is changed from the default value.*

9.27 wav.srdiv

Idx.	Parameter	Type	Default	Valid Range/Values	Unit	Description
41	wav.srdiv	uint8	8	[0, 254]	$(+1)\ Hz/Hz$	Sample rate divider



Table 43: Sample modes.

Value	Mode
`wav.smode = 0`	IMU polled sampling.
`wav.smode = 1`	IMU polled interrupt-driven sampling,
`wav.smode = 2`	IMU interrupt-driven sampling.

This parameter sets the sample rate divider which determines the downsample rate, resulting in the effective sample rate, f_e, defined in Equation (13). This parameter affects the run duration (see Section 6.4.1: Run Duration) and, in spectral output modes, the spectra frequency bins (see Section 7.2: Spectra Frequencies).

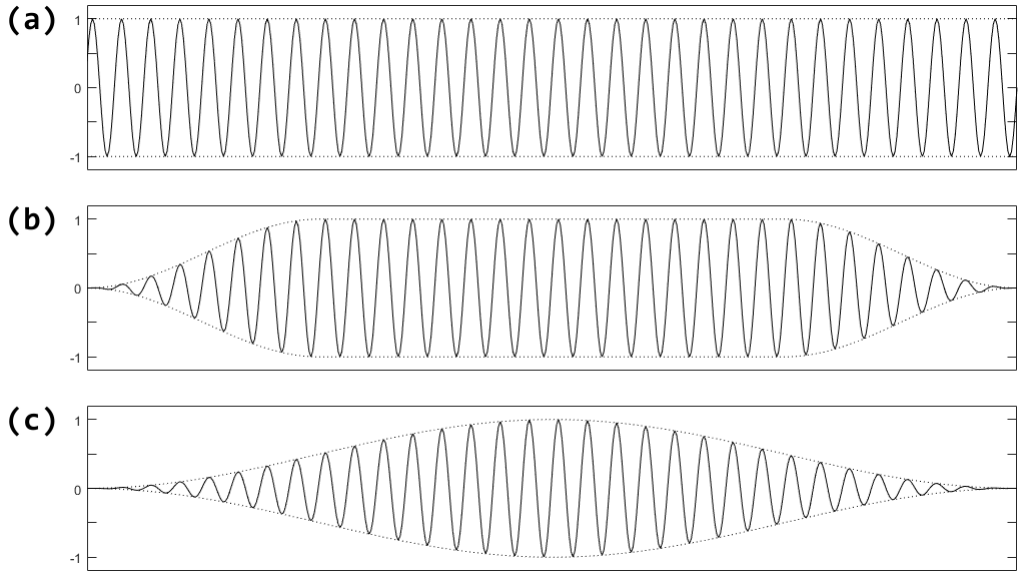
> **NOTE:** *In spectral output modes, it is recommended to set this parameter to the default, 8, with* `imu.srate` *= 45 for an effective sample rate of* $5Hz$*. Firmware versions up to and including v2.01.00616b had a default of 17, for an effective sample rate of* $2.5Hz$*.*

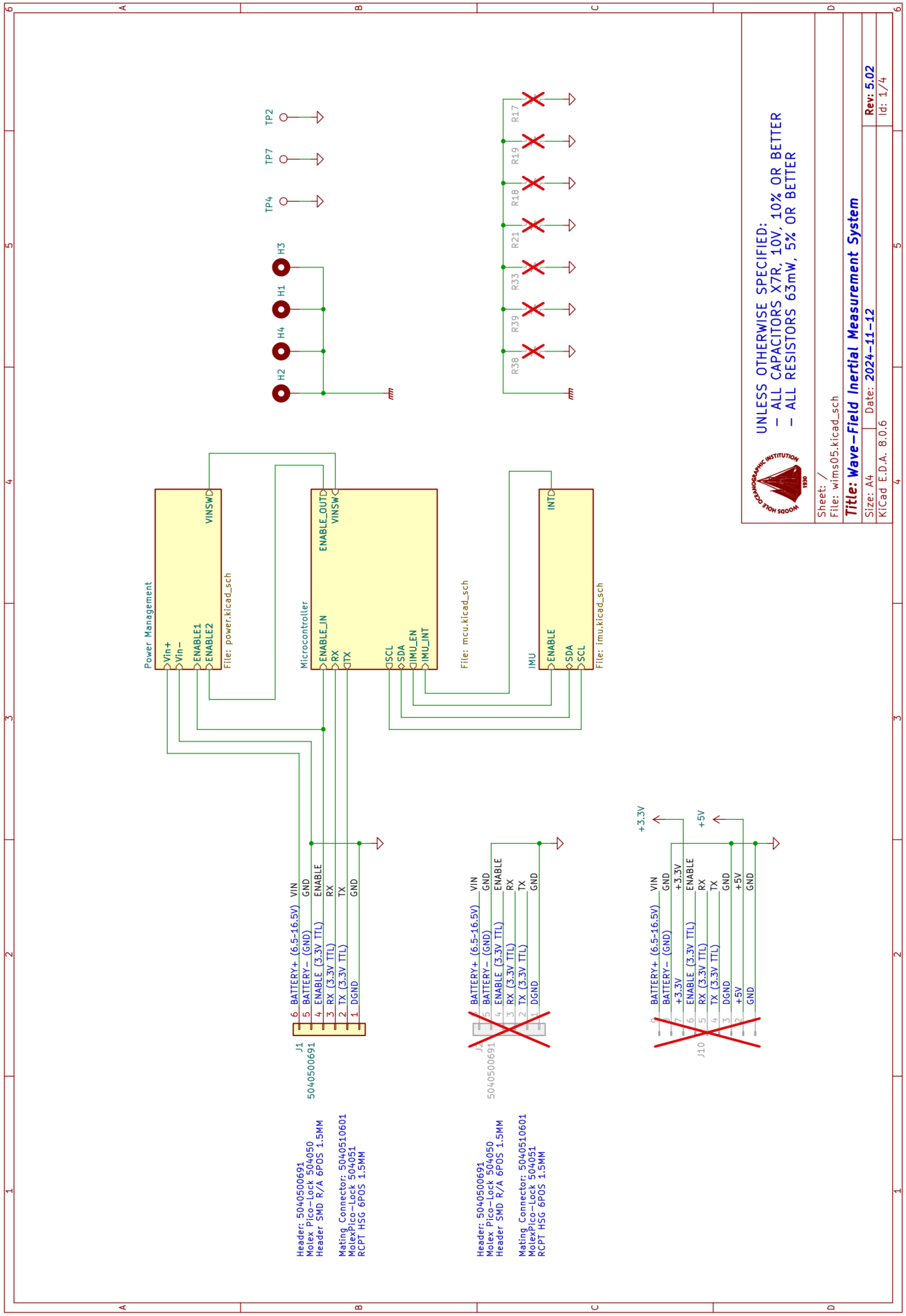
9.28 wav.twalp

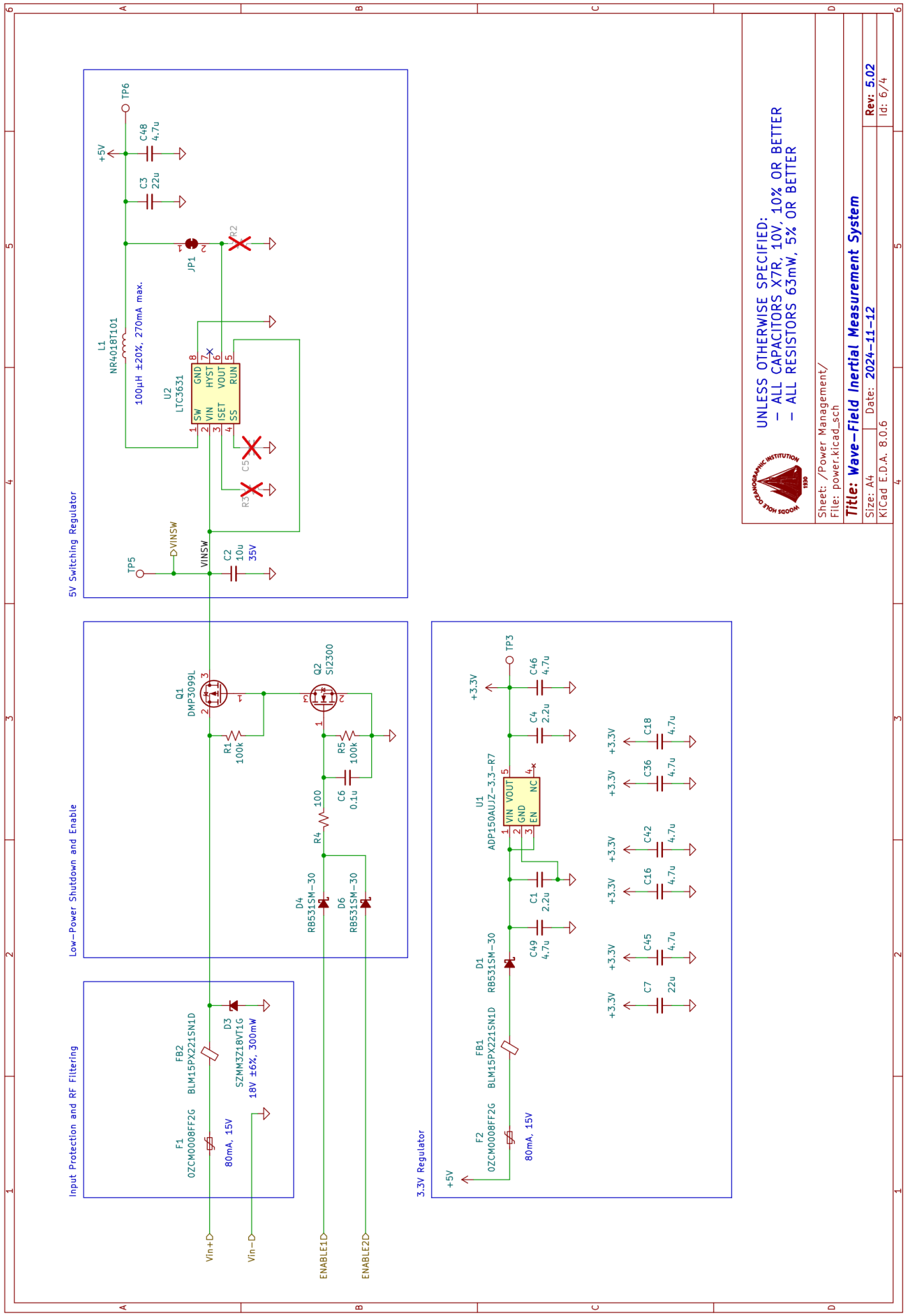
Idx.	Parameter	Type	Default	Valid Range/Values	Unit	Description
42	`wav.twalp`	uint8	64 (0.500)	[0, 128]	2^{-7}	Tukey window function alpha

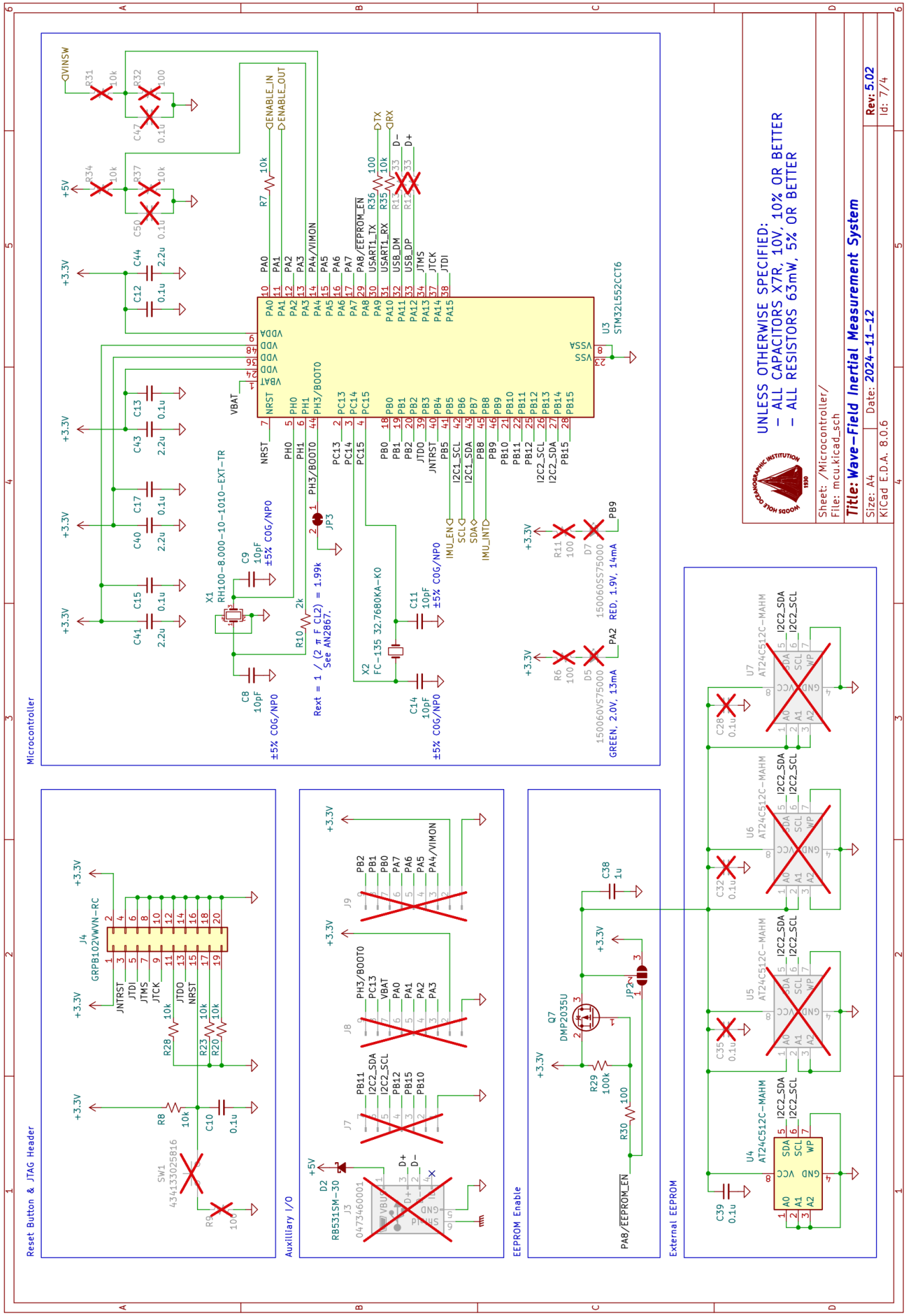
This parameter sets the Tukey window alpha parameter. The Tukey window is applied to each segment in spectral output modes before the CFFT is applied for spectral leakage reduction (see Section 6: Operation). The effect of the alpha parameter is shown in Figure 29.

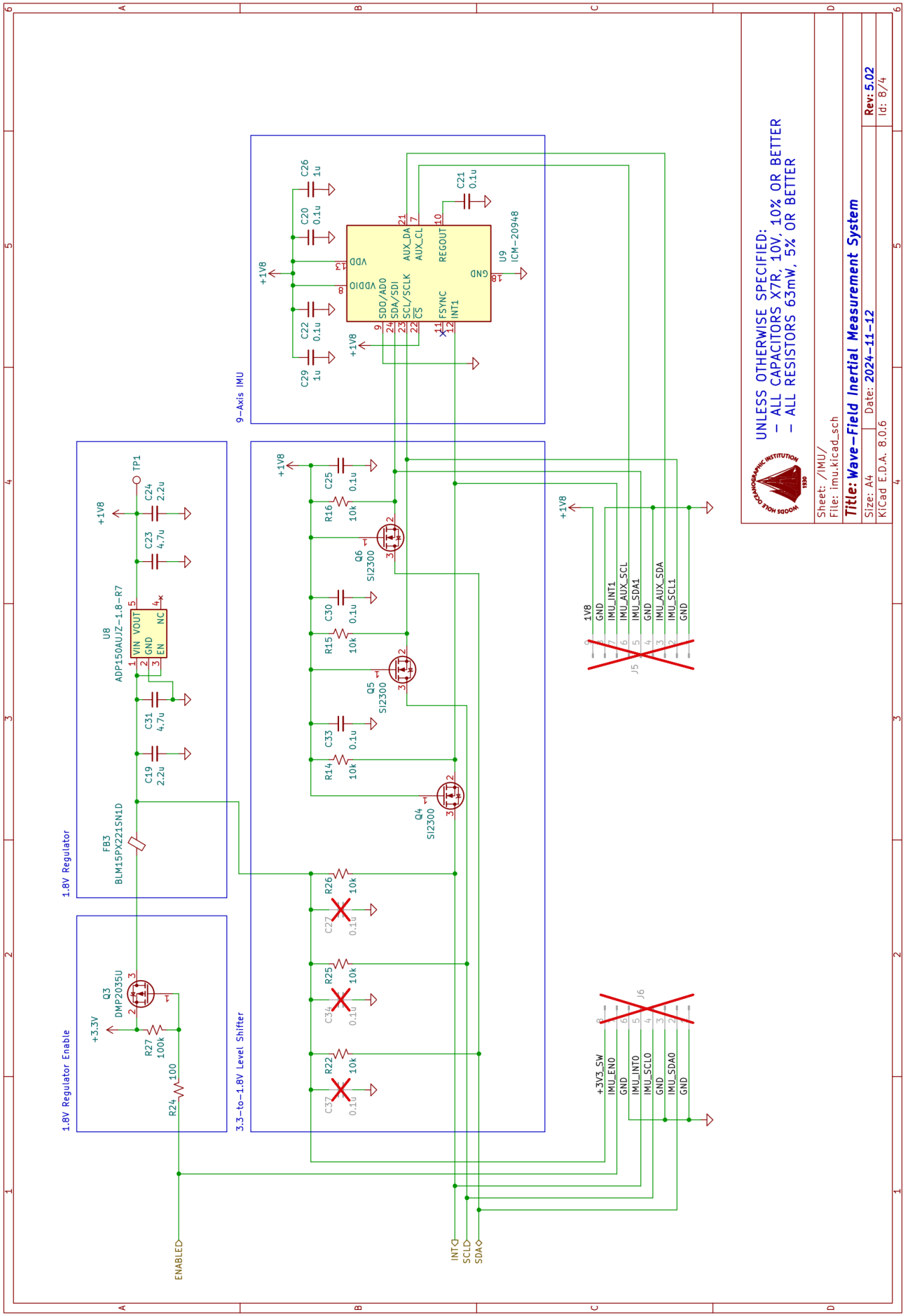
Figure 29: Effect of Tukey window cosine taper for (a) $\alpha = 0.0$, (b) $\alpha = 0.5$, and (c) $\alpha = 1.0$.



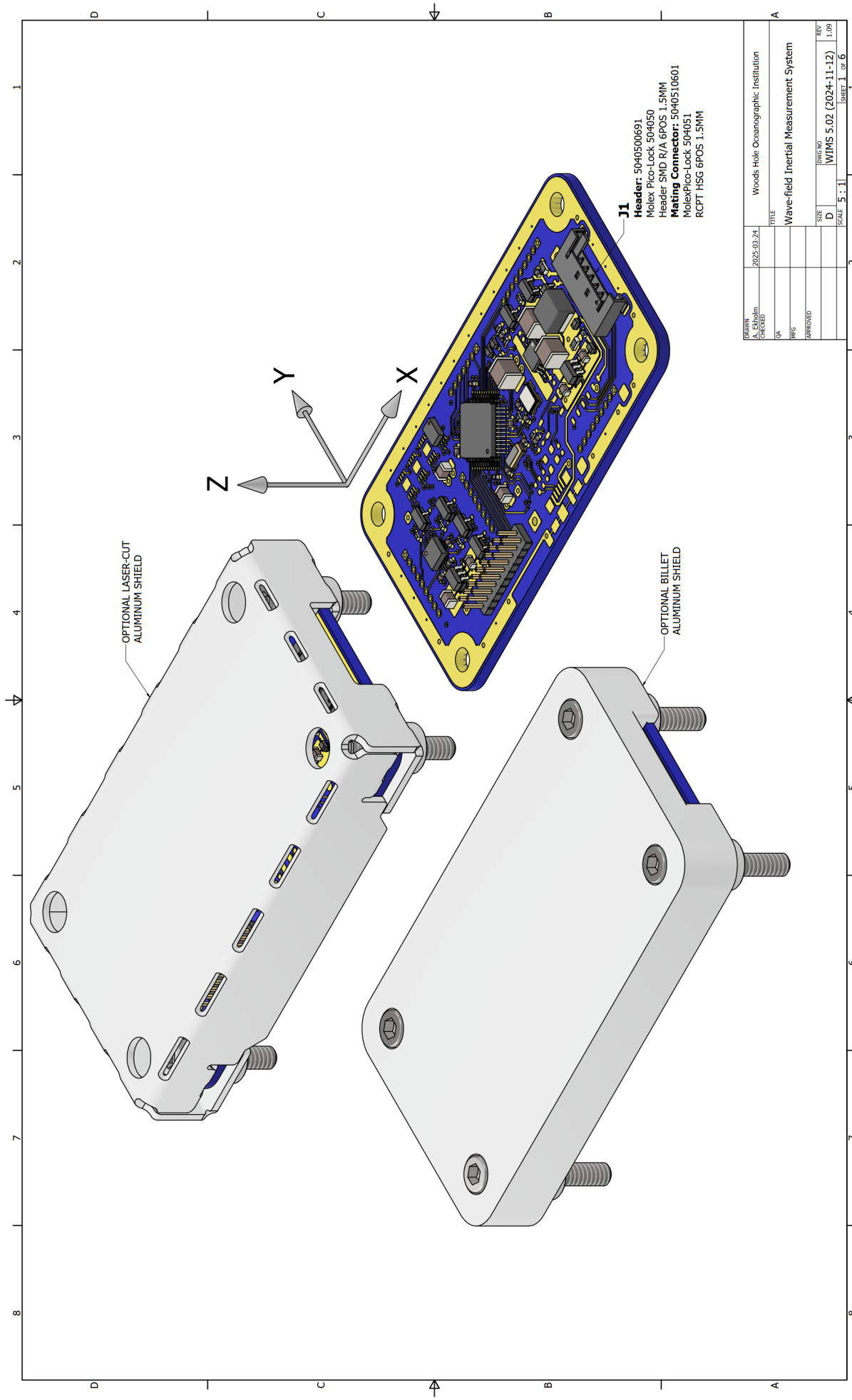

UNLESS OTHERWISE SPECIFIED:
- ALL CAPACITORS X7R, 10V, 10% OR BETTER
- ALL RESISTORS 63mW, 5% OR BETTER
Sheet: /
File: wims05.kicad_sch
Title: Wave-Field Inertial Measurement System
Size: A4
Date: 2024-11-12
Rev: 5.02
KiCad E.D.A. 8.0.6
Id: 1/4
Power Management
Vin+
Vin-
ENABLE1
ENABLE2
VINSW
File: power.kicad_sch
Microcontroller
ENABLE_IN
RX
TX
ENABLE_OUT
VINSW
SCL
SDA
IMU_EN
IMU_INT
File: mcu.kicad_sch
IMU
ENABLE
SDA
SCL
INT
File: imu.kicad_sch
H1
H2
H3
H4
TP2
TP4
TP7
R17
R19
R18
R21
R33
R39
R38
J1
5040500691
6 BATTERY+ (6.5-16.5V)
5 BATTERY- (GND)
4 ENABLE (3.3V TTL)
3 RX (3.3V TTL)
2 TX (3.3V TTL)
1 DGND
VIN
GND
ENABLE
RX
TX
GND
Header: 5040500691
Molex Pico-Lock 504050
Header SMD R/A 6POS 1.5MM
Mating Connector: 5040510601
MolexPico-Lock 504051
RCPT HSG 6POS 1.5MM
J2
5040500691
BATTERY+ (6.5-16.5V)
BATTERY- (GND)
ENABLE (3.3V TTL)
RX (3.3V TTL)
TX (3.3V TTL)
DGND
VIN
GND
ENABLE
RX
TX
GND
Header: 5040500691
Molex Pico-Lock 504050
Header SMD R/A 6POS 1.5MM
Mating Connector: 5040510601
MolexPico-Lock 504051
RCPT HSG 6POS 1.5MM
J10
+3.3V
+5V
BATTERY+ (6.5-16.5V)
BATTERY- (GND)
+3.3V
ENABLE (3.3V TTL)
RX (3.3V TTL)
TX (3.3V TTL)
DGND
+5V
GND
VIN
GND
+3.3V
ENABLE
RX
TX
GND
+5V
GND

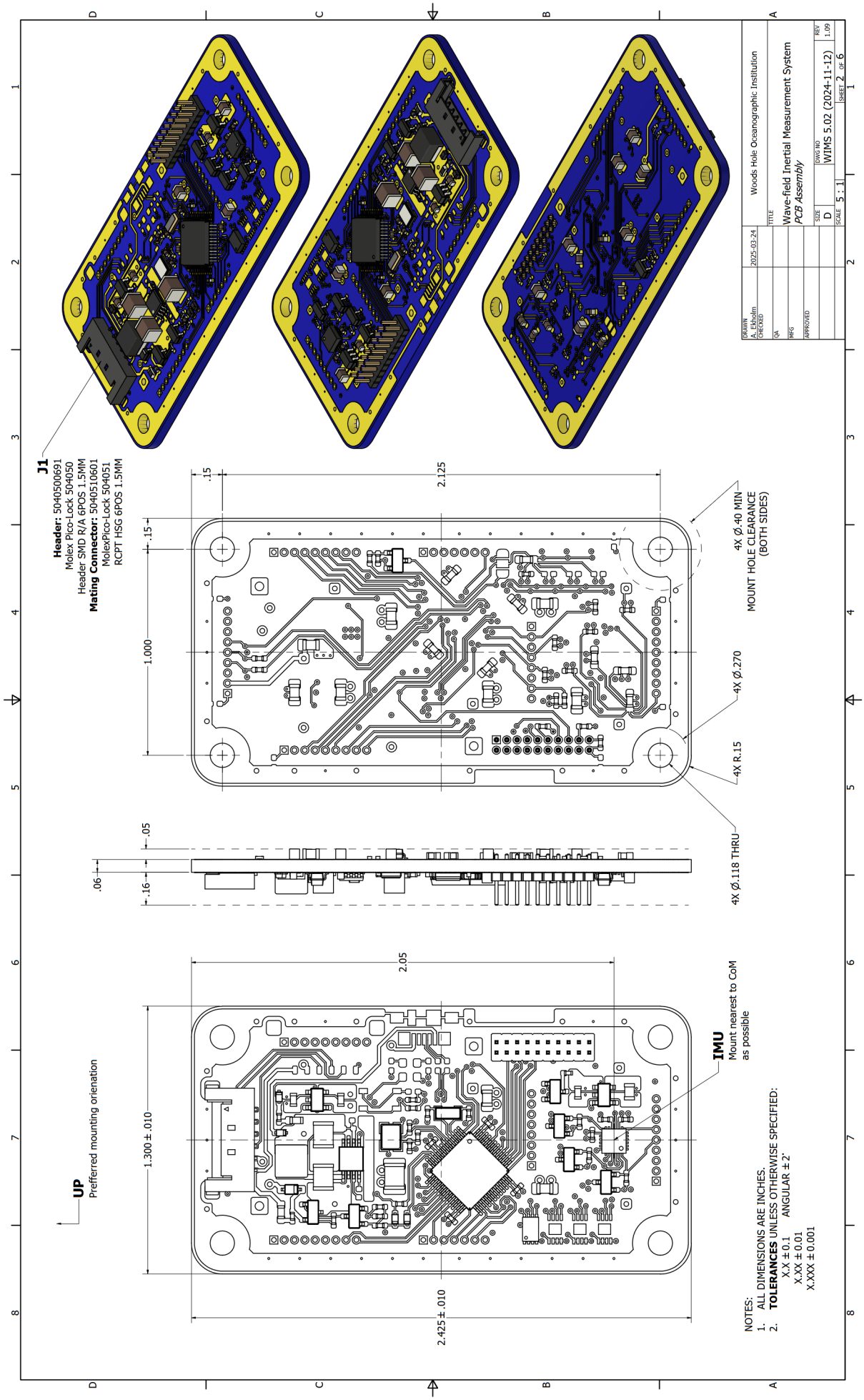

UNLESS OTHERWISE SPECIFIED:
– ALL CAPACITORS X7R, 10V, 10% OR BETTER
– ALL RESISTORS 63mW, 5% OR BETTER
WOODS HOLE OCEANOGRAPHIC INSTITUTION 1930
Sheet: /Power Management/
File: power.kicad_sch
Title: Wave–Field Inertial Measurement System
Size: A4
Date: 2024–11–12
Rev: 5.02
KiCad E.D.A. 8.0.6
Id: 6/4
5V Switching Regulator
TP6
+5V
C48 4.7u
C3 22u
JP1
R2
L1
NR4018T101
100µH ±20%, 270mA max.
U2
LTC3631
GND HYST VOUT RUN
SW VIN ISET SS
C5
R3
TP5
VINSW
C2 10u 35V
Low–Power Shutdown and Enable
Q1
DMP3099L
Q2
SI2300
R1 100k
R5 100k
C6 0.1u
R4 100
D4
RB531SM–30
D6
RB531SM–30
3.3V Regulator
TP3
+3.3V
C46 4.7u
C4 2.2u
U1
ADP150AUJZ–3.3–R7
VIN VOUT GND NC EN
C1 2.2u
C49 4.7u
D1
RB531SM–30
FB1
BLM15PX221SN1D
F2
0ZCM0008FF2G
80mA, 15V
C18 4.7u
C36 4.7u
C42 4.7u
C16 4.7u
C45 4.7u
C7 22u
Input Protection and RF Filtering
FB2
BLM15PX221SN1D
D3
SZMM3Z18VT1G
18V ±6%, 300mW
F1
0ZCM0008FF2G
80mA, 15V
Vin+
Vin–
ENABLE1
ENABLE2

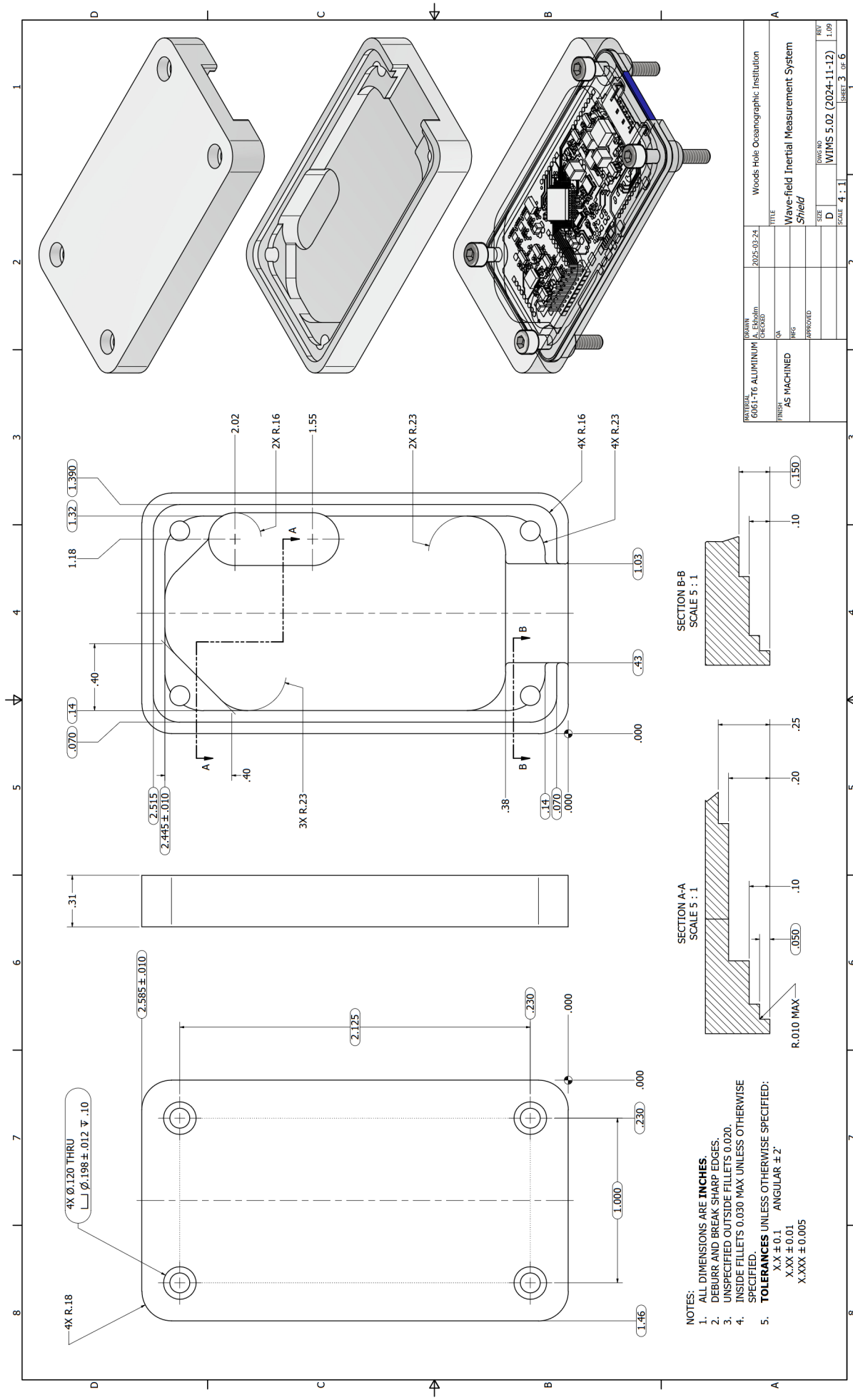

Microcontroller
Reset Button & JTAG Header
Auxiliary I/O
EEPROM Enable
External EEPROM
STM32L552CCT6
AT24C512C-MAHM
GRPB102VWVN-RC
RB531SM-30
DMP2035U
UNLESS OTHERWISE SPECIFIED:
- ALL CAPACITORS X7R, 10V, 10% OR BETTER
- ALL RESISTORS 63mW, 5% OR BETTER
Title: Wave-Field Inertial Measurement System
Rev: 5.02
Size: A4
Date: 2024-11-12
KiCad E.D.A. 8.0.6
Id: 7/4
Sheet: /Microcontroller/
File: mcu.kicad_sch

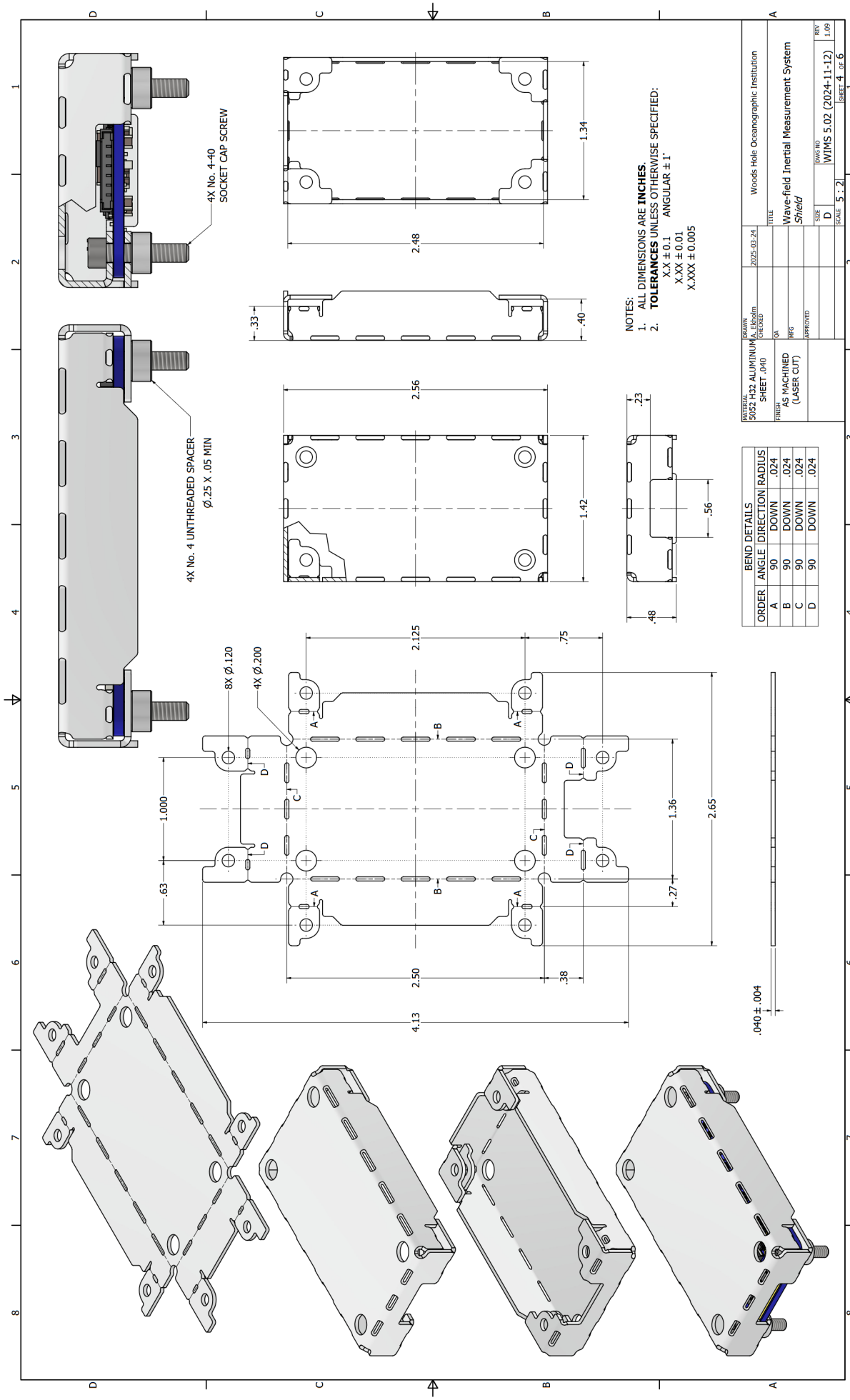

UNLESS OTHERWISE SPECIFIED:
- ALL CAPACITORS X7R, 10V, 10% OR BETTER
- ALL RESISTORS 63mW, 5% OR BETTER
Sheet: /IMU/
File: imu.kicad_sch
Title: Wave-Field Inertial Measurement System
Size: A4
Date: 2024-11-12
Rev: 5.02
KiCad E.D.A. 8.0.6
Id: 8/4
9-Axis IMU
U9
ICM-20948
1.8V Regulator
U8
ADP150AUJZ-1.8-R7
FB3
BLM15PX221SN1D
1.8V Regulator Enable
Q3
DMP2035U
3.3-to-1.8V Level Shifter
Q4
Q5
Q6
SI2300
TP1
ENABLED
INT
SCL
SDA
+1V8
+3.3V
+3V3_SW
GND
IMU_INT1
IMU_AUX_SCL
IMU_SDA1
IMU_AUX_SDA
IMU_SCL1
IMU_EN0
IMU_INT0
IMU_SCL0
IMU_SDA0

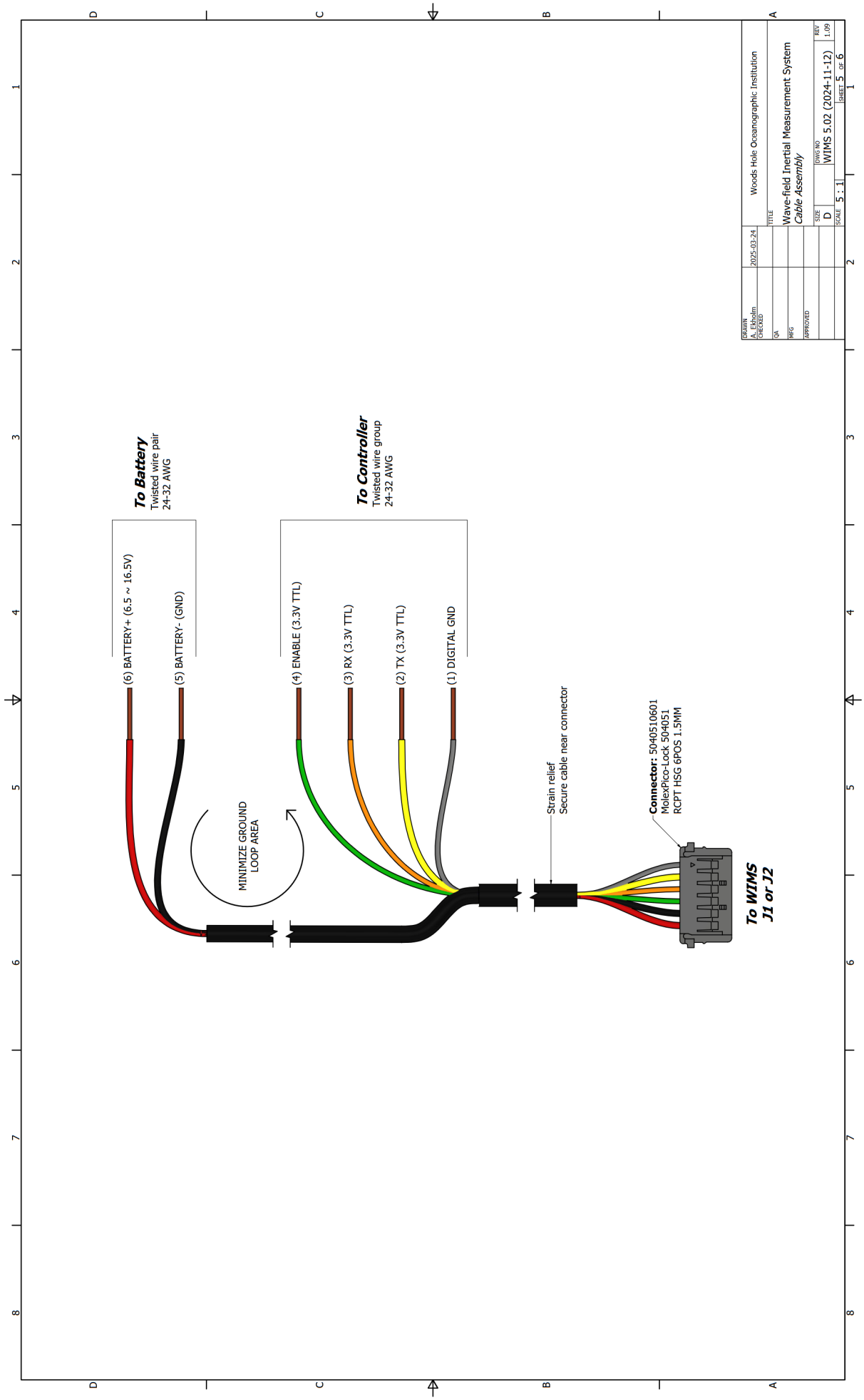


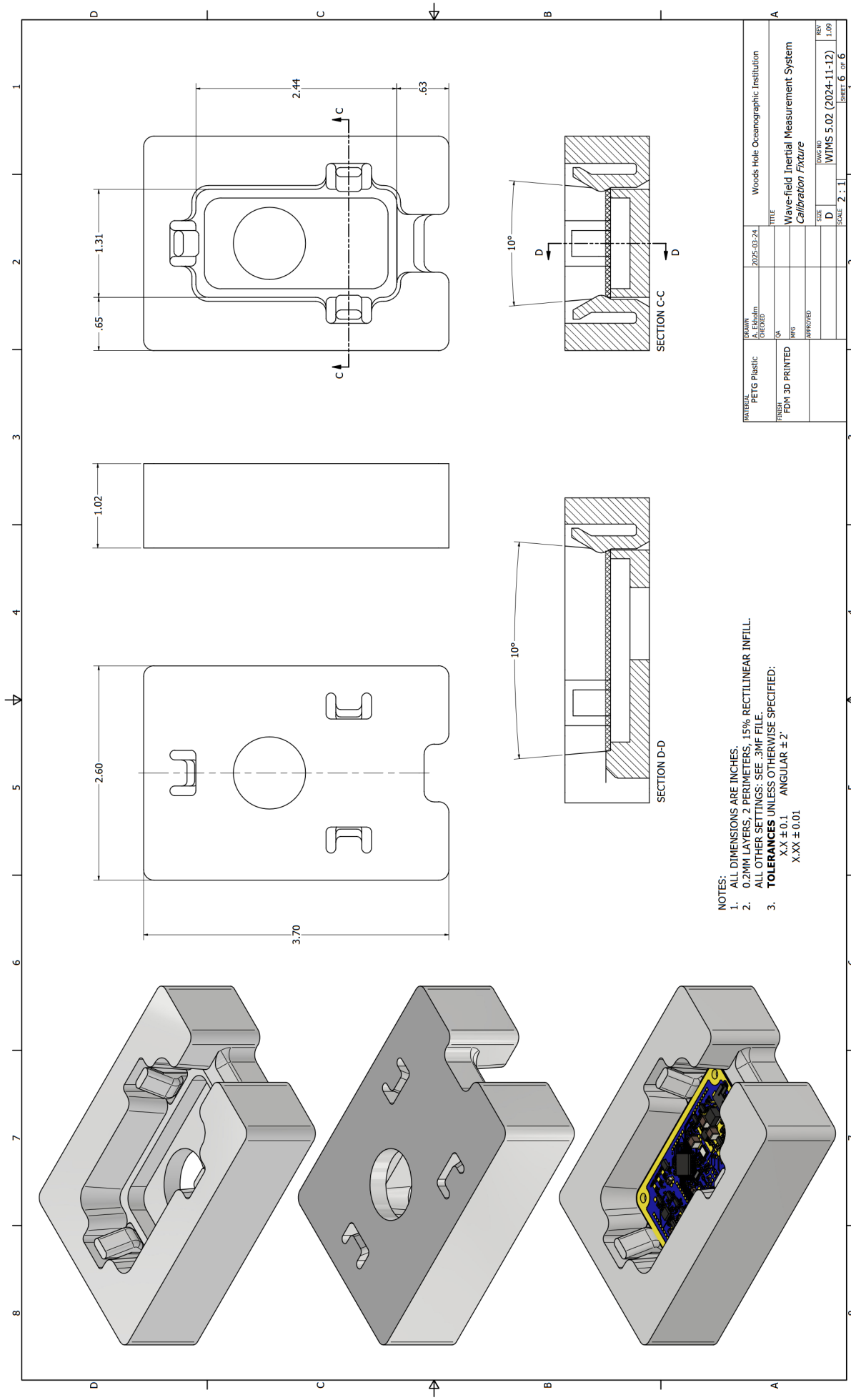

J1
Header: 5040500691
Molex Pico-Lock 504050
Header SMD R/A 6POS 1.5MM
Mating Connector: 5040510601
MolexPico-Lock 504051
RCPT HSG 6POS 1.5MM
OPTIONAL LASER-CUT
ALUMINUM SHIELD
OPTIONAL BILLET
ALUMINUM SHIELD
Z
Y
X
DRAWN
A. Elholm
2025-03-24
CHECKED
QA
MFG
APPROVED
Woods Hole Oceanographic Institution
TITLE
Wave-field Inertial Measurement System
SIZE
D
DWG NO
WIMS 5.02 (2024-11-12)
REV
1.09
SCALE
5 : 1
SHEET 1 OF 6


J1
Header: 5040500691
Molex Pico-Lock 504050
Header SMD R/A 6POS 1.5MM
Mating Connector: 5040510601
MolexPico-Lock 504051
RCPT HSG 6POS 1.5MM
UP
Prefferred mounting orienation
IMU
Mount nearest to CoM as possible
4X Ø.40 MIN
MOUNT HOLE CLEARANCE
(BOTH SIDES)
4X Ø.270
4X R.15
4X Ø.118 THRU
2.125
1.000
2.05
1.300 ± .010
2.425 ± .010
.15
.05
.06
.16
NOTES:
1. ALL DIMENSIONS ARE INCHES.
2. TOLERANCES UNLESS OTHERWISE SPECIFIED:
X.X ± 0.1 ANGULAR ± 2°
X.XX ± 0.01
X.XXX ± 0.001
DRAWN A. Eiholm 2025-03-24
CHECKED
QA
MFG
APPROVED
Woods Hole Oceanographic Institution
TITLE
Wave-field Inertial Measurement System
PCB Assembly
SIZE D
DWG NO WIMS 5.02 (2024-11-12)
REV 1.09
SCALE 5 : 1
SHEET 2 OF 6


Woods Hole Oceanographic Institution
Wave-Field Inertial Measurement System
Shield
WIMS 5.02 (2024-11-12)
MATERIAL 6061-T6 ALUMINUM
FINISH AS MACHINED
SCALE 4 : 1
SHEET 3 OF 6
SECTION A-A SCALE 5 : 1
SECTION B-B SCALE 5 : 1
4X Ø.120 THRU ⌴ Ø.198 ± .012 ↧ .10
4X R.18
R.010 MAX
NOTES:
1. ALL DIMENSIONS ARE **INCHES**.
2. DEBURR AND BREAK SHARP EDGES.
3. UNSPECIFIED OUTSIDE FILLETS 0.020.
4. INSIDE FILLETS 0.030 MAX UNLESS OTHERWISE SPECIFIED.
5. **TOLERANCES** UNLESS OTHERWISE SPECIFIED:
X.X ± 0.1 ANGULAR ± 2°
X.XX ± 0.01
X.XXX ± 0.005


4X No. 4-40
SOCKET CAP SCREW
4X No. 4 UNTHREADED SPACER
Ø.25 X .05 MIN
NOTES:
1. ALL DIMENSIONS ARE **INCHES**.
2. **TOLERANCES** UNLESS OTHERWISE SPECIFIED:
X.X ± 0.1 ANGULAR ± 1°
X.XX ± 0.01
X.XXX ± 0.005
BEND DETAILS
ORDER ANGLE DIRECTION RADIUS
A 90 DOWN .024
B 90 DOWN .024
C 90 DOWN .024
D 90 DOWN .024
8X Ø.120
4X Ø.200
.040 ± .004
MATERIAL
5052 H32 ALUMINUM
SHEET .040
FINISH
AS MACHINED
(LASER CUT)
DRAWN
A. Elholm
CHECKED
QA
MFG
APPROVED
2025-03-24
Woods Hole Oceanographic Institution
TITLE
Wave-field Inertial Measurement System
Shield
SIZE
D
DWG NO
WIMS 5.02 (2024-11-12)
REV
1.09
SCALE
5 : 2
SHEET 4 OF 6


To Battery
Twisted wire pair
24-32 AWG
(6) BATTERY+ (6.5 ~ 16.5V)
(5) BATTERY- (GND)
To Controller
Twisted wire group
24-32 AWG
(4) ENABLE (3.3V TTL)
(3) RX (3.3V TTL)
(2) TX (3.3V TTL)
(1) DIGITAL GND
MINIMIZE GROUND
LOOP AREA
Strain relief
Secure cable near connector
Connector: 5040510601
MolexPico-Lock 504051
RCPT HSG 6POS 1.5MM
To WIMS
J1 or J2
DRAWN
A. Ekholm
2025-03-24
CHECKED
QA
MFG
APPROVED
Woods Hole Oceanographic Institution
TITLE
Wave-field Inertial Measurement System
Cable Assembly
SIZE
D
DWG NO
WIMS 5.02 (2024-11-12)
REV
1.09
SCALE
5 : 1
SHEET 5 OF 6


2.44
.63
1.31
.65
C
C
10°
D
D
SECTION C-C
1.02
2.60
3.70
10°
SECTION D-D
NOTES:
1. ALL DIMENSIONS ARE INCHES.
2. 0.2MM LAYERS, 2 PERIMETERS, 15% RECTILINEAR INFILL.
3. ALL OTHER SETTINGS: SEE .3MF FILE.
4. TOLERANCES UNLESS OTHERWISE SPECIFIED:
X.X ± 0.1 ANGULAR ± 2°
X.XX ± 0.01
MATERIAL PETG Plastic
FINISH FDM 3D PRINTED
DRAWN A. Ekholm 2025-03-24
CHECKED
QA
MFG
APPROVED
Woods Hole Oceanographic Institution
TITLE
Wave-field Inertial Measurement System
Calibration Fixture
SIZE D
DWG NO WIMS 5.02 (2024-11-12)
REV 1.09
SCALE 2 : 1
SHEET 6 OF 6

12 Firmware Change Log

v2.01.00617b (2026-10-27)

- The default sample rate divider, `wav.srdiv`, is 8 (was 17), for an effective sample rate of 5 Hz (was 2.5 Hz) with the default `imu.srate` of 45 Hz. With the default segment length, the spectra bin bandwidth is 0.0195 Hz, the segment duration is 51 seconds, and the default run time is about 6.5 minutes. The spectral sensitivity scale factor increases by a factor of 4 (see Section 7.3: Scale Sensitivity).
- Fixed the linear trend removal for segment lengths of 512 and 1024, for which an integer overflow made the estimated slope 4 times too small, so that most of the trend was not removed.
- The trend intercept is computed exactly; previously the mean sample index was truncated, leaving an offset of half the slope.
- The vertical spectral output mode, `wav.omode` = 4, uses the earth-frame vertical acceleration, filtered and downsampled as in full spectral output mode. It previously used the sensor-frame Z-axis acceleration, which was not rotated to the earth frame or filtered with `wav.afilt`, and its trend removal left an offset in each segment.
- `load default` resets `cal.acofx`, which was previously left unchanged.
- `save` no longer resets the wave module configuration parameters when EEPROM is unavailable.
- `imu.srate` is limited to the range 5 to 225 Hz, and `wav.mxsam` and `wav.mxseg` to the range 0 to 65535.

v2.01.00616b (2026-10-26)

- The processor sleeps (Sleep mode, wait for interrupt) when it has no work: during a run in the interrupt-driven sample mode, between IMU samples, and in the idle state, while waiting for serial input. Peripherals keep running, and the processor wakes on the next IMU sample, received character, or system tick. This reduces the supply current; the polled sample modes are unchanged.
- Removed the `-mtune=cortex-a35` compiler option, which tuned code generation for an application processor. Code is now tuned for the Cortex-M33 processor, reducing the program size by about 4.7 kB.

v2.01.00615b (2026-10-26)

- Corrected spectra bin frequencies: bin n is now labelled $nf_e/2N$, with bin 0 the DC bin. Earlier versions labelled bin n with $(n+1)f_e/2N$. The spectral values are unchanged.
- The `runinfo` command reports the spectra bin bandwidth instead of the minimum bin frequency, which is now 0 Hz.

- Spectra min/max frequency limits are inclusive for all spectral output, as for single-spectrum output.

v2.01.00614b (2026-10-26)

- Fixed `CFG_PARAM_RUN_RMODE` configuration parameter identifier declaration so the committed source builds. This fix was already included in the v2.01.00613b release binaries.
- Added STM32CubeIDE project files, linker scripts, and Doxygen configuration to the source repository. The Release build now also generates `.hex` and `.bin` images.

v2.01.00613b (2025-05-14)

- Fixed configuration parameter indexing bug.
- Changed behavior of spectra min/max frequency to be inclusive of boundaries.

v2.01.00612b (2025-05-06)

- Initial production release candidate.

v2.01.00611a (2025-03-25)

- Orientation filter optimizations.

v2.01.00604a (2025-03-21)

- Added functionality to measure IMU sample period using MCU clock for more accurate orientation updates from angular rate.

v2.01.00596a (2025-03-18)

- Implemented baud command.

v2.01.00591a (2025-03-18)

- AT24C512C driver bugfixes
  - Corrected I2C addresses bug.
  - Fixed write timestamp comparisons
- ICM-20948 driver bugfixes.

  - Now enables low-power mode while sampling (disables some digital circuitry for power reduction).
  - Fixed bug where mag data not correctly adjusted to account for magnetometer orientation.
  - I2C master clock frequency now set to correct value.

- Orientation filter – implemented new method for initial orientation filter settling that ignores gyro data initially.
- Wave module
  - Fixed rotations for normally forward and upward axes.
  - Streamlined wave packet processing.
- Quaternion utility - fixed calculation of Euler angle from quaternion.

v2.00.00487a (2024-12-27)

- Added "run.rmode" and "run.smode" configuration parameters.
- Updates to user comms utility task function.
- Updates to math utility.
- Updates and bugfixes for wave module.

v2.00.00426a (2024-12-03)

- Updates to wave module acceleration trend removal (linear regression).
- Updates to board driver LED sequence handling.

v2.00.00416a (2024-11-22)

- Bugfixes for EEPROM utility and AT24C512C driver.
- Changed wave module output of spectral data to improved format.
- Added "load", "runinfo", and "save" commands.
- Added wav.fbmax and wav.fbmin configuration parameters.
- Changed MCU timebase to run from TIMER1

v2.00.00394a (2024-11-18)

- Implemented EEPROM utility and AT24C512C driver.
- Implemented "reset", "magst", "shutdown", and "sleep" commands.
- Implemented magnetometer self-test capability.
- Updates for user comms utility.

v2.00.00365a (2024-11-12)

- Implemented configuration parameters and user commands.
- Implemented "set" and "get" commands.
- Fixed bug in user comms that caused hang when tx buffer filled.

v2.00.00336a (2024-11-06)

- User comms utility and ICM-20948 driver bugfixes.

v2.00.00324a (2024-11-05)

- Implemented run command.
- Fixes for interrupt-driven behavior for reading ICM-20948 FIFO packet buffer.
- Updates for user comms module.
- Updates for circular buffer utility.

v2.00.00323a (2024-11-04)

- Ported orientation filter and wave modules. Overhaul of wave module for new ICM-20948 driver.
- Implemented FIR filter, math, and quaternion utilities.
- Fixed include structure.

v2.00.00322a (2024-11-04)

- Implementation/rewrite of ICM-20948 driver.
- Added CMSIS-DSP source.
- Fixes and updates for interrupt driven behavior of user comms utility.
- Created board driver for v5.02 hardware

v2.00.00317a (2024-09-17)

- Initial port for v5.02 hardware.
- Created initial configuration files for ARM Cortex-M33 STM32L552xx.
- Ported circular buffer, user comms, and common utilities.

v1.09

- Added support for hardware revision 2.06 hardware including new ICM-20948 IMU.
- Updated default configuration parameter values for new hardware. Removed deprecated parameters.
- Implemented new accelerometer low-pass filter options corresponding to new default sample rate.
- Implemented software gain option for accelerometer and added corresponding configuration parameter.

v1.08

- Implemented functionality to load and store configuration parameters to nonvolatile memory. Additionally, a hash of the configuration parameters is computed and stored in nonvolatile memory to verify that parameters loaded parameters are valid.
- Implemented functionality to load configuration parameters on boot and validate the configuration parameter hash. If parameters are loaded with an invalid hash, the default parameters are automatically loaded and save to nonvolatile memory.
- Added "load", "save", and "reset" commands to allow user to control manipulate configuration parameters stored in nonvolatile memory.
- Implemented function in DEBUG build for testing response of FIR filters to (1) impulse and (2) step functions.
- Added "read" command to print one or more spectra after a run has completed.
- Implemented FIR filtering of magnetometer data during calibration. The magnetometer data is filtered using the filter specified by "wav.afilt".
- Deprecated magnetic declination correction.
- Performance optimizations for wave module.

v1.07

- Implemented finite-impulse response filtering for accelerometer data and added coefficients for three selectable filters, selectable using new configuration parameter "wav.afilt".
- Added "wav.ostsc" parameter which determines the duration allow to let the orientation filter to settle at the start of the run.
- Changed default maximum segments from 16 to 12 so that default run time is approximately 10 minutes.
- Changed default accelerometer full-scale range from $\pm 4g$ to $\pm 2g$, resulting in a change in the default cross-spectra full-scale range from $\pm 16g^2/Hz$ to $\pm 4g^2/Hz$.

v1.06

- Completed implementation of improved, full orientation filter described by Madgwick et al.
- Added optional magnetic distortion compensation for full orientation filter.
- Removed deprecated output modes.
- Added Gyroscope bias drift compensation and related parameter "wav.ozeta". This parameter determines the rate of convergence of the gyroscope bias drift compensation.

v1.05

- Implemented optional normalization of acceleration vector in orientation filter.
- Added parameter "wav.nfwax" for defining normally forward facing axis. Allows measurements to be referenced to direction of the measurement platform.

v1.04

- Added 100ms delay on startup before splash text is printed. This helps mitigate garbage being printed to the serial port when the power switching circuit is transitioning to the low power sleep state and prevents the device from setting the D04 signal high, preventing the power circuit from switching off.
- Added check to ensure that average power-spectral densities (e.g. "Szz") are saturated to the range of uint16_t.
- Changed "sleep" command behavior so that user can cancel power down by entering the ESC character 10 times (before the power circuit switches off). Previously, the sleep command would be canceled if any character was received from the user.



v1.03

- Suppressed intermediate "a_v" and "qs2e" output in output mode 8 (WAVE_OUTPUT_MODE_SPECTRA_VERTICAL) when log.level is less than 3 (UCOM_LOG_LEVEL_INF).

v1.02

- Added parameter "wav.nupax" for defining normally upward facing axis. Allows orientation filter to settle faster on start of run with better guess of initial orientation.
- Added "baud" command for changing serial port BAUD rate.
- Implemented "vers" command for getting firmware version identification. Firmware version now also printed at startup.

v1.01

- Initial release.

13 Document Revision Change Log

v3.22 (2026-11-03)

- Refitted the low-frequency response correction, Table 13, with the center and direction of motion of the storm at the time of each spectrum taken from a cubic spline through the best track positions, for the storm quadrants of the colocated pairs: $f_0 = 0.02622$ Hz and $w = 0.08951$ Hz, from 0.02595 Hz and 0.08834 Hz. The correction is 1 above 0.116 Hz, from 0.114 Hz, and the root-mean-square residual of the fit is 0.051, from 0.057.

- Took the time and position of each WIMS spectrum from the profile position determined by the `xmtps` software, with the Iridium position for the few profiles without a GPS fix (Section 7.8.1). The water depth of the WIMS spectra of Section 7.10.1 is now available at all of these positions; 346 spectra without one, 277 of them of float 9282, were previously excluded. The NDBC pairs increase from 3548 to 3940, mostly at NDBC 42003, 42039, and 42040.

- Updated the results, tables, and figures of Sections 7.8 to 7.10 accordingly.

v3.21 (2026-10-31)

- Refitted the low-frequency response correction, Table 13, to the colocated pairs whose WIMS and reference positions are in the same storm quadrant or both more than 600 km from the center of the storm, as in Sections 7.9 and 7.10, with the A-DWSD outliers excluded: $f_0 = 0.02595$ Hz and $w = 0.08834$ Hz, from 0.01445 Hz and 0.10457 Hz. Added the A-DWSD outlier criteria to Section 7.8.1. Updated the results of Sections 7.8 to 7.10 with the refitted correction, and added its sensitivity to the pair selection to Section 7.8.6.

- Cited the National Hurricane Center best track data and the Tropical Cyclone Report of Hurricane Erin for the storm tracks, in place of the description of the Atlantic hurricane database (HURDAT2).

- Added the NDBC buoy pairs measured during tropical cyclones, Section 7.10.3: Teddy (2020), Ida, Mindy, and Nicholas (2021), Chantal, Erin, Humberto, Imelda, and Melissa (2025), and Josephine (2020).

- Applied the storm-quadrant selection of the colocated pairs with all the storms active during the deployments, not only Erin and Lowell; the NDBC 41047 pairs during Hurricanes Humberto, Imelda, and Melissa are now in the same quadrant of that storm or excluded.

- Added a disclaimers page: WIMS data are not to be used for decisions about actions in response to storm or other weather conditions, for which the guidance of the authorities is to be sought, and Claude Code was used in producing the analysis of Sections 7.8 to 7.10, which has been reviewed by the author.

- Drew the maps of Figures 11, 12 and 27 in the Robinson projection.

- Added the distance of the A-DWSD drifters from the center of the storm to Figures 11 and 12c, labelled the floats as ALAMO floats, enlarged the A-DWSD markers, and placed the track date labels inside the map borders.
- Drew Figures 11 and 12b over the GOES infrared image of the closest approach of the storm.
- Limited Figure 18 to 400 km from the center of the storm, enlarged it, and added the storm-relative significant wave heights and swell and wind-wave directions of all the WIMS spectra of the two storms, Figures 19 to 21, with the storm-relative positions from a cubic spline through the best track positions.

v3.20 (2026-10-29)

- Corrected the unit of the RTC clock frequency, f_{RTC}, from MHz to kHz.
- Corrected the caption of the back PCB assembly drawing.
- Corrected the sign of the exponent of the accelerometer offset correction in Section 9.2: cal.acof[A] and cal.acsc[A], to $2^{(r_a-14)}$.
- Removed the note in Section 7.8 that the correction applies only to WIMS installed in ALAMO floats.
- Revised the description of the differences between the per-bin scale factors of the data sets: from 0.06 Hz to 0.1 Hz, the higher NDBC 41047 ratio of the means comes from a minority of high-energy pairs, consistent with the position of the buoy relative to the storm, and below 0.055 Hz the differences depend on the sensor noise floors and the long-period swell (Section 7.8.3: Results).
- Revised the NDBC buoy intercomparison (Section 7.10: NDBC Buoy Intercomparison) with the WIMS spectra of all ALAMO floats and all NDBC buoys within the colocation limits, including stations no longer reporting, at the buoy position of the deployment in effect at each spectrum: 3595 pairs at 15 buoys in water deeper than 50 m, with the WIMS spectra in water deeper than 50 m (ETOPO 2022 bathymetry), from 21 floats, from August 2020 to July 2026, including the NDBC 41047 pairs of Hurricane Erin used to fit the low-frequency response correction that have the WIMS spectrum and the buoy in the same storm quadrant or both more than 600 km from the center. The buoys are selected by water depth instead of as deep-water or continental shelf buoys. The position of NDBC 41002 used previously was about 430 km from its actual position. Added the table of buoy locations and positions, with the water depth of each deployment position from the ETOPO 2022 bathymetry, Table 24. Updated the NDBC buoy results of the directional coefficient intercomparison (Section 7.9.1: Directional Fourier Coefficients and Spreading Parameters).
- Started each section and subsection on a new page, with the figures and tables of a section placed within it, except the reference entries of the configuration parameters and the change log entries.
- Placed the track date labels of Figure 12 without overlap, and the quadrant labels of Figure 18 inside the plot borders.

- Reduced the colocated spectra figures, Figures 14 to 16, to the differences of the colocated spectra, and moved the legend of Figure 12b to the upper left.
- Added notes to Tables 24 and 25 that the NDBC 41047 data of Hurricane Erin were used to calculate the low-frequency response correction, and set the period of Figure 12c to 2 to 10 September.
- Used, in Sections 7.9, 7.9.1 and 7.10, the pairs with both positions in the same storm quadrant or both more than 600 km from the center of the storm, excluding only the pairs in different quadrants, and moved the colorbar of Figure 18 below the plots.

v3.19 (2026-10-29)

- Replaced the mechanical properties table, which had no values, with Table 6, from the dimensions and mechanical drawings.
- The no-wave-energy rejection criterion is $m_0 = 0$, since S_{zz} is never negative (Section 7.7.2: Post-Processing Steps).
- Moved Table 13 to the post-processing step that first refers to it.

v3.18 (2026-10-29)

- Added Section 6.2.1: Formulation, the full formulation of the orientation filter.
- Removed the recommendation that the host reset WIMS.
- Gave the recommendations for mechanical integration and for the primary cable assembly the format of those for electrical integration, with a bold label for each item, and renamed Section 5.2: Recommendations for Primary Cable Assembly, whose figure is now on the same page.

v3.17 (2026-10-29)

- Added Section 7.9.1: Directional Fourier Coefficients and Spreading Parameters, an intercomparison of the WIMS directional Fourier coefficients and spreading parameters with those of the A-DWSD drifters and NDBC buoys of Sections 7.8 to 7.10, and referenced it from Sections 7.8 and 7.10.

v3.16 (2026-10-29)

- The noise floor and the low-frequency response correction are applied to all six spectra, as in the current `xmtps` software, not to the vertical spectrum only (Section 7.7.2: Post-Processing Steps). The stored acceleration spectra are those before the correction.

- Stated that the low-frequency response correction was determined with, and applies to, the ALAMO floats deployed to date, with firmware versions earlier than v2.01.00617b, and added its limitations below 0.055 Hz and for the trend removal of floats 9287 and 9291 (Section 7.8: Low-Frequency Response Correction).
- Corrected the data sets to which the low-frequency response correction is fitted in Section 7.8.4: Storm-Relative Position.
- The firmware and document revision change logs list the newest version first.

v3.15 (2026-10-28)

- Updated for firmware v2.01.00617b, including the default `wav.srdiv` of 8, the example output, and the `runinfo` examples.
- Updated the spectral sensitivity scale factor, Equation (23), and the reported spectra type.
- Spectral moments exclude the DC bin.
- Documented the run output record formats, the `mcal` command output and magnetometer calibration procedure, the `OUT` log tag, and the effect of `wav.gaina` = 0.
- Added Section 8.3.3: Error Messages and Status Codes.
- Corrected the `imu.srate` and `wav.mxseg` ranges, and the `wav.afilt` = 0 filter characteristics for the default `wav.srdiv`.
- Added Section 3.3: Recommendations for Electrical Integration.
- Repeated the intercomparisons of Sections 7.8 to 7.10 with the corrected scale factor, added the Hurricane Lowell A-DWSD intercomparison, including the wave direction validation, which now uses only pairs in the same storm quadrant, and replaced the low-frequency response correction, Equation (42), with a cosine taper fitted to the ratio of the means of all data sets. Rewrote these sections more concisely.
- Added Section 7.8.4: Storm-Relative Position, and repeated Section 7.8.5: Rejection Criteria Evaluation with the corrected scale factor.
- Removed the statement that the A-DWSD drifter spectra are shifted in frequency relative to the NDBC spectra, and the evaluation of the bin frequency labels of earlier firmware from the intercomparison.
- Added the track of Hurricane Erin and the distance of the floats and the buoy from the storm to Figure 11.
- Added references to the external data sets used: the NDBC, A-DWSD, and NHC best track data, and IGRF-14.
- The magnetic declination of a dive without a valid position is that of the most recent valid position of the float (Section 7.7.2: Post-Processing Steps).

v3.14 (2026-10-27)

- Added Section 7.10: NDBC Buoy Intercomparison.

v3.13 (2026-10-26)

- Updated for firmware v2.01.00616b.

v3.12 (2026-10-26)

- Updated for firmware v2.01.00615b.
- Corrected spectra bin frequencies in Section 7.2: Spectra Frequencies, and the example output.
- Added Section 7.7: Shore-Side Data Validation and Post-Processing.
- Rewrote Section 7.5: Directional Spectra for displacement measurements, removing the wavenumber, and documented that wave directions give the direction toward which waves propagate.
- Added Section 7.8: Low-Frequency Response Correction.
- The principal wave direction, θ_2, is resolved to the range $[0°, 360°)$ using the mean wave direction, Equation (36).
- Added an evaluation of the spectra rejection criteria, Section 7.8.5: Rejection Criteria Evaluation, and noted that the low-frequency response correction applies only to WIMS installed in ALAMO floats.
- Wave directions are corrected for the magnetic declination in the shore-side processing and referenced to true north.
- Added Section 7.9: Wave Direction Validation.

v3.11 (2026-10-26)

- Updated for firmware v2.01.00614b.
- Added dates to Section 12: Firmware Change Log.
- Corrected default values of `wav.obeta`, `log.level`, and `serialnum`, and the gyroscope full-scale range description.
- Corrected principal wave direction, directional spreading function, deep-water approximation, spectral moment, and maximum segment run time equations.
- Corrected accelerometer and gyroscope calibration procedure steps.

- Documented `runinfo` output fields, `load` and `baud` side effects, continuous run behavior, IMU DLPF cutoff selection, and IMU sample rate rounding.
- Corrected typographical errors.

v3.10 (2025-10-16)

- Added Section 4.4: Recommendations for Mechanical Integration.
- Updated document revision change log cross-references.

v3.09 (2025-09-02)

- Changed Equations (34) and (36), mean and principal wave direction, to reference clockwise angle from magnetic north.
- Updated Table 42: Output modes..

v3.08 (2025-08-27)

- Fixed error in Equation (22): base spectral sensitivity scale factor.

v3.07 (2025-05-28)

- Added Section 5.2: Recommendations for Primary Cable Assembly.
- Added equivalent orientation representation for combinations for wav.nfwax and wav.nupax in Table 41.

v3.06 (2025-05-15)

- Added configuration parameter descriptions in Section 9.
- Added description of serial interface special characters and strings in Section 8.1.

v3.05 (2025-05-14)

- Added configuration parameter descriptions in Section 9.

v3.04 (2025-05-12)

- Added naming conventions, directional spectra, and derived wave parameters subsections in Section 7: Spectral Data Processing.

v3.03 (2025-05-08)

- Added Section 6.4.1: Run Duration.
- Added Section 7: Spectral Data Processing.
- Updated parameter and command cross-references.

v3.02 (2025-05-07)

- Updated Section 12: Firmware Change Log.
- Added Section 6.3: Reset Behavior.
- Added Section 6.5: Low-power Shutdown.
- Added Section 9: Configuration Parameters.

v3.01 (2025-05-06)

- Added PCB characteristics, assembly drawings, and renders.
- Added connectors tables.
- Added interface commands table and command descriptions.
- Updated Section 12: Firmware Change Log.

v3.00 (2025-05-02)

- Initial updates for v5.02 hardware.

14 References

[1] A. K. Ekholm, "Wave-field inertial measurement system," U.S. Patent 12 650 303, Jun. 9, 2026.

[2] S. R. Jayne, W. B. Owens, P. E. Robbins, A. K. Ekholm, N. M. Bogue, and E. R. Sanabia, "The air-launched autonomous micro observer," *Journal of Atmospheric and Oceanic Technology*, vol. 39, no. 4, pp. 491–502, 2022. DOI: 10.1175/JTECH-D-21-0046.1.

[3] S. O. Madgwick, A. J. Harrison, and R. Vaidyanathan, "Estimation of imu and marg orientation using a gradient descent algorithm," in *2011 IEEE international conference on rehabilitation robotics*, Ieee, 2011, pp. 1–7.

[4] S. Wilson, H. Eberle, Y. Hayashi, *et al.*, "Formulation of a new gradient descent marg orientation algorithm: Case study on robot teleoperation," *Mechanical Systems and Signal Processing*, vol. 130, pp. 183–200, 2019.

[5] M. D. Earle, "Nondirectional and directional wave data analysis procedures," National Data Buoy Center, Stennis Space Center, MS, NDBC Technical Document 03-01, 2003.

[6] L. Centurioni, L. Braasch, E. Di Lauro, *et al.*, "A new strategic wave measurement station off Naples port main breakwater," *Coastal Engineering Proceedings*, vol. 1, no. 35, waves.36, 2017. DOI: 10.9753/icce.v35.waves.36.

[7] C. D. Beggan, C. Kloss, P. Amblard, *et al.*, "International geomagnetic reference field: The fourteenth generation," *Earth, Planets and Space*, vol. 78, p. 127, 2026. DOI: 10.1186/s40623-025-02360-0.

[8] Lagrangian Drifter Laboratory, Scripps Institution of Oceanography. "SASCWATCH first5 wave data." ERDDAP dataset ONR_SASCWATCH_First5, ONR SASCWATCH drifter wave observations, Hurricane Erin (accessed 2025-09-23) and Hurricane Lowell. (2025), [Online]. Available: https://erddap.ldl.ucsd.edu/erddap/info/ONR_SASCWATCH_First5/index.html (visited on 10/28/2026).

[9] Lagrangian Drifter Laboratory, Scripps Institution of Oceanography. "SASCWATCH data." ERDDAP dataset ONR_SASCWATCH, ONR SASCWATCH drifter observations, Hurricane Erin (accessed 2025-09-23) and Hurricane Lowell. (2025), [Online]. Available: https://erddap.ldl.ucsd.edu/erddap/info/ONR_SASCWATCH/index.html (visited on 10/28/2026).

[10] National Hurricane Center. "Automated tropical cyclone forecasting system (ATCF) best track data." Best tracks of Hurricane Erin (AL052025, bal052025.dat) and Hurricane Lowell (EP122026, bep122026.dat). (2026), [Online]. Available: https://ftp.nhc.noaa.gov/atcf/ (visited on 11/01/2026).

[11] R. J. Pasch and A. D. Mahoney, "Hurricane Erin (AL052025), 11–22 August 2025," National Hurricane Center, Tropical Cyclone Report, Jan. 30, 2026. [Online]. Available: https://www.nhc.noaa.gov/data/tcr/AL052025_Erin.pdf (visited on 11/01/2026).

[12] GOES-R Calibration Working Group and GOES-R Series Program. "NOAA GOES-R series advanced baseline imager (ABI) level 2+ cloud and moisture imagery (CMIP)." Band 13, GOES-18 and GOES-19, NOAA Open Data Dissemination Program, buckets noaa-goes18 and noaa-goes19 on Amazon Web Services. (2017), [Online]. Available: https://registry.opendata.aws/noaa-goes/ (visited on 10/31/2026).

[13] M. S. Longuet-Higgins, D. E. Cartwright, and N. D. Smith, "Observations of the directional spectrum of sea waves using the motions of a floating buoy," in *Ocean Wave Spectra*, Englewood Cliffs, NJ: Prentice-Hall, 1963, pp. 111–136.

[14] NOAA National Centers for Environmental Information, *ETOPO 2022 15 arc-second global relief model*, 2022. DOI: 10.25921/fd45-gt74.

[15] C. W. Landsea and J. L. Franklin, "Atlantic hurricane database uncertainty and presentation of a new database format," *Monthly Weather Review*, vol. 141, no. 10, pp. 3576–3592, 2013. DOI: 10.1175/MWR-D-12-00254.1.

